SMITHSONIAN CONTRIBUTIONS TO THE EARTH SCIENCES

NUMBER 9

William G. Melson
EDITOR

Mineral Sciences Investigations, 1969-1971

SMITHSONIAN INSTITUTION PRESS
CITY OF WASHINGTON
1972

ABSTRACT

Melson, William G., editor. Mineral Sciences Investigations, 1969–1971. *Smithsonian Contributions to the Earth Sciences,* number 9, 94 pages, 34 figures, 1972.—Seventeen short contributions from the Smithsonian's Department of Mineral Sciences from 1969 to 1971 are gathered together in this volume. The scientific and technological subjects treated in these contributions include studies of lunar samples from Apollo 12, meteorites, petrology and volcanology, and descriptive mineralogy, as well as of the history and description of one of the Smithsonian Institution's most important recent acquisitions—the Carl Bosch Collection of Minerals and Meteorites.

Official publication date is handstamped in a limited number of initial copies and is recorded in the Institution's annual report, Smithsonian Year.

Library of Congress Cataloging in Publication Data
Melson, William G., 1938– comp.
Mineral sciences investigations, 1969–1971.
(Smithsonian contributions to the earth sciences, no. 9)
"Seventeen short contributions from the Smithsonian's Department of Mineral Sciences."
1. Mineralogy—Addresses, essays, lectures. 2. Petrology—Addresses, essays, lectures. I. National Museum of Natural History. Dept. of Mineral Sciences. II. Title. III. Series: Smithsonian Institution. Smithsonian contributions to the earth sciences, no. 9.
QE1.S227 no. 9 [QE369] 550'.8s [549'.1] 72–355

For sale by the Superintendent of Documents, U.S. Government Printing Office
Washington, D.C. 20402 - Price $1.25 (paper cover)

Contents

LUNAR STUDIES

Brian Mason, William G. Melson, E. P. Henderson, Eugene Jarosewich, and Joseph Nelen

Mineralogy and Petrography of Some Apollo 12 Samples

ABSTRACT

Samples of the Apollo 12 fines contain fragments of crystalline rocks and breccias, mineral grains, and glassy particles. The mineral grains are mainly pyroxene (pigeonite and augite) and olivine, with minor amounts of plagioclase and ilmenite, and rare metal grains. The compositions of the metal grains indicate that some are of meteoritic origin and some are derived from lunar rocks. A single pyroxene crystal has a pigeonite core, an augite mantle, and a rim of ferrohedenbergite, with a narrow zone of pyroxferroite along a central fissure. One rock fragment from a sample of coarse fines (12032) is a silica-rich hedenbergite granophyre, consisting of sanidine (50%), quartz (30%), hedenbergite (10%), plagioclase (7%), fayalite (3%), and accessory apatite, whitlockite, and zircon. A complete chemical analysis of 12001 fines has been made, and also a determination of the water-soluble cations, a noteworthy feature being the presence of 103 ppm water-soluble calcium.

The Smithsonian received the following samples from the Apollo 12 collections:

Fines (−1 mm):	12001 (3.0 g); 12003 (0.5 g); 12033 (0.5 g); 12042 (0.5 g); 12057 (2.0 g); 12070 (2.0 g)
Coarse fines:	(1 mm–1 cm): 12032 (0.5 g)
Rock sections:	12009, 12022, 12045, 12051

Each sample of the fines was sieved through 60-mesh (0.250-mm opening) and 200-mesh (0.074-mm opening) sieves. The grain-size distribution was similar in all, the weight proportions being: +60 mesh, 10–20%; 60–200 mesh, 20-30%; −200 mesh, 50–60%. The fines contained fragments of crystalline rocks and breccias, mineral grains, and glassy particles. The coarser fractions were density-separated, using methylene iodide (D = 3.32). The fraction with D>3.32 comprised about 30%, and consisted almost entirely of grains of pyroxene (major), olivine (minor), and opaque minerals (small amount). The fraction with D<3.32 (about 70%) consisted of rock and breccia fragments, glass spherules and fragments, and feldspar grains.

The −200-mesh fraction of 12,001 was further separated with a 325-mesh sieve (0.044-mm opening), and a portion of the −325-mesh fraction analysed. The results are given in Table 1, along with two analyses of Apollo 11 fines. The compositions of the Apollo 12 and the Apollo 11 fines are rather similar, except that the Apollo 12 fines contain about half as much titanium as the Apollo 11 material; this has already been noted in earlier reports (LSPET 1970). Our analyses also show distinctly higher potassium and chromium in Apollo 12 fines. Since microscopic examination showed minute particles of metallic iron in the glassy fraction of the fines, we attempted to determine this in the Apollo 12 fines (by dissolution in $KCuCl_3$ solution). The figure obtained, 0.33% Fe, is certainly a minimum value, since the procedure would only dissolve those metal particles exposed on the surface of the glass fragments, and not those totally enclosed. The high summation of the analysis of the Apollo 12 fines probably results from the reporting of some metallic iron as FeO, and possibly some trivalent titanium as TiO_2.

The calculated mineral compositions (norms) of these analyses show about 40% feldspar of anorthitic composition and about 45% pyroxene. The composi-

Brian Mason, William G. Melson, E. P. Henderson, Eugene Jarosewich, and Joseph Nelen, Department of Mineral Sciences, Smithsonian Institution, Washington, D.C. 20560.

TABLE 1.—*Analyses and norms of Apollo 11 and Apollo 12 fines*
(Eugene Jarosewich, analyst)

Constituent	*Analyses (weight percent)*			Constituent	*Norms (weight percent)*		
	12001 —325 mesh	*10084 —325 mesh*	*10084 glass concentrate*		*12001 —325 mesh*	*10084 —325 mesh*	*10084 glass concentrate*
SiO_2	45.83	42.02	43.28	An	33.9	37.4	37.8
Al_2O_3	13.45	14.61	14.83	Ab	4.0	3.8	4.1
TiO_2	2.99	6.38	5.43	Or	1.5	0.9	1.1
FeO	15.78	15.59	14.91	Di	14.4	18.4	19.4
MgO	10.28	7.92	7.63	Hy	33.0	20.4	22.5
CaO	10.63	12.39	12.56	Ol	7.0	6.2	4.1
Na_2O	0.47	0.45	0.48	Il	5.7	12.1	10.3
K_2O	0.25	0.15	0.19	Cr	0.7	0.3	0.2
P_2O_5	0.22	0.27	0.17	Ap	0.5	0.6	0.4
H_2O-	0.00	0.00	0.00	Metal	0.3	—	—
MnO	0.21	0.15	0.18	FeS	0.5	—	0.4
Cr_2O_3	0.45	0.17	0.10				
Ni	0.03	0.03	0.03				
S	0.17	—	0.13				
Fe_{met}	0.33	100.13	99.92				
Sum	101.09						
S=O	0.09		0.07				
Sum	101.00		99.85				

tions are slightly undersaturated in SiO_2, giving small amounts of olivine. The Apollo 12 fines contain the equivalent of about 5% ilmenite, compared to about 10% in the Apollo 11 material. After subtracting the ilmenite, the FeO/FeO + MgO molecular percentage is remarkably similar in all these analyses (42 for the Apollo 12; 41 and 43 for the Apollo 11 analyses).

We also determined the water-extractable cations in both Apollo 11 and Apollo 12 fines. A control experiment without sample yielded less than 1 ppm of the cations determined. A sample of the Allende meteorite was extracted for comparison. The results are as follows (in ppm):

	Na	*K*	*Mg*	*Ca*	*Fe*	*Ni*
12001	14	5	31	103	5	5
10084	21	5	16	325	5	5
Allende	238	5	25	20	5	5

The notable feature is the comparatively high amount of extractable calcium, considerably less, however, in 12001 than in 10084. The extractable cations are not present in the fines as halides, since Reed and Jovanovic (1970) report less than 2 ppm water-soluble halogens in 10084. The high surface area and reactivity of the fresh lunar glass may be responsible. The water-extractable calcium perhaps explains the reported stimulating effect of lunar dust on plant growth.

Thirty grains of olivine in the Apollo 12 fines were analysed with the microprobe. The range in composition, in mole percent Fe_2SiO_4 (Fa), is Fa_{26-60}, with no marked compositional preference; the mean is Fa_{41}. Minor elements detected with the microprobe were Ca (average 0.28%), Mn (0.24%), Cr (0.14%) and Ti (0.08%). The contents of calcium are notably high for olivine; in meteoritic olivines which we have measured Ca is usually 0.01–0.02%, and Cr 0.02–0.04%. This probably reflects a high temperature of crystallization for the lunar olivine, and rapid chilling preventing readjustment at lower temperatures.

Some sixty pyroxene grains in the Apollo 12 fines were also analysed. They showed two compositional clusters, one for pigeonite and the other for augite-subcalcic augite. The mean composition of the pigeonite cluster is $Wo_{11}En_{55}Fs_{33}$, of the augite-subcalcic augite cluster $Wo_{33}En_{40}Fs_{27}$. The principal minor elements are aluminum and titanium. The pigeonite grains average 1.4% Al_2O_3 and 0.9% TiO_2, the augite and subcalcic augite 2.3% Al_2O_3 and 1.3% TiO_2.

The range of compositions shown by the isolated

pyroxene grains are essentially duplicated in a single pyroxene crystal fragment picked from 12057. This crystal fragment, 1.1 mm by 0.7 mm, has a central core of pigeonite of rather uniform composition ($Wo_{10}En_{57}Fs_{33}$) with a mantle of subcalcic augite ($Wo_{37}En_{37}Fs_{26}$), and on one edge a narrow rim of ferrohedenbergite ($Wo_{30}En_{7}Fs_{63}$). A narrow rift in the central core is lined with a thin zone of pyroxferroite. The individual minerals are clearly distinguished in crossed polars by the increase in birefrigence in passing from pyroxferroite to pigeonite to augite to ferrohedenbergite. The compositional variation across this grain is given in Figure 1 in terms of the pyroxene end members. A similar pyroxene crystal from Apollo 12 material has been described by Bence et al. (1970).

Plagioclase grains from the Apollo 12 fines show a range of composition from An_{82} to An_{96}, with a mean of An_{90}. The plagioclase contains detectable iron (average 0.4% FeO), potassium (average 0.1% K_2O), and titanium (average 0.08% TiO_2).

Several metal-rich particles were extracted from the Apollo 12 fines by means of a hand magnet. The total amount in any sample is small, making up much less than 1%. Two types of metal were distinguished; one type is finely granular and shows deformation structures, the other is coarse grained and undeformed. Microprobe analyses of the deformed grains give figures for nickel and cobalt comparable with those for meteoritic nickel-iron, suggesting that these grains have been derived from meteorite impacts on the lunar surface. The coarse-grained undeformed metal usually has lower nickel concentrations than meteoritic nickel-iron, and sometimes more cobalt than nickel; these fragments are presumably indigenous to the Moon, probably formed by localized reduction of basaltic material. One such fragment is essentially pure iron, with no detectable amounts of other elements; it is extremely soft, comparable with the purest strain-free iron we have been able to obtain. This metal fragment contains inclusions of olivine and ilmenite similar to these minerals in the lunar basalts, from which it was presumably derived.

Our 0.5-g sample of coarse fines (12032, from the rim of Bench Crater) was washed with acetone to remove dust, and then density-fractionated in methylene iodide-acetone mixtures. The density fractions were sorted by hand under a binocular microscope into breccia fragments and crystalline rock fragments. The results are set out in Table 2. The average weight of individual fragments is 3.5 mg, and the percentages of breccia and crystalline rocks are 82 and 18 respectively.

Several crystalline rock fragments were selected for detailed examination. The most remarkable one was a lone white fragment in the D<2.70 fraction, which otherwise consisted of highly vesiculated black breccia fragments. This crystalline fragment, 3-mm long, proved to consist largely of sanidine, with minor amounts of quartz, plagioclase, fayalite, and heden-

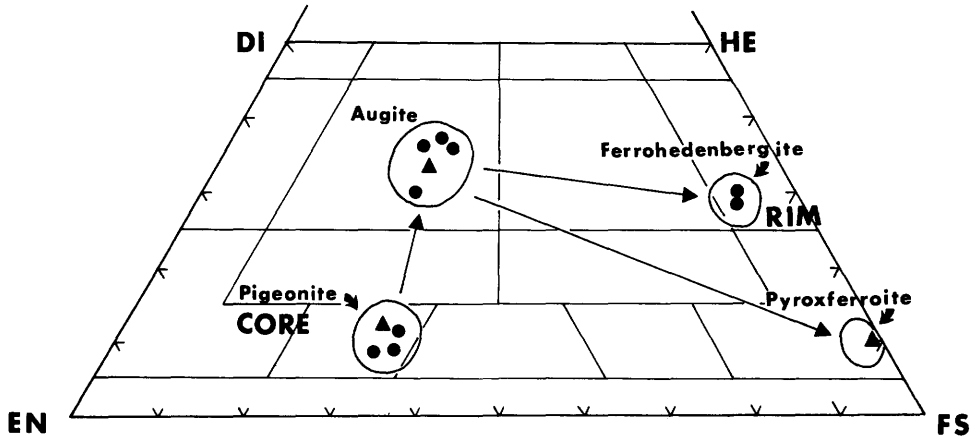

FIGURE 1.—Compositional zoning across a single pyroxene crystal from sample 12057, projected in the system enstatite (En), ferrosilite (Fs), wollastonite (Wo); arrows indicate crystallization sequence from core (pigeonite) through mantle (augite) to rim (ferrohedenbergite); a thin zone of pyroxferroite occurs along the central fissure.

bergite, and accessory zircon, apatite, and whitlockite. The composition of the individual minerals, determined by the microprobe, is given in Table 3, along with the calculated bulk composition.

The hedenbergite and fayalite are present as phenocrysts, up to 1-mm long, in a fine-grained groundmass of quartz and feldspar, much of it in micrographic intergrowth. The percentages of sanidine and quartz in this intergrowth are approximately 65:35, a composition close to the temperature minimum on the liquidus in the system $KAlSi_3O_8$–$NaAlSi_3O_8$–SiO_2. The rock is comparable to some terrestrial granophyres, specifically the hedenbergite granophyres of the Skaergaard intrusion. One of these (EG 3021) has essentially identical mineralogy, consisting of hedenbergite ($Wo_{44}En_6Fs_{50}$), fayalite (Fa_{95}), plagioclase (An_{40}), potash feldspar, and quartz and tridymite. Lindsley et al. (1969) estimate temperatures of 950°–980°C and an oxygen fugacity ranging from $10^{-13.0}$ to $10^{-13.6}$ atm for the crystallization of the Skaergaard rock, and these figures should be equally applicable to the lunar granophyre.

The chemical, mineralogical, and textural features of this rock strongly suggest that it represents the last liquid differentiate from the fractional crystallization of a large body of lunar basaltic magma (or possibly an initial product of partial melting). Its composition is similar to that of the high-silica glassy mesostasis of many of the Apollo 11 igneous rocks, described by Roedder and Weiblen (1970). It is also comparable with the light-colored, silica-rich parts of the unique rock 12013. Whether it was formed at or near the locale of the Apollo 12 landing, or whether it is an exotic fragment, possibly from a Copernicus ray, remains an open question.

This work has been supported by NASA Contract 9–8016.

TABLE 2.—*Fractionation of 0.5-g coarse fines from the rim of Bench Crater (12032, 46)*

Density	*Weight percent*	*Number of fragments*	
		Breccia	*Crystalline rocks*
2.70	8	11	1
2.70–2.90	33	43	3
2.90–3.10	44	58	6
3.10–3.32	12	5	12
3.32	3	—	4
Totals	100	117	26

TABLE 3.—*Analyses (microprobe) of minerals in hedenbergite granophyre (12032, 46–2)*

Constituent	*Microprobe Analyses (weight percent)*					
	*1**	*2**	*3**	*4**	*5**	*6**
SiO_2	65.4	57.0	99.72‡	48.8	29.8	72.0
TiO_2	—	—	—	0.75	0.21	0.1
Al_2O_3	18.6	26.8	0.28	0.45	0.04	11.1
Cr_2O_3	—	—	—	0.06	0.13	—
FeO	0.82	1.10	n.d.	28.0	67.8	5.3
MnO	n.d.	n.d.	n.d.	0.39	0.95	0.1
MgO	n.d.	n.d.	n.d.	1.55	1.22	0.2
CaO	0.31	8.74	n.d.	19.3	0.67	2.7
Na_2O	2.96	6.85	n.d.	0.10	n.d.	2.1
K_2O	11.6	0.15	—	—	—	5.8
SrO	n.d.	n.d.	—	—	—	—
BaO	1.21	n.d.	—	—	—	0.6
	100.9	100.6	(100.0)	99.4	100.8	100.0

n.d. = not detected (<0.05%).
* Column 1: Sanidine ($Or_{69}Ab_{28}Cn_2An_1$); 50%.
Column 2: Plagioclase feldspar ($Ab_{58}An_{41}Or_1$); 7%.
Column 3: Quartz; 30%.
Column 4: Hedenbergite ($Wo_{47}En_5Fs_{50}$); 10%.
Column 5: Fayalite (Fa_{95}); 3%.
Column 6: Bulk composition (calculated).
‡ Calculated by difference.

Literature Cited

Bence, A. E., J. J. Papike, and C. T. Prewitt
1970. Apollo 12 Clinopyroxenes: Chemical Trends. *Earth and Planetary Science Letters,* 8:393.

Lindsley, D. H., G. M. Brown, and I. D. Muir
1969. Conditions of the Ferrowollastonite-Ferrohedenbergite Inversion in the Skaergaard Intrusion, East Greenland. *Mineralogical Society of America Special Paper* 2:193.

LSPET (Lunar Sample Preliminary Examination Team)
1970. Preliminary Examination of Lunar Samples from Apollo 12. *Science,* 1967:1325.

Reed, G. W., and S. Jovanovich
1970. Halogens, Mercury, Lithium and Osmium in Apollo 11 Samples. *Geochimica et Cosmochimica Acta, Supplement* 1:1487.

Roedder, E., and P. W. Weiblen
1970. Lunar Petrology of Silicate Melt Inclusions, Apollo 11 Rocks. *Geochimica et Cosmochimica Acta, Supplement* 1:801.

E. P. Henderson,
R. D. Buchheit,
and J. L. McCall

Microhardness of a Lunar Iron Particle and High-Purity Iron Samples

Introduction

Lunar soil recovered by the Apollo 11 and 12 missions is continually being subjected to critical analyses and examinations by numerous scientists and engineers. A sample of the lunar soil, Sample 12032, 46–1 from the Apollo 12 mission which had been sieved to a particle size of about 3 mm, was received for studies by the Smithsonian Institution from the Manned Space Flight Center. During the studies, one particle of the lunar soil sample attracted attention because it was so strongly magnetic. Metallographic examinations showed the magnetic particle to be metallic iron possessing an unusually low microhardness. A comparison of the microhardness of this particle of metallic iron with the microhardness of high-purity iron samples is reported herein.

Examinations of Lunar Iron Particle

The particle of lunar soil which exhibited a strong magnetic attraction is shown in Figure 1 as a metallographic specimen etched in 1% Nital for about 20 seconds. Polishing was done using mechanical methods. The maximum diameter of the particle was about 2.3 mm. The microstructure of the particle consisted of a coarse-grained mass of iron (kamacite) with numerous nonmetallic inclusions concentrated in a peripheral zone. The dark inclusions are essentially olivine but some ilmenite is associated with the olivine.

The dark inclusion, left of center, Figure 1, which is surrounded with a swathing zone, is shown at higher magnification in Figure 2. The electron microprobe study of the inclusion showed that calcium and phosphorus are present in about the proportions in which they exist in apatite; since the surface of the black material was chipped, a satisfactory probe study was impossible.

A small metallic inclusion with a slightly different reflectivity than the metal was found along the interface of the swathing metal around the apatite (?) and the matrix. This grain was probed by Dr. K. F. J. Heinrich and Mr. Charles Fiori of the National Bureau of Standards who reported that although it has essentially the composition of the surrounding metal it probably contains a light element—carbon, boron or nitrogen—in amounts too small to be measured. On this evidence, we suspect that this inclusion is a carbide.

The average diameter of the metal grains in the lunar particle, determined by a lineal intercept method, was found to be about 0.25 mm. We observed no work hardening or other physical damage in the microstructure of this lunar iron.

Microhardness Determinations

The microhardness values obtained on this Apollo 12 sample were lower than the values normally reported

E. P. Henderson, Department of Mineral Sciences, Smithsonian Institution, Washington, D.C. 20560. R. D. Buchheit and J. L. McCall, Battelle Memorial Institute, Columbus Laboratories, Columbus, Ohio 43201.

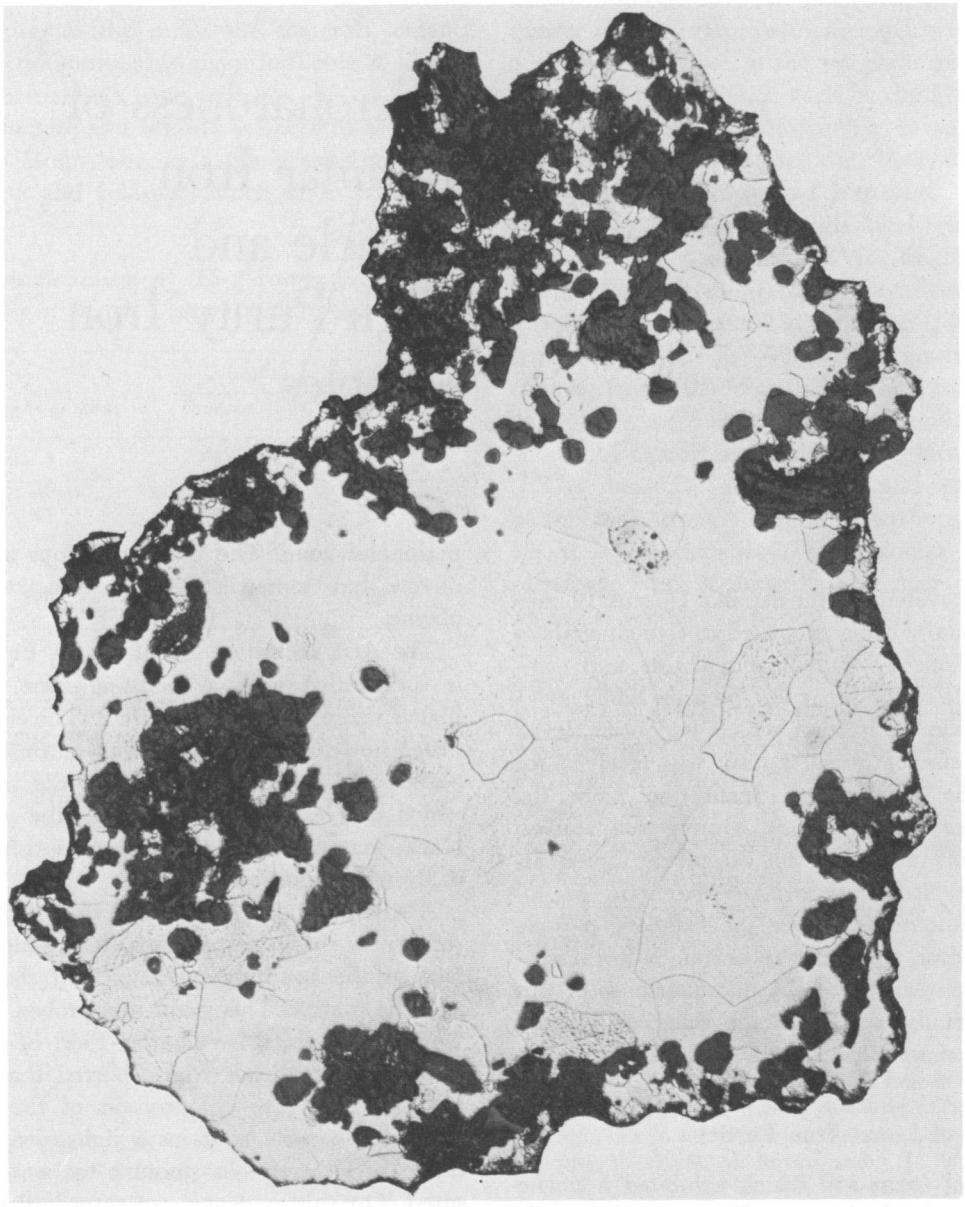

FIGURE 1.—Microstructure of lunar iron particle. Maximum dimension is 2.3 mm.

for commercially pure iron and much below the microhardness of kamacite in iron meteorites.

Recently E. P. Henderson found what is assumed to be kamacite grains in stony meteorites which are unusually soft. Some of these grains, when measured with the Vickers diamond indenter, using a 25-gram loan, gave a Vickers Hardness Number (V.H.N.) between 120 and 130. The study of these soft Ni-Fe grains in stony meteorite has not been completed.

The Vickers 136° diamond pyramid was chosen for all these microhardness measurements because it required a smaller area for a given load than the Knoop indenter and it generally provides more precise data than ball-type indenters (Lea 1936). The average value of the microhardness found with the weight loads given below are:

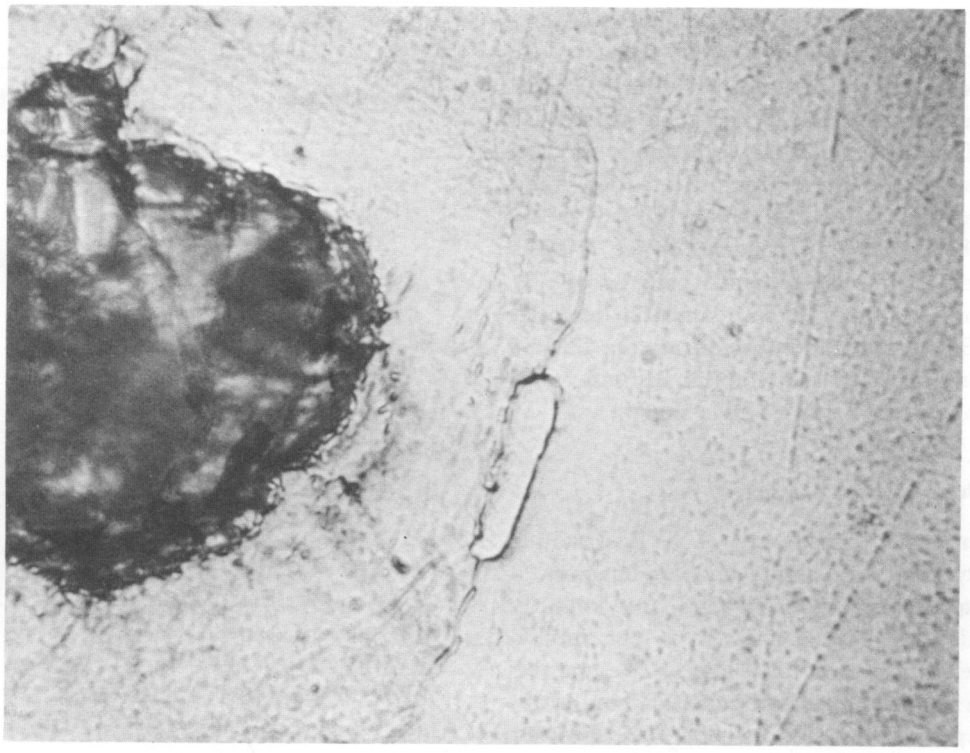

FIGURE 2.—The dark rough area at the left is tentatively identified as apatite. Along the interface of the apatite and metal there is some ilmenite. The metallic inclusion between the two metallic areas may be a carbide. Width of field is about 0.1 mm.

Weight load (grams)	*V.H.N.*	*Indentations*
25	80.6	3
50	78.6	8
100	72.6	8

Mr. T. B. Shives of the National Bureau of Standards measured the microhardness of the lunar particle using a 100-gram load and reported an average value of 69 V.H.N. Various loads were used for all these and other microhardness measurements reported in this paper because of the known variation in hardness number when low-load microhardness testing is performed (Small 1960; Lysaght and DeBellis 1969; Edmond 1958).

A recent study involving laboratory annealing of kamacite with 7% nickel for long periods of time, at temperatures of 300–700°C, showed the lowest microhardness attained was 153 Knoop Hardness Number, which is equivalent to about 140 V.H.N. (Staub and McCall, 1969).

It is widely accepted that the hardness of meteoritic iron (kamacite) is approximately proportional to the nickel content suggesting that the low hardness values obtained from the lunar iron particle could be a result of high purity, essentially fully annealed, iron. To check this out, electron microprobe analyses were made on the lunar iron particle and the microhardness of the lunar iron was compared with the microhardness of three different high-purity iron samples.

ELECTRON MICROPROBE ANALYSES

Electron microprobe analyses of the particle of lunar iron detected only iron and failed to detect the presence of Ni, Co, or P, elements generally found in meteoritic iron. The detectability limits of the electron microprobe analyser used were 0.1% for Co and 0.05% for Ni. No other analytical techniques were used on this particle because of its small size and the desire to preserve as much of it as possible.

Microhardness Determinations of High-Purity Iron Samples

A literature search for microhardness data for high-purity iron samples revealed a complete absence of useful data. Therefore, an effort was made to procure some samples of high-purity iron and to determine their microhardness for comparison with the microhardness of the lunar iron particle. Three samples of high-purity iron were obtained, one from the Edger C. Bain Laboratory for Fundamental Research of the U. S. Steel Corporation,[1] one from the Columbus Laboratories of Battelle Memorial Institute,[2] and the third sample from Lehigh University.[3]

Bain High-Purity Iron Sample

Details concerning the preparation of the Bain sample of high-purity iron were not available; however, a chemical analysis was reported and the impurity elements and their contents in parts per million (ppm) by weight are given in Table 1. The analyses for all of the impurity elements except carbon, nitrogen, and oxygen were determined by mass spectroscopy. The analyses of carbon and nitrogen were made by chemical determinations, and the analysis of oxygen was made by vacuum fusion. These analyses indicate the sample to be 99.985+ percent iron.

The Bain sample was mounted in Bakelite at a pressure of 5000 psi and a temperature of about 130°C. The mounted sample was ground and polished metallographically and etched for 30 seconds in 1% Nital. Subsequently, microhardness tests were made in several places on the polished and etched surface.

All of the microhardness indentations were made with a Vickers diamond microhardness tester attached to a Vickers metallograph. The microhardness determinations were performed by one operator over an interval of several days. Each day the balance pan on the microhardness tester was reset. In order to evaluate the uniformity of the microhardness values and their reproductibility in the Bain high-purity iron sample, four series of microhardness determinations were made. The first series consisted of four identations equally spaced along a straight line and made with a load of 50 grams. The second series was made near the first series and consisted of four rows of four indentations in each row. The indentations in the first and fourth rows were made with a 50-gram load, and the indentations in the second and third rows were made with a 25-gram load. The third series consisted of two rows of four indentations in each row made with a 100-gram load. The fourth and last series of microhardness determinations consisted of three rows of five indentations in each row made with a 25-gram load. The microhardness values obtained from each of the four series of determinations in the Bain high-purity iron sample are given in Table 2, and the average values are plotted versus load in Figure 3. Included in Figure 3 is a plot of the average Vickers microhardness values of the lunar iron.

TABLE 1.—*Impurity content of the Bain high-purity iron sample*

Impurity element	*Weight, ppm*
Carbon	11[a]
Nitrogen, N_2	7[a]
Oxygen	12[b]
Aluminum	0.2[c]
Calcium	2.1[c]
Chlorine	12.7[c]
Cobalt	15.7[c]
Chromium	8.4[c]
Copper	1.7[c]
Germanium	5.2[c]
Potassium	7.0[c]
Manganese	1.0[c]
Sodium	20.6[c]
Nitrogen, N	15.8[c]
Phosphorus	4.4[c]
Sulfur	0.6[c]

[a] Combustion analysis.
[b] Vacuum fusion analysis.
[c] Mass spectrographic analysis.

Battelle High-Purity Iron Sample

The Battelle high-purity iron sample was floating zone purified (Rengstorff 1968). The process of purification begins with commercially available iron, usually high-purity electrolytic iron. The starting material is electron-beam melted in a vacuum furnace and

[1] Courtesy of Dr. John Bromback.
[2] Courtesy of American Iron and Steel Institute.
[3] Courtesy of Dr. Joseph Goldstein.

TABLE 2.—*Vickers Microhardness Numbers for three high-purity iron samples and the Apollo 12 lunar iron particle and the total impurity content for the three high-purity iron samples*

Sample	Total impurities, ppm	Load grams							
		10	25	50	100	200	300	400	500
Battelle Iron	35–50	78.9 (70.5–83.8)	74.5 (73.7–75.5)	70.0 (69.0–71.2)	65.4 (64.7–66.3)	60.6 (58.5–62.4)	59.5 (57.2–60.9)	58.1 (56.3–61.3)	57.4 (55.5–60.0)
Lunar Iron ..	unknown	—	80.6 (78–85)	78.3 (74.2–82.5)	72.6 (70.7–74.5)	—	—	—	—
Bain Iron	124.4	—	81.9 (77.2–85.7)	78.3 (76.0–80.0)	77.9 (75.7–79.8)	—	—	—	—
Lehigh Iron	700.5	135.5 (122–159)	118.5 (109–131)	110.7 (106–116)	105.2 (100–112)	—	—	—	—

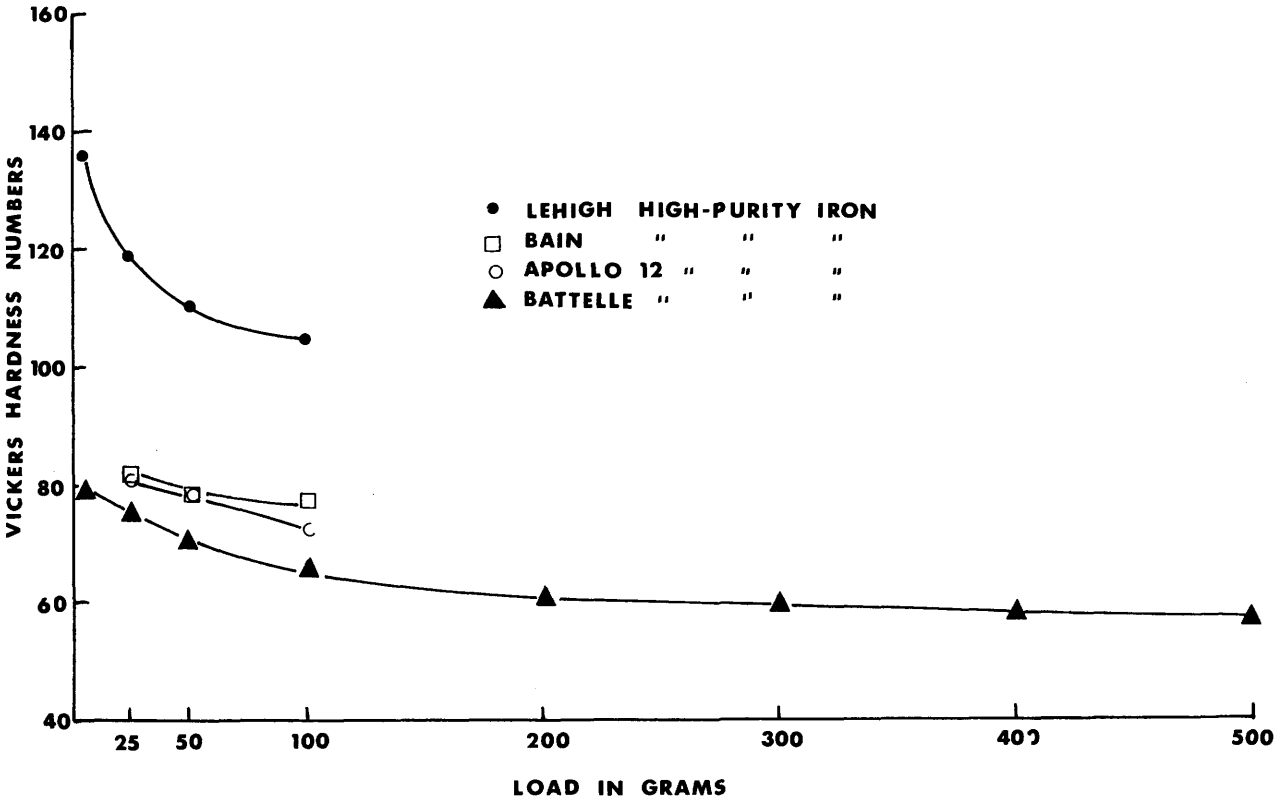

FIGURE 3.—Vickers microhardness number versus load for three high-purity iron samples and the Apollo 12 lunar iron particle.

cast into 1⅞-inch-diameter ingots. Four zone-melting passes of the electron-beam-melted ingots complete the purification process. No chemical analysis of the elemental impurity content was obtained for the particular sample made available, but the total impurity content was known to be 35–50 ppm by weight. This means the sample was 99.9950+ percent iron.

The Battelle sample was mounted in a room-temperature setting epoxy resin, ground and polished metallographically, and finally electropolished. Subsequently, microhardness determinations were made on the electropolished surface.

All of the microhardness determinations were made with a Vickers diamond indenter or an MO Tukon Microhardness Tester using loads of 10, 25, 50, 100, 200, 300, 400, and 500 grams. The various loads were used because of the previously shown variations of hardness reading with load. The microhardness indentations were placed in 11 rows of 6 indentations in each row. The spacing between rows and between adjacent indentations was approximately 4 mils for low load (50 grams and less) indentations and 8 mils for the heavier load indentations. Twelve microhardness determinations were made for each of the 10-, 25-, and 50-gram loads; six determinations were made for each of the 100-, 200-, 300-, 400-, and 500-gram loads. The microhardness indentations were measured with a filar micrometer eyepiece in conjunction with a 50× objective. The results of the microhardness survey on the Battelle high-purity iron sample are given in Table 2 and the average microhardness values versus load are plotted in Figure 3.

Lehigh Sample

The Lehigh sample, although regarded as high-purity iron, differed from the Bain and Battelle samples in that it consisted of a fine-grained microstructure containing many dark nonmetallic inclusions. The Lehigh iron was cast as a cylinder and then heat treated at 1000°C for 12 hours. The reported analysis of the Lehigh iron sample, shown in Table 3, indicates it to be 99.9+ percent iron. The sample was mounted in Bakelite and prepared metallographically for the microhardness measurements.

The microhardness measurements were made using loads of 10, 25, 50, and 100 grams by the same procedure described for the Battelle iron sample. The microhardness values obtained are given in Table 2, and the average values are plotted versus load in Figure 3.

Discussion of Results

The comparison, shown in Figure 3, of the microhardness of the lunar iron particle with the microhardness of three different high-purity iron samples indicates that the lunar particle also is high-purity iron. This indication is supported further by the electron microprobe analyses made on the lunar particle which revealed no detectable elements other than iron.

Table 3.—*Impurity content of the Lehigh iron sample*

Impurity element	*ppm*
Carbon	70[a]
Oxygen	200[b]
Nitrogen	10[b]
Hydrogen	<0.5[b]
Tungsten	<300[c]
Nickel	<40[c]
Al, Ba, B, Ca, Zr	<50[c]
Co, Cu, Ge, Mn, Mo, V	<20[c]
Cr, Pb, Mg, Si, Sn, Ti, Zn	<10[c]

[a] Combustion analysis.
[b] Vacuum fusion analysis.
[c] Emission spectrographic analysis.

The hardness of a material usually is affected by only three factors: the structure and grain orientation, the amount of strain (cold work), and the composition. The structures of the three high-purity iron samples, as well as the structure of the lunar iron particle, consisted of single-phase alpha iron (kamacite). The only difference among the structures which might affect hardness (O'Neill 1967) was the difference of grain sizes, but, since the grain sizes of all the samples were large enough to entirely contain a microhardness impression at all the loads used, this effect is not believed to be significant. Another factor known to affect hardness is the crystallographic orientation of the grains with respect to the plane on which the microhardness measurements are made. This effect is particularly significant for anisotropic materials, but has been shown to be relatively minor for isotropic materials such as alpha iron. Furthermore, the hardness measurements made on the samples in this study were found to be rather consistent from reading to reading (grain to grain) within each sample, indicating little or no orientation effect.

The amount of strain in a material very significantly affects hardness with the lowest hardness always being obtained for the condition of 0 percent strain, i.e., fully annealed. The three high-purity iron

samples were intentionally prepared in this condition and, in all cases, care was taken to metallographically prepare their surfaces such that no strain was introduced (Vitovec and Binder 1955). The only indication that the lunar iron particle was strain free, other than its low hardness, is its microstructure which revealed equiaxed grains with no "strain lines." Further confirmation of this probably would require a destructive technique of examination, such as transmission electron microscopy which was not permitted in this study.

Finally, the hardness of materials are affected by their compositions. This is well known for alloys and probably is the most important reason for alloying (strength is directly related to hardness (Lenhart 1955)). Less well known, however, is the effect of small amounts of impurity elements on the hardness of otherwise pure elements. Since the other contributing factors to hardness described above are believed to provide only minor effects on the materials in this study, it is believed that the present data (Figure 3) show only the effects of impurities on the hardness of pure iron. The three high-purity iron samples were found to have different impurity levels; the Battelle iron had about 35–50 ppm of impurities, the Bain sample had about 110 ppm of impurities, and the Lehigh sample had about 700 ppm of impurities. The microhardness data show that, for these samples, the microhardness increases with increasing impurity content.

Assuming that the microhardness of the three iron samples and the lunar iron particle is affected primarily by the impurity content, as discussed above, and that the effect is related only to the total impurity content and not to the content of selected impurities (perhaps a poor assumption since interstitial elements generally have a more pronounced influence on the hardness of iron than do substitutional elements), the close match between the microhardness of the lunar iron particle and the Bain sample suggests the total impurity content of the lunar iron sample is in the order of 100+ ppm. Unfortunately, the small size of the particle and the requirement not to destroy it prevented analyses for impurities to verify the correlation indicated between microhardness and the total impurity content.

Acknowledgments

We are indebted to Dr. K. F. J. Heinrich and Mr. Charles Fiori of the Bureau of Standards for the electron microprobe studies made on the small metallic inclusion, and also to Messrs. Grover C. Moreland and Harold Moore for mounting and preparing the polished surface we studied.

Literature Cited

Edmond, L.
1958. Vickers-Knoop Hardness Conversion. *Metals Progress,* 74(3):97.

Lea, F. C.
1936. *Hardness of Metals.* London: C. Griffin and Co.

Lenhart, R. E.
1955. The Relationship of Hardness Measurements to the Tensile and Compression Flow Curves. *Wright Air Development Center Technical Report,* 55: 114.

Lysaght, V. E., and A. DeBellis
1969. *Hardness Testing Handbook.* New York: American Chain and Cable Company.

O'Neill, H.
1967. *Hardness Measurements of Metals and Alloys.* 2nd edition. London: Chapman and Hall, 238 pages.

Rengstorff, G. W. P.
1968. Zone Purification and Analysis of Large Bars of Iron. *Memoires Scientifiques de la Revue de Metallurgie,* LXV:85–90.

Small, L.
1960. *Hardness, Theory and Practice.* Ferndale, Michigan: Service Diamond Tool Company.

Staub, R. E., and J. L. McCall
1969. Metallographic Studies of an Iron-Nickel Meteorite Following Long-Time Heat Treatments. *Proceedings of the International Metallographic Society Second Annual Meeting,* San Francisco, California.

Vitovec, F. H., and H. F. Binder
1955. The Effect of Surface Preparation and Condition on Microhardness. *Wright Air Development Center Technical Report,* 55:372.

PETROLOGY AND VOLCANOLOGY

William G. Melson,
Eugene Jarosewich,
George Switzer,
and Geoffrey Thompson

Basaltic Nuées Ardentes of the 1970 Eruption of Ulawun Volcano, New Britain

ABSTRACT

Ulawan volcano, New Britain, (5°02′40″S., 151°20′15″E.) erupted between January 9, 1970, and February 10, 1970, producing a small nuée ardente about 0405 hours local time, January 22, 1970. Ash eruptions of various intensities occurred throughout the episode, and a 5.6-kilometer-long lava flow was produced during the final phases. The main nuée ardente was essentially a hot avalanche of basaltic scoria which could not have emitted large volumes of gases during flow, but had the high mobility and marginal hot "hurricane" winds which characterise nuees ardentes. These features lend support to the experimental evidence of McTaggart (1956) that high temperatures alone can greatly increase the mobility of avalanching materials.

The chemical composition of the eruptives which produced the nuées ardentes and the lava flows are identical. The nuées ardentes evidently occurred when exteremely large volumes of scoria were disgorged at low ejection velocities, such that they fell back as coherent fragmental flows on the upper slopes, creating hot avalanches. The preferential direction of the main avalanche, down the Northwest Valley reflects the existence of a "notch," or low point in the crater wall, at the head of this valley.

The ejecta of the 1970 eruption are plagioclase phyric high-alumina basalts, which are compositionally like previous eruptive rocks. Three new analyses, petrographic features, and electron probe analyses are given. Of special interest are the compositions of glass inclusions in phenocrysts, which give evidence for the existence of high-alumina basaltic liquids, and may indicate mixing of basaltic and dacitic magmas prior to eruptions.

This eruption of Ulawun was a comparatively small one. The combined volume of the nuée ardente deposits and lava flows probably are between 0.002 and 0.010 cubic kilometers. The area devastated by the nuées ardentes is about 2 square kilometers—a small area compared to most historic nuées ardentes.

William G. Melson, Eugene Jarosewich, and George Switzer, Department of Mineral Sciences, National Museum of Natural History, Smithsonian Institution, Washington, D.C. 20560. Geoffrey Thompson, Woods Hole Oceanographic Institution, Woods Hole, Massachusetts 02543. (Mr. Jarosewich made the chemical analyses; Dr. Switzer, the electron probe analyses; and Dr. Thompson, the trace element analyses.)

Introduction

Ulawun volcano, New Britain, had an eruption early in 1970. First reports to the Smithsonian Center for Short-Lived Phenomena indicated that a well-developed nuée ardente (glowing-cloud eruption) had been produced on January 22, 1970. This led to a field study of the eruption as part of an ongoing project on the classification, properties, and origin of nuées ardentes. Two other nuée-ardente-producing eruptions were recently studied as part of this project (1968 eruption of Mayon volcano, Phillippines, see Moore and Melson 1969; 1968 eruption of Arenal

volcano, Costa Rica, see Melson and Saenz 1968). This is an interim report dealing briefly with the results of the field observations at Ulawun volcano, and of the laboratory studies of the samples from the nuée ardente deposits and from an associated lava flow.

Mr. R. Citron and the writer were at the volcano from February 7 to 14, 1970. In addition to the results reported here, extensive still photography and 16-mm cinematography were obtained by Mr. Citron. We had hoped to use cinematography to get quantitative information on the velocity and other features of nuées ardentes, but we arrived too late. Nonethless, extensive photographic coverage was obtained of the nuées ardentes deposits and the surrounding devastated zone. The still photographs (35-mm slides) and motion pictures are now on deposit at the Smithsonian Institution.

We were accompanied throughout the field investigations by R. A. Davies, and part of the time by G. A. M. Taylor and David Palfreyman, of the Rabaul Volcanological Observatory, an organization which is maintained by the Administration of the Territory of Papua, New Guinea, and draws its professional staff from the Australian Bureau of Mineral Resources, Geology, and Geophysics. We acknowledge the kind assistance and free exchange of information given by these gentlemen. R. A. Davies (1970 and 1971) has discussed this eruption, and R. W. Johnson (1970a) has described the volcano and its petrology prior to the 1970 eruption. Further publications on this eruption are contemplated by Davies, who reached the scene of the eruption almost at its inception, and remained at hand until its termination.

Nuées Ardentes

Nuées ardentes ("glowing-cloud eruptions") have received much attention because of their incredible destructive potential, as demonstrated by the obliteration of St. Pierre, Martinique, and its 30,000 inhabitants by a nuée ardente from Mount Pelée, an eruption described in the classic work on nuées ardentes by A. Lacroix (1904). Since that time, numerous other nuées ardentes have been described, and much has been written about their mechanism of flow. One of the most recent reviews is by McTaggart (1960).

Nuées ardentes are defined somewhat differently by different authors, but perhaps the following definition is acceptable to most; it is the one used in this report:

A nuée ardente is a type of volcanic eruption involving two components: (1) a hot, normally but not always incandescent, highly mobile avalanche composed of either essential or accidental material or a combination of the two, and (2) a hot envelope of gases and ash, which is derived from the avalanche but includes much heated air, which expands vertically in billowing, ash-laden clouds, and also travels laterally, predominantly parallel and extending beyond the sides of the avalanche, and may extend very far beyond the final terminus of the avalanche; these lateral, ground-following ash and gas clouds can attain "hurricane" velocities, on the order of 100 mph, and are responsible for most of the loss of life and extensive damage associated with historic nuées ardentes.

Ulawun Volcano: Background Information

The following summary is drawn largely from Johnson (1970a), who gives an account of the morphology, geology, and petrology of Ulawun prior to its 1970 eruption, and gives a schematic topographic map. Johnson (1970b) also has reviewed the relationship between lava composition, volcano position, and the Benioff zone beneath New Britain. Ulawun (The Father) is a symmetrical stratovolcano on the north coast of central New Britain which rises from a base at sea level to 2,300 meters. It has a pronounced summit crater about 300 meters wide and up to 130 meters deep, with notches which feed into the major valleys, of which the Northwestern Valley (Figure 1) was the course of the 1970 nuée ardente. This Northwestern Valley is a pronounced "scar" on the mainly smooth cone (Figure 1), and appears to have been eroded by hot avalanches as well as by normal erosive processes.

A pronounced older, deeply eroded, volcanic edific trends roughly east-west along the south side of the volcano (Figure 1), and is marked by a 160-meter-high escarpment, which may be the remains of a caldera or linear graben.

Eruptions of Ulawun appear to be characterized by a mixture of strombolian and vulcanian eruptions. Lava flows typically occur, and move as thin ribbons down one or more valleys. These flows are interlayered with the volcanic fragmental debris, mainly

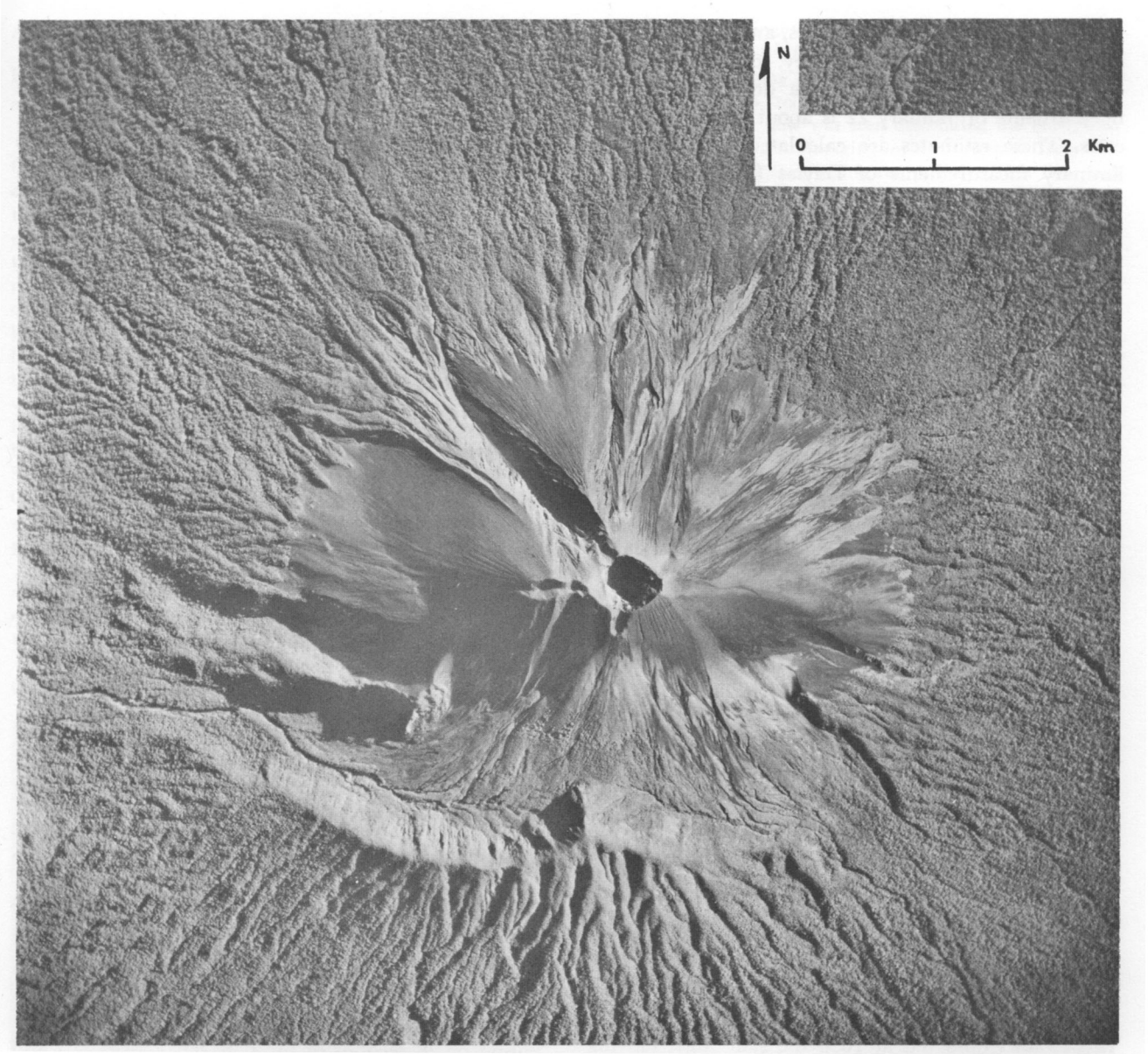

FIGURE 1.—Vertical aerial photograph of Ulawun volcano, New Britain, taken June 17, 1948.

scoria, and buttress the volcano with an interleaved framework emanating from the summit. The relative proportion of fragmental deposits and coherent flows is unknown, but they are perhaps on the order of 1:1.

Observations of the 1970 eruption show that nuées ardentes at Ulawun are of the avalanche type (St. Vincent type, or d'explosion vulcanienne type of Lacroix, 1904), and occur when the volcano disgorges large quantities of fragmental debris at low ejection velocities, such that large quantities fall immediately back on the slopes, coalescing to form hot avalanches.

Table 1 summarizes some of the principal features of Ulawun volcano.

Summary of the 1970 Eruption

The eruption was a brief one (about 32 days) and, in terms of total volumes of ejecta, was not a major eruption. Based on preliminary measurements, the hot avalanche and associated marginal ash deposits

total about 0.005 cubic kilometers, and the main lava flow, that in the Southwest Valley, totals about 0.003 cubic kilometers. The total area devastated by the nuée ardente of January 22 is about 2 square kilometers. These estimates are calculated from the preliminary measurements of Davies (1970). No estimate can yet be made of the volume of airfall ash.

The area devastated by the nuée ardente is extremely small compared to the destruction caused a major nuée ardente, such as that of January 21, 1951, at Mount Lamington, which ravaged over 200 square kilometers (Taylor 1958).

TABLE 1.—*Summary of features of Ulawun volcano, mainly from Johnson (1970a) and Fisher (1957)*

SYNONYMS: Ulawon, Uluwun, The Father

TYPE: Stratovolcano

LOCATION: New Britain, Territory of New Guinea and Papua; opposite Lolobau Island (also an active volcano), and 16 kilometers west of Bamus, an older dissected stratovolcano.

COORDINATES: 5°02′40″S., 151°20′15″E.

HEIGHT ABOVE SEA LEVEL: 2,300 meters, which slopes down to sea level; height above adjacent sea floor 3,000 meters.

PREVIOUS ERUPTIONS: A number of mildly explosive events were recorded between 1915 and 1967, the most violent of these were in April 1915, and January 1967. No lava flows or nuées ardentes were reported during these eruptions. The initial explosions seem to have been most violent, and were followed by less violent eruptions for several months. Zones of ash deposition are dependent on wind directions, which have ranged widely on the different times of eruption.

PETROLOGY: Mainly porphyritic basic lavas, with plagioclase as dominant phenocryst, although a few percent of pyroxene and olivine phenocrysts occur in most. Chemically, these lavas are basalts, which are tholeiitic, i.e., they have low total alkalies. High alumina content (17–19%) is a characteristic feature. Johnson (1970a) gives 4 chemical analyses, and 32 modal analyses of Ulawun rocks.

Davies (1970) has broken the eruption of Ulawun into three overlapping phases:

1. **January 9–14, 1970.** Quiet vapor and ash emission, white to grey vapor, occasional ejections of ash, no audible activity.

2. **January 15–27, 1970.** Audible explosions; climactic explosion at 0405 local time, on January 22, 1970. Flows observed at 1650 the same day, moving down Northwest Valley.

3. **January 27–February 10, 1970.** Quiet, effusive phase, characterized by the major aa lava flow which moved down the Southwest Valley. Activity slowly declined, until February 10, 1970, when the main flow ceased moving, and vapor-phase activity continued to decline.

A number of vents were active during the eruption, all located circumferentially to the summit crater. The elevation of Ulawun grew through cone building during the eruption, starting at about 2,250 meters high, and ending at about 2,340 meters high.

GEOPHYSICAL CHANGES ASSOCIATED WITH THE EMISSION OF THE NUÉES ARDENTES

Davies (1970) also reports the changes in tilt and seismicity associated with the major explosive activity of January 22, 1970. Tiltmeter readings of the tangential component indicate a high in the inflation of the volcano prior to this event, and a rapid deflation of 28 seconds of arc between February 5 and 8, 1970. Continuous harmonic tremor characterized the seismicity. Impulsive tremors were not noted. Ground motion increased steadily from January 16, 1970, when measurements began, and reached a peak in excess of 25 microns during the night of January 21–22, 1970, which coincided with the first eruption of a nuée ardente. Ground motion decreased after that, although significant peaks were recorded on the afternoon of January 25 and the night of January 27, 1970, the latter coinciding with the production of three nuées ardentes, and the beginning of the quiet effusive phase.

Account of the Major Nuee Ardente

Davies (1970), who was near the volcano, gives this account of the event:

A "major" eruption from the northwest vent occurred at 0405 hours LT. The eruption, of Pelean type, was not preceded by any abnormal audible activity and explosive ejections of lava fragments and ash were observed prior to the eruption. Dense ash-laden vapour clouds accumulated above the summit, successive emissions gradually enveloping the northwest vent. An eye witness described how some 40 seconds later, abundant spots of light could be seen on the lower northwestern slopes. This can be ascribed to the avalanche (ash-flow) component of the nuée emerging from the Northwest Valley. Incandescent blocks and igniting vegetation marked the path of the nuée down into the forested region. The dark ash cloud component, which had blanketed the northwestern slopes, expanded rapidly to above 3,000 meters within 10 minutes. Between 0412 hours and 0432 hours an electric storm raged within the ash cloud and at 0430 hours a light shower of accretionary lapilli (mud pellets) and rain fell on the Mission.

Aerial inspection at 0700 hours (LT) revealed an area of almost total devastation 2.4 kilometers long and 0.8 kilometers wide, extending down through the forested region on the lower northwestern flanks of the volcano.

The northwest and northeast vents were continually active throughout the day, with little response from the southwest vent. Ash-laden vapour emission was again voluminous, dense clouds rising to over 5,000 meters. Cumulus cloud, together with smoke haze rising from burning vegetation marginal to the devastated area, rendered observation difficult. At 1650 hours (LT) a lava flow was seen descending the Northwest Valley, formed by the merging of two streams from the northeast and northwest vents, respectively. This flow was probably initiated during the early morning and by 1800 hours it had reached an altitude of 1,000 meters above sea level.

During the night all four vents were active, the lava temperature on emission being estimated at 1000–1100°C (by comparison with temperature-colour charts). Occasionally explosive ejections from two or more vents were synchronised, the more rhythmic ejections from the northeast and northwest vents littering the upper slopes with great volumes of incandescent blocks. Pulses of lava were frequently expelled from the north and northwest vents, the incandescent fronts surging down into the Northwest Valley. Audible explosions, which had persisted at irregular intervals throughout the day, increased in intensity during the night.

Observations on the Devastated Zone and Hot Avalanche Deposits

There was insufficient time during our field work to prepare a detailed account of our observations on the

FIGURE 2.—Hot avalanche (light gray deposit in middle of photograph) filling lower portion of Northwest Valley, February 7, 1970. Low altitude, oblique aerial photography.

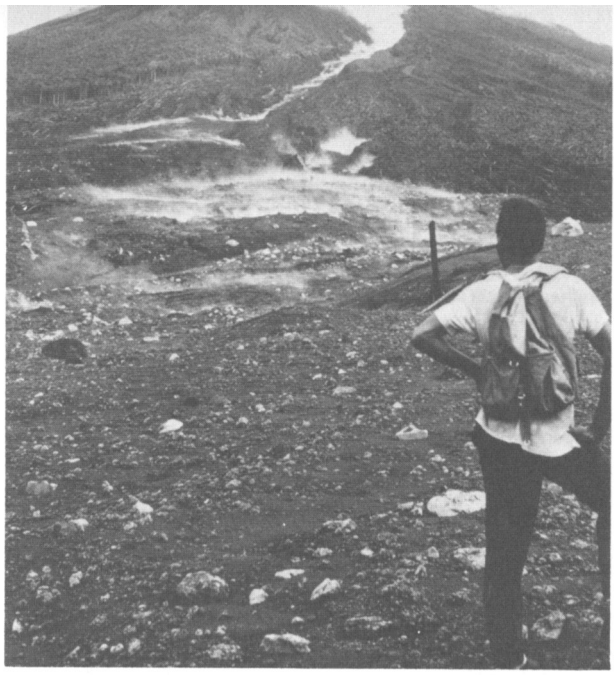

FIGURE 3.—Hot avalanche deposits in Northwest Valley, looking southeast toward Ulawun, at an elevation of about 500 meters. February 10, 1970.

devastated zone and hot avalanche deposits, or to refine our initial observations. Some of these observations, recorded in a field journal immediately after our first entry into the devastated zone, follow. Figures 2–12, all taken by Mr. R. Citron, illustrate some features of the devastated zone and the hot avalanche deposits.

We reached the devastated zone on February 7, 1970, some 16 days after the major nuée ardente had occurred. To reach the zone, we travelled south from a point near the airstrip, which is north of Ulawun and on the coast, through heavy rain forest along a gradually rising stream course, which, at an altitude of 450 meters, intersected the devastated zone. The first evidence of nearing the devastation was the smell of smoldering wood and evidence of a clearing of the rain forest ahead. The first damage we found was yellowed, withered vegetation. This withering became ubiquitous within ten to a few tens of feet after these first, irregularly distributed signs, and gave way to a totally devastated zone, where all trees had been either uprooted or snapped off a short distance up their trunks. Uprooted trees were aligned pointing down slope, that is, away from the

FIGURE 4.—Water vapor rising from the hot avalanche deposits after a rainstorm, February 8, 1970.

volcano. These fallen trees included eucalyptus trees which were up to 150 feet long. We noted very little ash in this zone, although a thin veneer, less than a centimeter thick, was present in places on the ground.

We traversed this zone of felled trees with difficulty, moving southwest so as to intersect the avalanche itself. After about 300 to 400 meters, we reached a blackened, ash-covered zone, where trees were slightly charcoalized on the side facing the volcano, and where some, those that had been ignited at the time of the avalanche, were still smoldering. This zone was a few hundred feet wide, and was confined to the margin of the channel down which the hot avalanche had traveled.

Remarkably, a small number of tree trunks were still standing near the margin but within the avalanche deposits, although their tops had been snapped off and carried away. These trees were smoldering from the portion buried in the avalanche deposits and, where their bases had been burned through, had collapsed.

Smoke rose from buried, smoldering wood in the ash flow, and there were small, only weakly active fumeroles. The avalanche here appeared to be several hundred feet wide, and was composed largely of dark grey, to black, sometimes red, scoriaceous basaltic bombs in a matrix of coarse ash, mainly composed of seriate fragments derived from the shattering and breaking up of the bombs during the avalanche. The bombs commonly had a knobby, "puffed-up" appearance, and typically their interiors were more vesicular than the outer portions, as if the outer vesicles had been flattened and compressed by pounding with other bombs and blocks during the avalanche. The "puffed-out" appearance suggests that expansion and gas release continued during the avalanche, and that the bombs were in a thick, pasty state during their ejection and subsequent avalanching. The bombs ranged widely in size, from large, up to five feet wide, on down to a few inches across.

Less abundant, but still conspicuous components, were angular light-colored, apparently holocrystalline medium-grained fragments, ranging up to large blocks, a few feet across. These appear to be accidental inclusions, perhaps from the plug and walls of the vent.

Subsequent field work gave a better overall view of the avalanche deposits. From place to place, the deposits range widely in the amount of coarse (e.g., greater than 6-inch maximum diameter) and the amount of fine clasts. There is no evidence of sorting in some places, whereas elsewhere there are areas,

FIGURE 5.—Hummucky topography of the avalanche near terminus. Direction of "flow" from left to right, and about parallel to the direction indicated by the alignment of fallen trees in the background. At an elevation of about 500 meters, February 8, 1970.

TABLE 2.—*Analyses of some 1970 eruptives of Ulawun volcano* (Chemical analyses by E. Jarosewich; trace element analyses by G. Thompson)

Constituent	*Chemical analyses (weight percent)*		
	*1**	*2**	*3**
SiO_2	52.77	52.62	51.51
Al_2O_3	18.00	18.31	18.96
Fe_2O_3	2.99	3.23	2.72
FeO	7.14	6.81	7.50
MgO	4.98	4.94	4.92
CaO	10.48	10.45	11.14
Na_2O	2.29	2.40	2.24
K_2O	0.37	0.40	0.32
H_2O+	<0.1	<0.1	<0.1
H_2O-	0.01	0.01	0.03
TiO_2	0.96	0.96	0.79
P_2O_5	0.08	0.08	0.07
MnO	0.14	0.14	0.16
Totals	100.21	100.35	100.36
	CIPW Norms		
Q	7.10	6.60	4.50
OR	2.19	2.36	1.89
AB	19.38	20.31	18.96
AN	37.74	38.01	40.74
DI	11.25	10.88	11.59
HY	16.20	15.49	17.06
MT	4.34	4.68	3.94
IL	1.82	1.82	1.50
AP	.19	0.19	.16
Fe/Mg	.36	.34	.40
	Trace element analyses (parts per million)		
B	30	28	15
Ba	100	110	75
Co	40	40	38
Cr	30	35	35
Cu	160	110	90
Ga	20	18	18
Li	10	8	7
Ni	21	23	22
Sr	350	300	280
V	300	300	300
Y	25	24	22
Zn	180	190	190
Zr	25	28	20

* Column *1:* Scoriaceous basalt bomb from 1,600 feet level of main avalanche produced by nuée ardente of January 22, 1970. Sample number USNM 112480.

TABLE 3.—*Comparison of the 1970 Ulawun ejecta, represented by the analysis of the scoria (Table 2) in column 1, with an average oceanic deep-sea basalt in column 2 (Melson et al. 1968), and overall average basalt and andesite (Taylor and White 1966) in columns 3, and 4 respectively*

Constituent	*Chemical analyses (weight percent)*			
	1	*2*	*3*	*4*
SiO_2	52.77	49.21	48.9	59.5
Al_2O_3	18.00	15.81	15.7	17.2
Fe_2O_3	2.99	2.21	—	—
FeO	7.14	7.19	10.7	6.10
MgO	4.98	8.53	8.70	3.42
CaO	10.48	11.14	10.8	7.03
Na_2O	2.29	2.71	2.32	3.68
K_2O	0.37	0.26	1.02	1.60
TiO_2	0.96	1.39	1.82	.70
P_2O_5	0.08			
MnO	0.14			
	Trace element analyses (parts per million)			
B	30	7	5	10
Ba	100	12	250	270
Co	40	32	48	24
Cr	30	296	200	56
Cu	160	87	100	54
Ga	20	18	12	16
Li	10	8	10	10
Ni	21	123	150	18
Sr	350	123	465	385
V	300	289	250	175
Y	25	43	25	21
Zn	180	122	—	—
Zr	25	100	110	110

some almost dune-shaped with their long axis in places perpendicular and in other places parallel to the direction of flow, which appear to be well sorted, consisting mainly of coarse—sand-sized fragments.

Typically, the deposits were estimated to be about 30 feet thick, although there was no way to accu-

Column *2:* Massive basalt from lava flow of 1970 eruption. Collected from terminus of slowly moving flow on February 8, 1970, at elevation of 1,450 feet along the upper dry course of the Matisibu River, the Southwest Valley of Ulawun volcano. Sample number USNM 112481.

Column *3:* Light-gray holocrystalline basalt xenolith from main avalanche deposit at 1,600 foot level of the Northwest Valley. Sample number USNM 112482.

rately measure this thickness. The deposits do not thin noticeably toward the terminus, but rather thin abruptly, in a distance of a few hundred feet, ending in a chaotic mélange of large blocks, bombs, and partly shattered and charcoalized tree trunks, with perhaps about 60 to 70 percent of finer material. To a first approximation, the deposits show no great range in thickness from their point of first "heavy" deposition, near the base of the northwest "shoot," to their terminus, another kilometer or so away.

The overlaying hot-ash "hurricane" proceeded beyond the terminus of the avalanche, withering vegetation up to 300 meters further down the "avalanche" course. Beyond the avalanche terminus, the dry, flattish stream bed curved gently. The totally withered zone gave way to zones where the withering alternates from one side, at one curve, to the other side, at the next curve, as if the "blast" became narrow, and ricocheted at each turn.

Composition of the Eruptives

Here, we search for significant chemical differences between the melts which produced the nuée ardente and those that produced the lava flow. We also selected a sample of a common variety of xenolith in the main nuée ardente avalanche deposit, which, in the field, appeared to be quite different from the essential ejecta.

Table 2 shows that all these eruptives are chemically basalts (between 45 and 55 percent silica), that they are slightly quartz normative (4.5 to 7.1 percent), and that they are remarkably similar to one another, even in their trace element compositions. The slightly higher ferric/ferrous iron ratio in the flow compared to the bomb is an expected consequence of the longer high-temperature exposure of the flow to the atmosphere. The very slightly lower contents of B, Ba, Sr, and Zr in the xenolith com-

FIGURE 6.—Felled trees, uprooted, or snapped off, during nuée ardente of January 22, 1970. Northeastern side of avalanche channel at about 400 meters elevation. Photograph taken February 8, 1970. Vapor from steaming avalanche deposits in foreground.

TABLE 4.—*Comparison of the 1970 eruptives (columns 1 and 2) with those of earlier eruptions (columns 3–6) compiled by Johnson (1970a)*

Constituent	Chemical analyses (weight percent)					
	1*	2	3	4	5	6
SiO_2	52.77	52.62	51.1	52.47	52.10	51.79
Al_2O_3	18.00	18.31	17.5	19.16	16.78	18.06
Fe_2O_3	2.99	3.23	4.30	3.40	3.07	2.51
FeO	7.14	6.81	6.35	5.82	7.32	7.25
MgO	4.98	4.94	5.85	4.90	6.52	5.85
CaO	10.48	10.45	10.8	10.76	10.84	10.98
Na_2O	2.29	2.40	2.40	2.45	2.19	2.19
K_2O	0.37	0.40	0.30	0.32	0.32	0.32
H_2O+	0.1	0.1	0.07	0.14	0.08	0.17
H_2O-	0.01	0.01	0.23	0.03	0.03	0.06
TiO_2	0.96	0.96	0.92	0.75	0.75	0.74
P_2O_5	0.08	0.08	0.07	0.09	0.09	0.09
MnO	0.14	0.14	0.13	0.17	0.19	0.17
	100.21	100.35	100.15	100.51	100.39	100.26

* Column *1:* Basaltic bomb, from hot avalanche deposits, 1970 eruptions. E. Jarosewich, analyst.

Column *2:* Lava flow, sampled at terminus, 1970 eruption. E. Jarosewich, analyst.

Column *3:* Ash, 1967 eruption, deposited on Lolobau Island (Jorgensen, analyst, in Johnson, 1970a).

Columns *4–6:* A.J.R. White, analyst, in Johnson (1970a).

Columns *4* and *5:* Prehistoric flows and a sill.

Column *6:* Bomb from southwestern slope.

pared to the essential ejecta are also small but noteworthy features of the analyses.

The Ulawun rocks have high alumina contents compared to most basalts. This is reflected modally by the abundance of plagioclase. Other differences with "average" basalts are brought out in Table 3, and include higher boron, and lower nickel, chromium, and zirconium.

The trace element abundances show both basaltic and andesitic affinities (Table 3). The very low nickel and chromium contents are close to the values for andesites, and low compared to most basalts. On the other hand, the cobalt and vanadium contents are close to those of basalts. The zirconium is anomalously low, and the copper, vanadium, boron, and zinc are anomalously high compared to both average basalts and average andesites. Gallium, yttrium, and lithium show little differences between the Ulawun samples, and the average basalts and andesite.

The Ulawun samples have low sodium contents compared to deep-sea basalts and to most island and continental basalts, and their potassium content, although higher than most deep-sea basalts, is lower than most island and continental basalts. The iron/magnesia ratio is higher, and the total iron is close to and magnesia is less than the average basalts.

Table 3 indicates that the Ulawun basalts cannot be related to either of the average basalts by a simple near-surface (low pressure) fractionation scheme. If we regard the average basalts as parents, we see that separation of some olivine and chromite would account for the lower Mg, Ni, and Cr, and higher Si of the Ulawun samples compared to these hypothetical parents. However, the low Na and Zr content of the Ulawun basalts is inconsistent with such near-surface olivine fractionation of these hypothetical parents.

The recent and prehistoric eruptives of Ulawun are of relatively uniform composition (Table 4). All are

TABLE 5.—*Hand-specimen and petrographic description of the analyzed basalts from the 1970 eruption of Ulawun Volcano. Mineral abundances in volume percent*

Bomb	*Flow*	*Xenolith*
	STRUCTURE (hand-specimen description)	
Black, highly vesicular, nubby, "puffed-out" outer portion; more vesicular in interior than on surface. Black to reddish oxidized glass on surfaces.	Dense; black; scattered irregular cavities; porphyritic.	Light gray; porphyritic; lacks significant pore space. Modal analysis (volume %): Plagioclase phenocrysts: 36.2; Plagioclase microlites: 21.4; Pyroxene (total): 29.3; Olivine: 2.0; Oxides: 2.7; Silica (cristobalite): 1.5; Interstitial glass and unresolvable material: 5.9; Pores: 1.0.
	GROUNDMASS	
Clear glass, plus microlites and quench crystals of plagioclase and pyroxene.	Brownish glass, with microlites of plagioclase, pyroxene and opaque(s).	Mainly crystalline, with about 40 percent pyroxene, 50 percent plagioclase, and a few percent oxide, and possibly clear interstitial glass.
	PHENOCRYSTS	
Plagioclase (1–5 mm; about 35% volume percent); olivine (mainly small, 1–2 mm across; less than 5 volume percent), rare rounded phenocrysts of clinopyroxene, and still rarer grains of hypersthene.	Plagioclase (1–5 mm across) about 35 volume percent; rounded olivine grains (mainly small, 1–2 mm, but some up to 7 mm across; less than 5%); rare rounded phenocrysts of clinopyroxene, and still rarer grains of hypersthene.	Plagioclase (1–5 mm; about 35 volume percent); olivine (small, 1–2 mm across; less than 5 percent), pyroxene (dark green clinopyroxene, a few large and rounded, up to 8 mm long).

high-alumina, quartz-normative basalts, with relatively low total alkali contents, and K_2O contents between 0.30 and 0.40 percent. Johnson (1970a) notes that they are comparable in chemistry and mineralogy to alumina-rich rocks with abundant plagioclase phenocrysts from various parts of Japan.

Mineralogy and Petrography

The three samples selected for chemical, electron microprobe, and petrographic analyses are all basalts, and all are porphyritic, with up to 40-volume-percent phenocrysts (crystals greater than about 0.5 mm in maximum dimension). The dominant phenocryst is plagioclase, which composes about 35-volume percent. These have highly calcic cores (bytownite, An_{85}, to anorthite, An_{90}) with weak zoning to An_{80} at their rims. In volume, there are less than 5 percent large, normally rounded pyroxene and olivine grains, which may be partially resorbed phenocrysts. Olivine occurs in all the samples, and is around Fo_{74}. No complete analyses were made of the opaques, but they appear to be mainly homogeneous titanmagnetite with about 17 percent TiO_2. Table 5 compares the hand speci-

TABLE 6.—*Pyroxene analyses via electron microprobe. George Switzer, analyst. First three pairs (1–2, 3–4, 5–6) are from the rims and cores of a single phenocryst in each of the three analyzed samples in Table 2, the basaltic bomb, the flow, and xenolith, respectively. The final analysis (Column 7), is of a pigeonite microlite in the groundmass of the basaltic xenolith*

Constituent	*Electron microprobe analyses (weight percent)*						
	Bomb		*Flow*			*Xenolith*	
	1	*2*	*3*	*4*	*5*	*6*	*7*
SiO_2	51.5	51.4	53.2	52.8	52.5	52.7	52.6
TiO_2	0.4	0.4	0.5	0.5	0.4	0.4	0.3
Al_2O_3	2.3	2.5	3.2	3.3	3.5	3.4	1.0
Fe	7.4	8.4	6.6	8.0	7.8	7.8	19.9
MnO	0.2	0.2	0.2	0.2	0.2	0.3	0.4
MgO	17.2	17.3	16.7	15.2	15.6	17.0	16.9
CaO	20.6	19.3	19.5	19.0	20.0	18.8	6.3
Na_2O	0.2	0.2	0.2	0.2	0.2	0.2	0.2
K_2O	0.05	0.05	0.05	0.05	—	—	—
	Molar ratios (mole percent)						
Fe	14.4	16.3	13.4	16.7	15.8	15.6	40.1
Mg	46.1	46.5	47.0	43.9	43.7	47.0	47.2
Ca	39.5	37.2	39.6	39.4	40.4	37.4	12.6

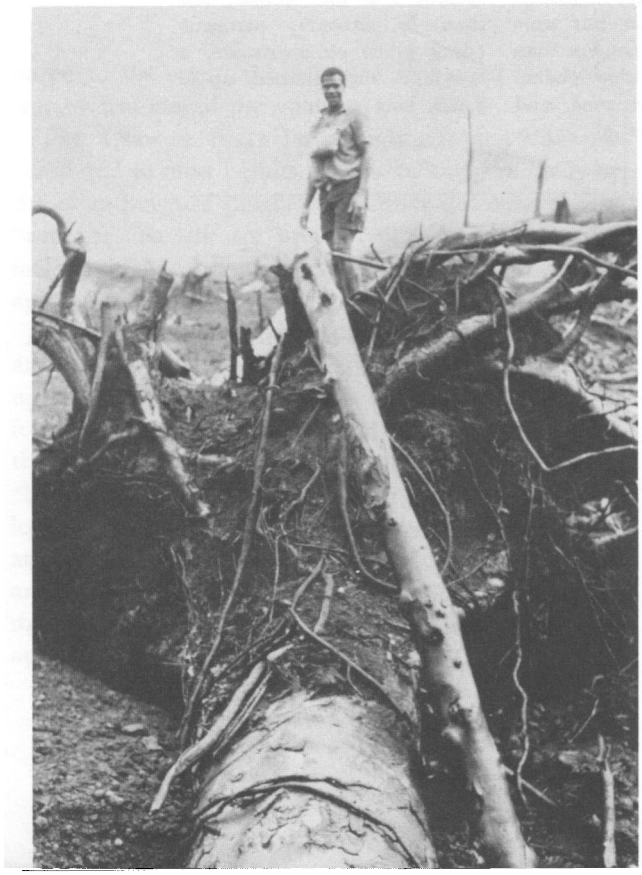

FIGURE 7.—Uprooted trunk of eucalyptus tree. Northeastern margin of avalanche channel. Note abrasion of trunk. February 10, 1970.

men and petrographic features in the three analyzed samples, and Figures 13 and 14 give comparisons of petrographic features.

The pyroxene phenocrysts are typically augite in all three samples (Table 6). Rarely, hypersthene phenocrysts occur, and intermediate pigeonite microlites (analysis 7, Table 6) were found in the matrix granules of the only holocrystalline basalt examined—the basaltic xenolith. Analyses of the rim and core of one augite phenocryst was made in each of the three samples (Table 6, analyses 1–6). These show that there is slight inverse zoning in the flow and bomb augites. The cores are slightly higher in Fe and lower in Ca than the rims.

The 1970 eruptives are petrographically similar to those of earlier eruptions described by Johnson

FIGURE 8.—Felled and snapped-off tree trunks near terminus devastated zone. Avalanche deposits to right (note vapor); looking northwest (downslope). Unaffected trees in background. February 8, 1970.

(1970a), except he reports that pigeonite phenocrysts are commonly present, although in small amounts. Johnson (1970a) gives more detailed descriptions of reactions between phenocrysts and liquids than given here, including oxidation and resorption of the olivine phenocrysts.

COMPOSITION OF GLASS INCLUSIONS IN PHENOCRYSTS: EVIDENCE FOR HIGH-ALUMINA BASALTIC LIQUIDS AND OF MIXED MAGMAS

Some of the phenocrysts and large rounded grains contain inclusions of clear to light brown glass (Figure 14). Electron probe analyses of some of these glass inclusions are in Table 7. The glass (analysis 3, Table 7) in a rounded olivine crystal in the analysed basaltic bomb is quite close to the bulk composition of the bomb, and suggests that this bulk analysis is in fact representative of a liquid composition of a high alumina basalt. In other words, the phenocrysts grew from a high alumina basaltic liquid, and phenocrysts have been neither added nor subtracted from this parent during crystallization. The glass inclusions in the plagioclase and augite phenocrysts are more difficult to understand, particularly the high silica (65.4%) glass in the augite phenocryst from the lava flow. This does not appear to be a residual glass, as the alkalies are not noticeably higher than in the bulk sample. One can explain this relationship by assuming that the clinopyroxene crystal grew in a different magma, e.g., a dacite, and that this magma was later mixed with basaltic magma. Indeed, cases of eruptions of mixed magmas have been reported (e.g., MacDonald and Katsura, 1965). All analysed Ulawun lavas (Table 4) have remarkably similar bulk composition, however, and thus if mixing of two

magmas is occurring, they must mix in the same proportions in each eruption, and involve mixing of basaltic magma with very small amounts of dacitic magma.

Significance of Nuées Ardentes from Basaltic Volcanoes

Normally, nuées ardentes are thought of as products of explosive eruptions of acid to intermediate rocks. Taylor (e.g., 1960) has pointed out that nuées ardentes are by no means restricted to such compositions, and reports of basaltic nuées ardentes of Manam volcano, New Guinea. He also notes the reports of nuées ardentes from basaltic eruptions recorded by Lacroix (1904) and by Hantke (1951, also at Manam volcano).

Gas emission during avalanching may be important in giving the characteristic high mobility and billowing ash emission in nuées ardentes (see Taylor, 1958, page 47, for a review of this mechanism). However, McTaggart (1960) has demonstrated that high temperature alone without gas emission during flow can account for the high mobility of nuées ardentes. He experimented by pouring sand at various temperatures down an incline and recording its distance of flow and geometry after deposition on a plane at the

TABLE 7.—*Composition of glass inclusions in plagioclase (column 1), augite (column 2), olivine (column 3), compared to the bulk composition (column 4, analysis 1, Table 1). Analyses by electron microprobe by G. Switzer. The glass inclusions are in the following samples: columns 1 and 3 are in sample 1, Table 2; column 2 is in sample 2, Table 2*

Constituent	*Electron microprobe analyses (weight percent)*			
	1	*2*	*3*	*4*
SiO_2	55.1	65.4	51.1	52.8
Al_2O_3	13.3	18.5	17.9	18.0
TiO_2	1.6	1.0	1.1	1.0
FeO*	15.8	5.0	10.3	10.8
MgO	4.2	2.5	4.7	5.0
CaO	7.1	5.9	10.7	10.5
Na_2O	2.0	2.1	n.d.	2.3
K_2O	0.7	0.6	n.d.	0.4
MnO	0.2	0.1	n.d.	0.2
	CIPW Norms			
Q	11.3	33.1	—	—
OR	0.4	0.4	—	—
AB	16.9	17.8	—	—
AN	27.1	29.3	—	—
DI	7.0	—	—	—
HY	33.7	14.0	—	—
IL	3.0	1.9	—	—

* All Fe recalculated as FeO.
n.d. = not determined.

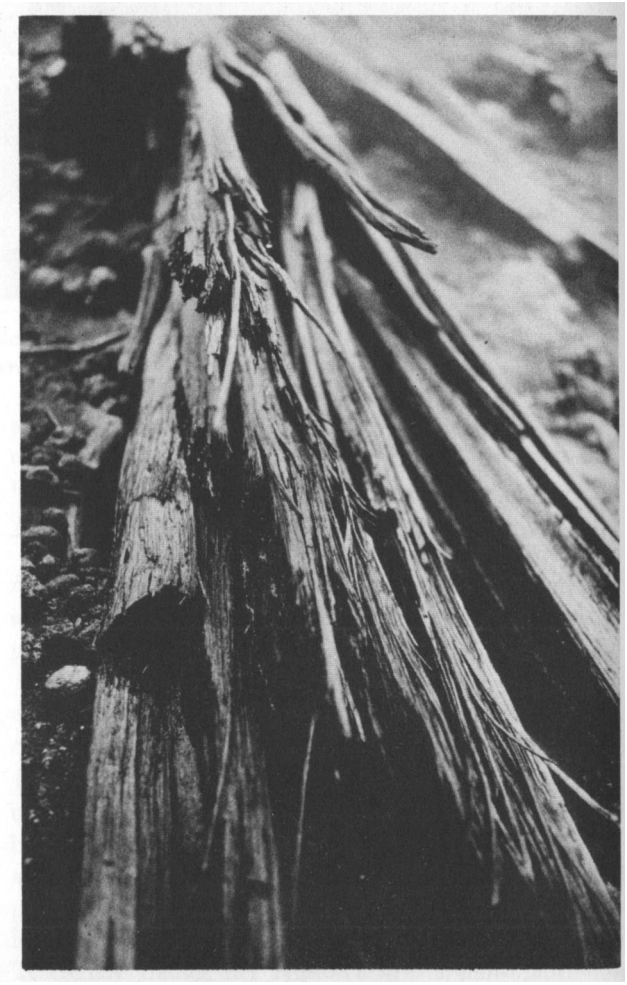

FIGURE 9.—Splintered tree trunk in avalanche deposits near terminus. This splintering occurred during transport of the trunk in the avalanche. February 10, 1970.

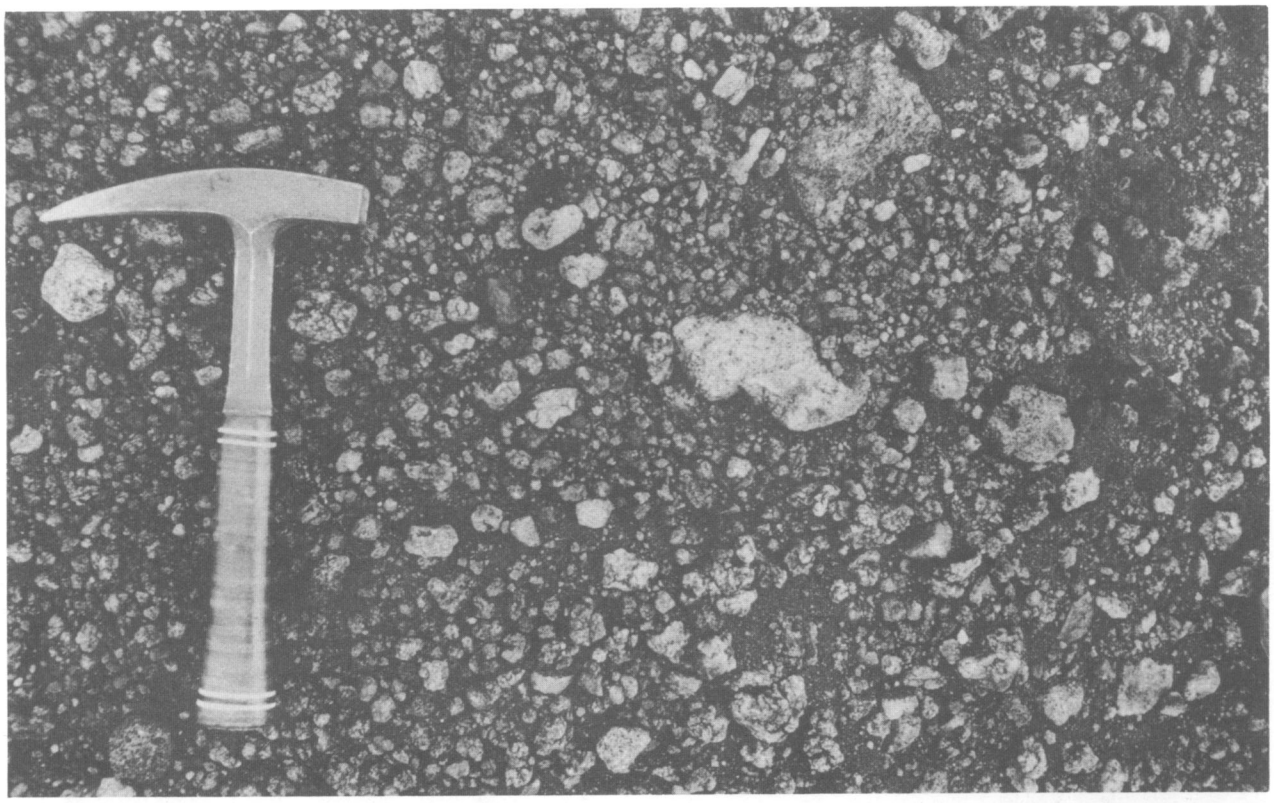

FIGURE 10.—Surface of the avalanche deposits, showing abundance of lapilli-sized fragments. February 10, 1970.

FIGURE 11.—Broken, scoriaceous bomb. Surface of avalanche deposits. February 10, 1970.

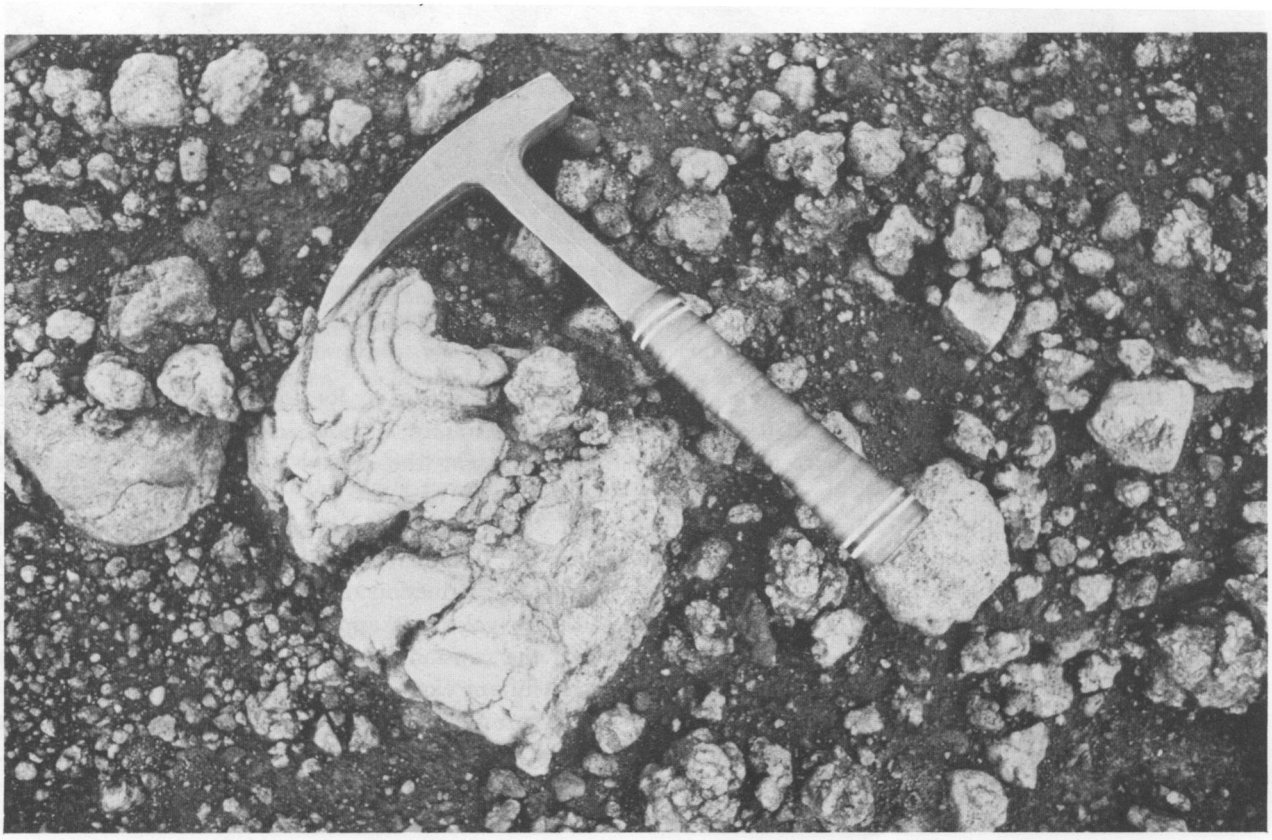

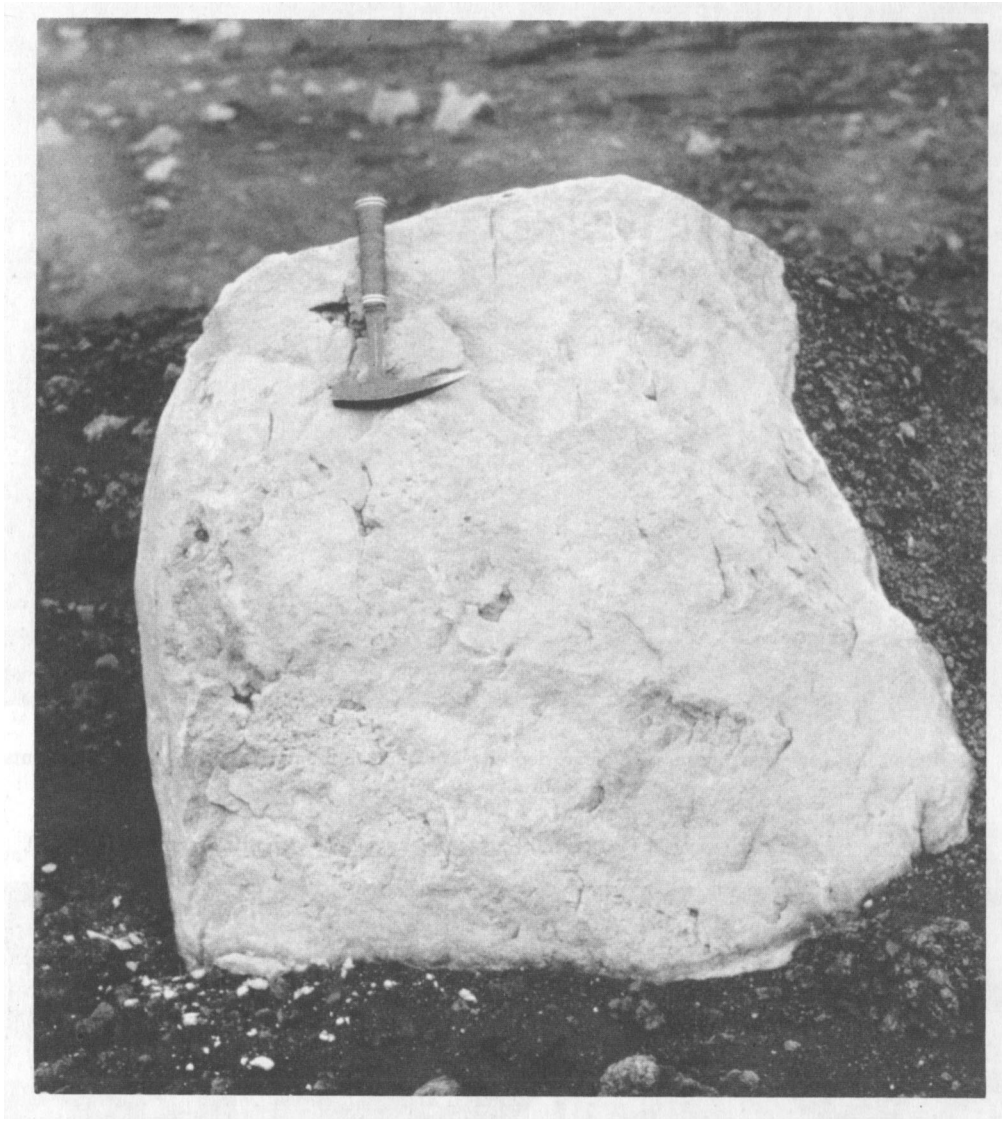

FIGURE 12.—Light-colored holocrystalline basalt xenoliths in the avalanche deposits.

base of the incline. The existence of basaltic nuées ardentes mentioned above and of the 1970 eruption of Ulawun volcano give strong support to McTaggart's idea. Basalts characteristically contain low contents of dissolved volatiles, and hence could not emit large volumes of gases during avalanching. True, the fragments in the avalanche deposits at Ulawun are vesicular, but are scoriaceous rather than pumiceous, and could not have emitted large quantities of volcanic gases. Gas emission from the avalanching material will enhance the mobility, but evidently is not a prerequisite of fragmental materials which will produce nuées ardentes. Recently, nuées ardentes were produced totally of nonessential, but hot material, ejected during the explosive opening of a new vent on the slopes of Arenal volcano, Costa Rica (Melson and Saenz 1968). Here, as at Ulawun, gas emission from the fragments in the avalanche had little to do with the production of nuées ardentes. The mobility at these volcanoes appears to have something to do with the constant inclusion and heating of air, with concomitant expansion. To my knowledge, an analysis of precisely how this mechanism works is not yet available, and is an objective of our further studies.

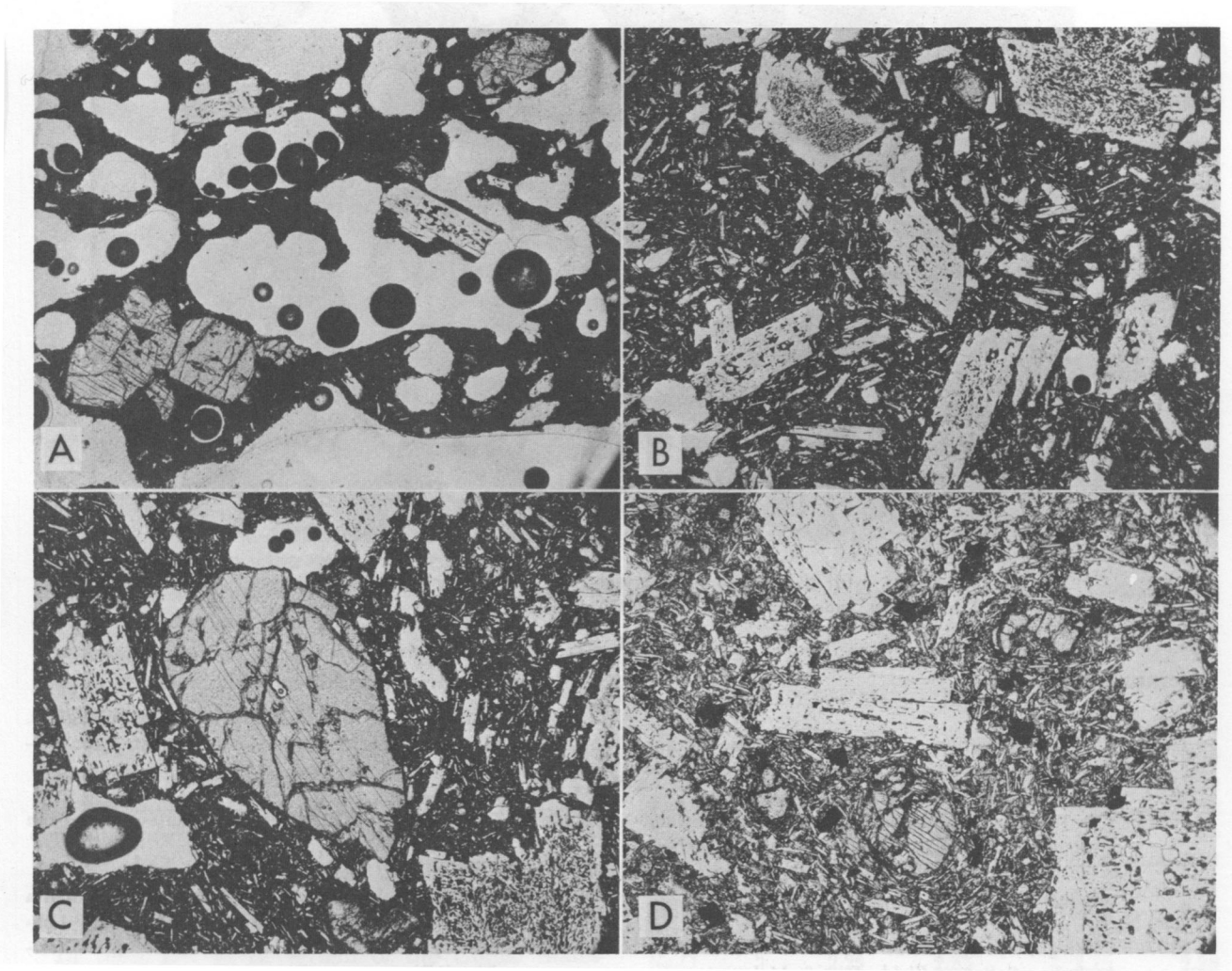

FIGURE 13.—Comparison of textures in the three analyzed ejecta of the 1970 eruption of Ulawun volcano. Width of field equals 2 mm in each photomicrograph. A. Central, vesicular portion of the analyzed basaltic breadcrust bomb (analysis 1, Table 2). Colorless phenocrysts are plagioclase; gray phenocrysts are augite. Matrix, crowded with microlites and minute oxide grains, is opaque. B. Basalt, from lava flow, showing abundance of devitrified glass inclusions in plagioclase phenocrysts and with clear overgrowths on margin. Plagioclase also abundant as microlites in matrix. Note scarcity of vesicles. C. Basalt, from lava flow, with large rounded phenocryst of augite. Analyzed sample (analysis 2, Table 2). D. Basaltic xenolith. Holocrystalline, with comparatively large grains of opaques (magnetite). Inclusions in plagioclase are holocrystalline, and mineralogically similar to the bulk sample (dominantly pagioclase and augite).

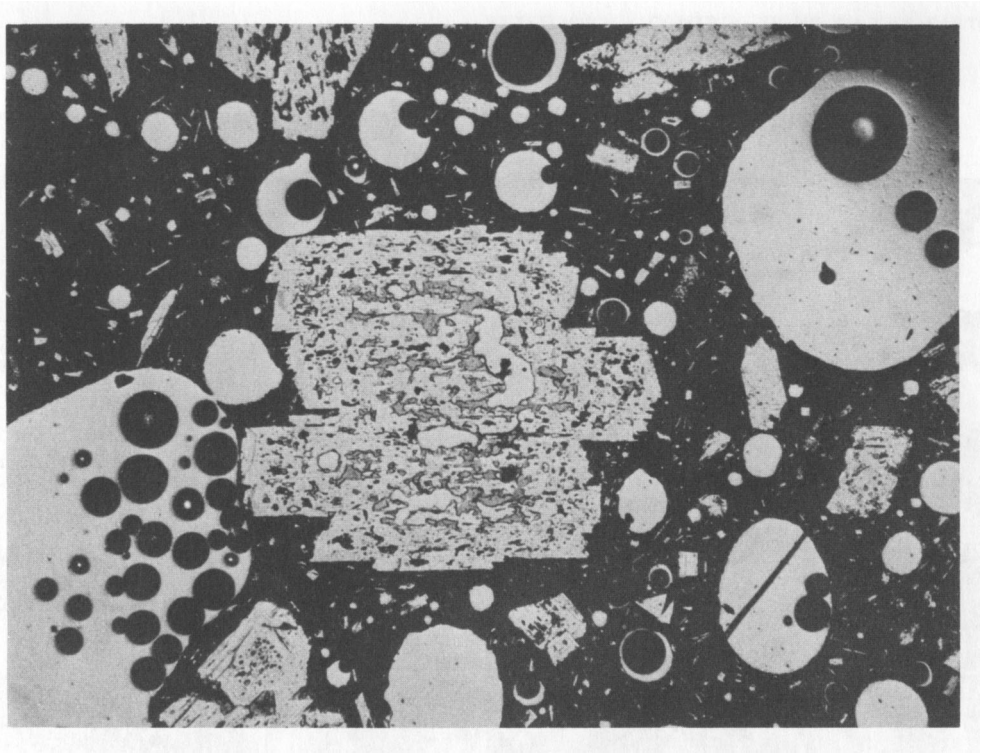

FIGURE 14.—Basalt, with plagioclase phenocrysts rich in glass inclusions. Phenocryst is about 1 millimeter wide. Analysis 1 (Table 7) is of one of these glass inclusions.

Literature Cited

Davies, R. A.

1970. The 1970 Eruption of Mt. Ulawun, New Britain. *Smithsonian Institution Center for Short-lived Phenomena Report, May 15, 1970:* 14.

1971. The 1970 Eruption of Mt. Ulawun, New Britain. *Note on Investigation,* 70501. 30 pages. Territory of Papua of New Guinea, Geological and Volcanological Branch.

Fisher, N. H.

1957. *Catalogue of the Active Volcanoes of the World Including Solfatara Fields, Part 5, Melanesia.* International Volcanological Association, Naples.

Hantke, G.

1951. Ubersicht uber die Vulkanische Tatigkeit 1941–1947. *Bulletin Volcanologique,* Series II, 11.

Johnson, R. W.

1970a. Ulawun volcano, New Britain: Geology, Petrology, and Eruptive History Between 1915 and 1967. *Australian Bureau of Mineral Resources, Geology and Geophysics, Report* 1970/21: 43.

1970b. Volcanoes of New Britain: a Summary of Preliminary Petrological Data. *Australian Bureau of Mineral Resources, Geology and Geophysics, Record* 1970/72: 2–5.

Lacroix, A.

1904. *La Montagne Pelee et Ses Eruptions.* Paris: Masson et Cie. 626 pages.

MacDonald, G. A., and T. Katsura

1965. Eruption of Lassen Peak, Cascade Range, California, in 1915: Example of Mixed Magmas. *Geological Society of America Bulletin,* 76:475–482.

McTaggart, K. C.

1960. The Mobility of Nuees Ardentes. *American Journal of Science,* 258:369–382.

Melson, W. G., and R. Saenz

1968. The 1968 Eruption of Volcano Arenal, Costa Rica: Preliminary Summary of Field and Laboratory Studies. *Smithsonian Center for Short-Lived Phenomena, Report, November 7, 1968.*

Melson, W. G., G. Thompson, and T. H. van Andel

1968. Volcanism and Metamorphism in the Mid-Atlantic Ridge: 22°N. *Journal of Geophysical Research,* 73:5925–5941.

Moore, J. G., and W. G. Melson

1969. Nuées Ardentes of the 1968 Eruption of Mayon Volcano, Philippines. *Bulletin Volcanologique,* 33(2):600–620.

Taylor, G. A.

1958. The 1951 Eruption of Mount Lamington, Papua. *Australian Bureau of Mineral Resources, Geology and Geophysics, Bulletin,* 38:117.

1960. An Experiment in Volcanic Prediction. *Australian Bureau of Mineral Resources, Geology, and Geophysics, Record,* 74.

Taylor, S. R., and A. J. R. White

1966. Trace Element Abundance and Andesites. *Bulletin Volcanologique,* 24:177–194.

R. F. Fudali

Experimental Data Bearing on the Paragenesis of Two Hawaiian Basalts from Kilaeua Volcano

Introduction

Mineral paragenesis (the order of formation of minerals in time succession) in igneous rocks is a matter of much interest to petrologists concerned with compositional trends in the residual melts, and with the genetic relations between different rock types which are associated in time and place.

Paragenesis is, of course, largely a function of the major element composition of the silicate melt but can also be influenced by such variables as: (1) Total confining pressure; (2) partial pressures (or fugacities) of H_2O and O_2; and (3) whether or not equilibrium between crystals and melt is maintained as the crystallization proceeds.

In 1968, Dr. T. L. Wright of the United States Geological Survey's Hawaiian Volcano Observatory sent me specimens of two basalts which had issued from the Summit of Kilauea Volcano in 1919 and 1954, respectively. Although separated in time by 35 years the two lavas are virtually identical in their major element content (Table 1).

However, these "isochemical" lavas apparently had different paragenetic sequences, presumably due to differences in one or more of the other variables mentioned above. This conclusion was based on the microscopic examination of samples from both rock units which exhibited varying crystal/glass ratios.

R. F. Fudali, Department of Mineral Sciences, National Museum of Natural History, Smithsonian Institution, Washington, D.C. 20560.

TABLE 1.—*Chemical analyses of two Kilauean basalts (weight percent)**

Constituent	1919		1954	
	1	*2*	*3*	*4*
SiO_2	50.20	50.02	50.20	50.09
Al_2O_3	14.04	13.87	13.73	13.79
TiO_2	2.74	2.76	2.72	2.68
Fe_2O_3	1.83	1.35	2.65	1.80
FeO	9.50	9.76	8.80	9.59
MgO	7.03	7.45	7.20	7.31
MnO	0.17	0.17	0.17	0.17
CaO	11.49	11.45	11.56	11.51
Na_2O	2.25	2.33	2.25	2.28
K_2O	0.57	0.53	0.57	0.53
H_2O+	0.1	0.08	0.00	0.08
H_2O-	0.02	0.02	0.00	0.02
P_2O_5	0.27	0.26	0.28	0.26
CO_2	0.02	0.02	0.01	0.01
Cl	—	0.02	0.02	0.01
F	—	0.04	0.05	0.05
Subtotal		100.07	100.21	100.18
Less 0		0.02	0.02	0.02
Total	100.14	100.05	100.19	100.16

* All analyses were performed at the U.S. Geological Survey Rock Analysis Laboratory, Denver. Column 1: Analyst, Lucille Tarrant. Column 2: Analyst, Ellen Danials. Column 3: Analyst, Lois Trumbull. Column 4: Analyst, Elaine Munson.

The change in crystal/melt ratio in the different specimens is normally a function of the temperature that portion of the rock unit attained before it was effectively quenched. Thus, by judicious selection of samples one can examine, at least in a crude way, a temperature and crystallization sequence for the rocks in question. Dr. Wright (personal communication) wrote:

> The Halemaumau lava lake overflows [1919] show subequal amounts of pyroxene and plagioclase at crystallinities varying from 5–20%. Evidently the two phases came out simultaneously . . . and the two minerals crystallized at nearly the same rate with falling temperature. By contrast, in the current series of flows [1954] which come up quickly from a depth of about 3 km* ($\sim$1000 bars total pressure) clinopyroxene comes out distinctly earlier than plagioclase (Cpx=8% by volume when plagioclase first appears) and the rate of plagioclase crystallization does not equal that of pyroxene until several tens of degrees lower temperature. I would like to explain the contrast by saying that the overflows from Halemaumau lava lake were degassed and equilibrated at approximately 1 atm. total pressure whereas the current flows retained a paragenesis on eruption characteristic of some P_{H_2O} lower than 1000 bars but much greater than 1 atm.

This theory was supported by the first chemical analysis of the 1954 basalt (Table 1, column 3) which reported a total iron content identical to that of the 1919 basalt but a substantially lower ferrous/ferric iron ratio—i.e., the 1954 basalt was apparently oxidized relative to the 1919 basalt, a natural consequence of higher associated water (and oxygen) fugacities.

However, subsequent chemical analyses and laboratory high-temperature, controlled atmosphere experiments performed here demonstrated this hypothesis to be incorrect. Further, total pressure differences and possible disequilibrium effects were also eliminated as possible causes of the observed paragenetic differences. The inescapable conclusion is that an apparently trivial difference in Al_2O_3 content (virtually within the analytical error of the analyses) was responsible for stabilizing plagioclase at significantly different temperatures in the two melts.

FeO and Total Iron Analyses

Divalent iron can be partially oxidized in sample preparation and digestion so that correct FeO determinations are notoriously difficult. For this reason one should always view reported FeO values with some scepticism, especially if the reported FeO value is lower than expected. One of the first things I did upon receiving the rock samples was to reanalyze them for FeO and total Fe as FeO.

The samples were very carefully ground to −80 mesh in an agate mortar, under alcohol. The analytical procedures used were standard wet chemical methods previously described by Muan and Osborn (1956) and myself (1965). Results of these analyses are shown in Table 2. My results indicate an identical ferrous/ferric iron ratio for the two rocks; a subsequent U.S. Geological Survey analysis (Table 1, column 4) supports this conclusion. The low ferrous iron reported in analysis number 3 must be due either to an analytical error or a nonrepresentative sample.

The identical ferrous/ferric ratios of the two rocks eliminates the possibility of different associated fo_2's, since such a difference would be reflected in a large difference between the two rocks in this ratio. The possibility of differences in f_{H_2O} is also eliminated since, in the absence of significant amounts of other gas species, H_2O and O_2 are inextricably related through the dissociation of water equation ($H_2O \rightleftarrows H_2 + \frac{1}{2}O_2$). Different total confining pressures and/or disequilibrium effects remained as possibilities.

TABLE 2.—*Ferrous iron and total iron analyses of 1919 and 1954 basalts (weight percent)*

Year and Iron Content	*Fudali analysis*	*USGS analyses*
1919:		
FeO	9.89	9.50– 9.76
Total Fe as FeO	11.20	10.98–11.15
1954:		
FeO	9.87	8.80– 9.59
Total Fe as FeO	11.18	11.18–11.21

Experimental Procedure

Representative samples of the two rocks were carefully crushed, under alcohol, to −80 mesh in an agate mortar, as for the chemical analyses. One to two hundred milligram charges of the homogenized powders were dryed at 110°C and placed in 60% Ag–40% Pd crucibles which, in turn, were placed in

* Determined from analyses of ground tilt.

vycor (silica glass) tubes, the ends of which had been previously sealed. The open ends of the vycor tubes were connected to a vacuum pump and, after the system was evacuated, short lengths of tubing (containing the Ag–Pd crucibles) were necked off in the flame of an oxy-hydrogen torch. The atmospheres inside the sealed vycor tubes were reduced to approximately ½ mm Hg by this procedure. This prevented the glass tubes from bursting at run temperatures. More importantly, the amount of gas remaining in the tube was so small, with respect to the weight of the powdered charge, that this rock charge could generate an equilibrium atmosphere at run temperature without a measurable change in its own composition.

The charges, so prepared, were placed in a standard, platinum-wound, vertical quench furnace. Temperature control was maintained within ±1°C during the course of the run. After sufficient time for the charge to equilibrate (in all but a few cases) at run temperature—usually 24 to 48 hours—the charges were quenched by plunging them in a beaker of cold water and the quenched phases examined under the petrographic microscope.

Temperatures were measured immediately before and after each run with a Pt–Pt/10Rh thermocouple, previously calibrated against the melting points of pure gold and diopside. Corrections were empirically determined for the difference in thermal profile of the reading thermocouple and the more massive vycor tube et al. Absolute accuracy of the indicated temperatures, as measured by this method, may be no better than ±2°C; however any error will be systematic rather than random. The indicated possible temperature spreads shown in Table 3 do not reflect such a systematic error. The indicated spread results largely from the spread between the temperatures of the two runs which most closely bracket the appearance or disappearance of given phase. One should therefore recognize that, although the absolute temperature scales could be roughly 2° higher or lower than those shown in Table 3, the relative temperature differences shown will not change.

Both rocks were run in the same furnace, using the same thermocouple, controller, and temperature-sensing instrument. Length of runs, quenching, and examination techniques were identical.

The paragenetic sequences of the two rocks, determined by these methods, are shown in Table 3.

Discussion of Experimental Results

The experimental results represent crystallization sequences under conditions of constant total composition. The ratio of ferrous to ferric iron in the charge does not change with falling temperature and the associated gas phase has a composition which is a function of the charge composition, rather than vice-versa. Down to about the appearance of an oxide phase the crystallization sequence is also an equilibrium sequence. With glassy starting charges it is an equilibrium sequence to the solidus. With crystalline starting materials crystallization at lower temperatures departs somewhat from equilibrium due to zoning effects in the crystals and the consequent inability of the largely crystalline charge to equilibrate in the experimental runs because of the low rate of solid state diffusion at these temperatures.

TABLE 3.—*Crystallization sequences of 1919 and 1954 Kilauean basalts—constant composition conditions*

1919:	
1182±2°C	olivine-liquidus
1174±2°	plagioclase
1162±3°	pyroxene
1105±5°	Fe oxide
1078±5°	Solidus 1
1050±5°	Solidus 2
1954:	
1179±3°C	olivine-liquidus
1163±2°	pyroxene
1161±2°	plagioclase
1100±3°	Fe oxide
1078±5°	Solidus

The 1954 lava sample used in this work was largely glass (~80%) and the determined sequence is therefore an equilibrium sequence. Both completely crystalline and glassy charges of the 1919 lava were used. The only difference between the two is that, with the crystalline charge, nonequilibrium effects as discussed above result in the persistence of a small amount of residual liquid to ~30° lower (solidus 2) than is the case with glassy charges (solidus 1). The sequence determined with crystalline starting charges represents the actual sequence that the rock experienced in nature.

The modal analyses of samples of the two rocks equilibrated at 1160°C are entirely consistent with the

modal observations reported by Dr. Wright (Table 4), and the experimental crystallization sequences do indeed show a significant difference with respect to the first appearance of plagioclase. However, the laboratory data does not support the *interpretation* based upon the modal analyses of the natural rocks.

TABLE 4.—*Modal analyses (volume percent)*

Constituent	*Experimental runs equilibrated at 1160°C*	**Original rock modes*
		(Analysis #1, Table 1)
1919:		
glass	91.7	89.2
pyroxene+olivine	4.4	5.1
plagioclase	3.8	5.7
		(Analysis #4, Table 1)
1954:		
glass	88.7	91.8
pyroxene+olivine	8.8	7.1
plagioclase	2.5	1.1

* Original rock modes supplied by Dr. T. L. Wright.

First, although plagioclase and pyroxene are present in subequal amounts in 1919 (at 8% total crystals) they did not begin to crystallize simultaneously. Plagioclase has a crystallization interval of ~12° before pyroxene becomes stable. Pyroxene then crystallizes more rapidly over a short temperature interval to approximately equal plagioclase in amount at 1160°C.

More importantly, since the observed differences in crystallization histories have been duplicated experimentally under low-pressure, equilibrium conditions, it is clear that neither confining pressure differences nor nonequilibrium effects need be invoked to explain the modal differences observed in the natural rock specimens. Clearly the true explanation is simply that the very slightly higher Al_2O_3 content of the 1919 lava stabilized plagioclase at a temperature approximately 13° higher than in the 1954 lava. Although the determined sequences are not precise enough to warrant further conclusions, the modal analyses at 1160° suggest that the temperature interval between the appearance of pyroxene and plagioclase in the 1954 lava is larger than the nominal 2° indicated in Table 4. Here again, very minor differences in major element content (most likely slightly lower MgO and slightly higher CaO as compared with the 1919 lava) probably favored pyroxene over olivine in the 1954 lava in comparison with the 1919 lava.

Conclusions and Implications

An obvious conclusion of this study is that paragenetic sequences are best determined in the laboratory, rather than by examination of natural, quenched rock samples supposed to represent different (but unknown) temperatures.

Equally obvious is that, while *gross* differences in paragenetic sequences may reflect significant differences in the governing parameters, modest differences in paragenesis (e.g., a 13°C change in the appearance of plagioclase out of a total crystallization range of ~100°C) may be caused by very small, indeed perhaps virtually undetectable, major element differences. Clearly, not a great deal of significance should normally be attached to such modest paragenetic differences.

The experimental data gives a reasonably precise estimate of the temperature of the 1954 magma prior to its expulsion from the 3 km deep magma chamber. The 1954 lava specimens contain abundant phenocrysts of olivine and pyroxene plus rare phenocrysts of plagioclase embedded in a matrix consisting of glass and thin plates and needles of plagioclase and pyroxene (obviously formed in the rapidly cooling lava after extrusion). In the absence of water (less than 0.1% by wt.) the low confining pressure in the shallow magma chamber (~1000 bars) would not cause a measurable change in the temperature of first appearance of the various mineral phases—with respect to the temperatures determined in the laboratory. Therefore, the temperature in the magma chamber must have been lower than 1160° (for plagioclase to be present) but no lower than 1155° (at which temperature plagioclase is approaching the abundance of pyroxene).

The situation is not as clear-cut with the 1919 lava since the crystallization which occurred at the surface in a slowly cooling lava lake is not readily distinguishable from that which occurred at depth. Only olivine phenocrysts can be identified with certainty as being a product of crystallization at depth. So the possible temperature spread for the 1919 lava prior to extrusion is 1155–1175°C. Interestingly enough,

the flank eruption that began on May 24, 1969, and is still continuing in the east rift zone of Kilauea, has produced lavas throughout the eruption "whose close-range, optical pyrometer temperatures are normally 1160–1165°C,"* in excellent agreement with the experimentally deduced temperatures of the 1919 and 1954 eruptions.

The similarity in the major element composition of the 1919 and 1954 lavas, and their deduced temperatures prior to eruption provide considerable information about the nature and location of the magma source, given the reasonable assumption that both magmas come from the same source.

The possibility that a constant composition silicate melt existed from 1919 thru 1954 in a shallow magma chamber and was thus able to erupt isochemical lavas 35 years apart is not tenable. At 1160° the magma contains significant amounts of olivine and pyroxene. Given these circumstances it would be remarkable that separation of crystals and liquid did not occur, yielding a more recent magma or magmas of substantially different composition(s) from the 1919 lava. Melt viscosity and density differences between crystals and melt result in effective laboratory separations in a matter of days, with temperatures and compositions similar to those indicated herein. Actually, volcanic activity during this period included two additional summit eruptions (1934 and 1952) and also periods of inflation and inferred injections into the east rift zone (T. L. Wright, personal communication). Neither the 1934 nor the 1952 lavas are chemically identical with the 1919 and 1954 lavas. No east rift lavas were actually erupted during this period but two separate flows erupted in the east rift zone in 1955 appear to be clearly derivative rocks, presumably formed by removal of pyroxene and plagioclase from a summit basalt composition. Thus not only should a shallow-seated magma differentiate, but given the opportunity, some Kilauean magmas *have* differentiated, to a recognizable extent, within a period of time much shorter than 35 years.

Since all the Hawaiian lavas clearly originate by partial melting in the upper mantle, a reasonable explanation of the isochemical 1919 and 1954 lavas is that they represent the primary melts of such a process and were erupted before they had time to differentiate.

The partial melting of mantle material most likely occurs at constant temperature, triggered by some sort of pressure release mechanism. Since the lavas carry phenocrysts rather than residual crystals they must have been entirely liquid at one time, presumably when they originated. This necessitates an absolute minimum source temperature of ~1180°C (liquidus temperature at 1 atm. pressure). A more realistic source temperature estimate is 1200–1220°C. To keep basaltic material solid (prior to the melting event) at such temperatures requires a depth of 60–80 km for the source rock (Yoder and Tilley, 1962). Such a depth is well within the earth's mantle and is consistent with the frequent occurrence of ultramafic xenoliths (considered by most geologists to be locally derived mantle material) in some Hawaiian basalts.

As the magmas migrated upward from their mantle source into the shallow chamber at 3 km depth they cooled to ~1160°C, with some attendant crystallization. In most cases some differentiation took place but the 1919 and 1954 lavas were erupted before the melt-crystal mixture could separate appreciably.

A remarkable aspect of this volcanic complex is demonstrated by the fact that two lavas, separated in time by 35 years, could move 60–80 km upward through the mantle and crust, from the same source, to issue at the same surface vent. Either the conduit system from the mantle source to the surface has remained continuously open because it is filled with magma, as suggested by T. L. Wright (personal communication) or the same conduit system has been repeatedly opened, along a continual zone of weakness, by a periodic pressure release mechanism. In any case it seems indisputable that the conduits have been well-established, stable features from the surface to a depth of 60–80 km over at least the last fifty years.

Acknowledgments

I thank Dr. T. L. Wright of the United States Geological Survey for supplying samples of the Hawaiian basalts and making available to me their major element analyses prior to publication. His enlightening discussions with me and his penetrating criticisms of this manuscript are also greatly appreciated.

* The Smithsonian Institution Center for Short-Lived Phenomena, Event no. 14–17, card 1075, 12/22/70. Source: Swanson and Peterson, U.S. Geological Survey, Hawaiian Volcano Observatory.

Literature Cited

Fudali, R. F.
1965. Oxygen Fugacities of Basaltic and Andesitic Magmas. *Geochimica et Cosmochimica Acta,* 29: 1063–1075.

Muan, A., and E. F. Osborn
1956. Phase Equilibra at Liquidus Temperatures in the System MgO-FeO-F_2O_3-SiO_2. *Journal of the American Ceramic Society,* 39:121–140.

Yoder, H. S., and C. E. Tilley
1962. Origin of Basalt Magmas: an Experimental Study of Natural and Synthetic Rock Systems. *Journal of Petrology,* 3(3):342–532.

Harold H. Banks, Jr.

Iron-rich Saponite: Additional Data on Samples Dredged from the Mid-Atlantic Ridge, 22° N Latitude

Banks and Melson (1966) reported the occurrence of saponite in hydrothermally altered basalts and basaltic tuffs from the crest of the Mid-Atlantic Ridge and in the median valley between 22° and 23° N latitude. The present paper gives the results of a chemical and X-ray study of that material as well as of identical material tentatively identified as nontronite by Melson and van Andel (1966).

The 22° N latitude area was first examined in detail during cruise 44 of R. V. *Chain* (September–October 1964) of the Woods Hole Oceanographic Institution and revisited in 1965 on cruise 1965–1 of R. V. *Thomas Washington* (December 1965) of Scripps Institution of Oceanography. The geological and geophysical results were presented by van Andel et al. (1965) and van Andel and Bowin (1968). The petrology of the area has been discussed by Melson and van Andel (1966) and Melson et al. (1968). Siever and Kastner (1967) have described the mineralogy of the sediments.

Saponite is a major constituent of massive basalts, metabasalts, basaltic tuffs, and metatuffs dredged at four stations in this area of the Mid-Atlantic Ridge (Table 1).

In massive basalts, olivine phenocrysts are entirely replaced, in some, by dark, gray-green saponite with iron oxide, possibly goethite, localized at the crystal-matrix interface and in fractures in the pseudomorphs. The pseudomorphs are commonly connected

Harold H. Banks, Jr., Department of Mineral Sciences, National Museum of Natural History, Smithsonian Institution, Washington, D.C. 20560.

TABLE 1.—*Location of dredge hauls on the Mid-Atlantic Ridge in the area between 22° and 23° N latitude containing abundant saponite-bearing rocks*

Station	*Latitude and longitude*	*Depth (m)*
Thomas Washington, cruise 1965–1:		
THV–4 (dredge 2)	22°31.5′N, 45°W to 44°59.8′W	1985–1735
THV–14 (dredge 17)	22°49.2′N, 45°8.8′W to 22°48.6′N, 45°10.1′W	3500–3000
THV–18 (dredge 10)	22°10′N, 45°14.2′W to 22°11.4′N, 45°16.6′W	3100–2600
Chain, cruise 44:		
DR–2	22°38.2′N, 44°58.6′W to 44°58′W	2400–2100

by veinlets of optically identical material. Saponite also occurs as thin films along cleavages and fractures in subcalcic augite grains and along grain boundaries. Plagioclase (ca. An_{65}) often exhibits peripheral alteration to saponite, and any glass inclusions in the plagioclase are entirely altered to saponite. Saponite is also present as vesicle, interstitial, and vein filling. Such relations may be seen in a single thin section.

Saponite occurs associated with albite (An_1–An_4), relict calcic plagioclase (as high as An_{75}), ripidolitic chlorite (MgO=20%, FeO=19%, Al_2O_3=18%), actinolite (47–64% tremolite molecule), epidote (average composition about 75% clinozoisite molecule), quartz, sphene, pyrite, and relict spinel in the metabasalts (Melson and van Andel 1966). It is commonly intergrown in vesicles and veins with material which optically resembles chlorite. Veinlets and shear planes in mylonitized and brecciated basalts which have been only slightly altered in mineral composition contain trace amounts of saponite associated with albite, actinolite, chlorite, epidote, pumpellyite, and zeolites (probably mainly natrolite).

Marine tuffs dredged from the 22° N area show considerable variation in texture and mineralogy, but most show an abundance of saponite in the matrix, absence of highly vesiculated fragments, and abundance of fragments of glassy, variolitic rinds as opposed to coarser-grained fragments.

The metatuffs are undeformed and consist of lapilli of originally glass-rich basalt in a fine-grained ashy matrix. The glass is completely replaced by ripidolitic cholorite which is commonly altered to saponite. The matrix is composed of abundant saponite and traces of actinolite.

Optically, the saponite is micaceous to fibrous in habit, gray-green to yellow-brown in color, exhibits moderate to high birefringence (ca. 0.02;N_z=1.56) and is weakly pleochroic. In hand-specimen, it is light to dark gray-green with a greasy luster. Massive pieces are extremely soft when wet but become harder and brittle upon drying.

The saponite was identified using the identification scheme of Warshaw and Roy (1961) for layer silicates. Samples were ground in a porcelain mortar, and care was taken to prevent or at least minimize the effects of fine grinding which can destroy the ordered crystalline structure. The powders were then mixed with a small amount of finely ground silicon as an internal standard for X-ray study. Oriented slides, glycolated and unglycolated (with ethylene glycol) were analyzed on a diffractometer at 1°—2θ/minute, with Cu radiation and a nickel filter. Resolution of the (060) smectite* reflection (1.49–1.52 Å for dioctahedral smectite and 1.53–1.54 Å for trioctahedral smectite) was obtained by powder photographs using nickel filtered copper radiation in a 114.6 mm diameter camera. Powder data for two massive samples of saponite (samples 2–17 and 10–116) are given in Table 2.

TABLE 2.—*X-ray powder data for saponite*

	dÅ		
Indices[1]	*Cahuenga Pass, California*[1]	*Mid-Atlantic Ridge Station THV–4 (Sample 2–17)*	*Mid-Atlantic Ridge Station THV–18 (Sample 10–116)*
001	15.4	12.538[2] (10)[3]	12.503[2] (10)[3]
002	7.9	—	—
003	5.28	—	—
11,02	4.60	4.605 (4)	4.563 (4)
004	3.93	—	—
005	3.13	—	—
13,20	2.648	2.640 (3)	2.618 (3B)
006	—	—	—
—	2.560	2.520	—
—	2.452	—	—
04,22	2.298	2.311 (1)	—
15,24	1.740	1.739 (1)	—
31	—	—	—
06,33	1.541	1.536 (4)	1.527 (5)
26,40	1.330	—	—
19,46	1.001	—	—
53	—	—	—
60,39	0.888	—	—

[1] Data for griffithite, an iron-rich saponite (Faust 1955).

[2] X-ray pattern was made using the following instrumental factors: CuK_α radiation, λ=1.54178Å; 38KV; 18MA; silicon served as an internal standard. Peak shifted to 16.61Å after treatment with ethylene glycol.

[3] Numbers in parentheses are estimated relative intensities. B-broad.

* I use the term "smectite," proposed by British clay mineralogists (Brown 1955), rather than "montmorillonite-type mineral," an approved, identical, but cumbersome name.

Semiquantitative chemical analyses of saponite (Table 3) from veins in a mylonitized olivine basalt (sample 2–17) and from hydrothermally altered basaltic glass (sample 10–116) were performed by electron microprobe and X-ray fluorescence analysis, respectively, of lithium tetraborate fusions, with analyzed oceanic basalt lithium tetraborate fusions serving as standards: the fusions were prepared following the procedure outlined by Rose et al. (1963). For sample 10–116, H_2O was determined by the Penfield method, Na_2O and K_2O by flame photometry: the FeO and Fe_2O_3 contents of both samples were determined by classical methods.

The chemical analyses of the samples were plotted on a FeO-Fe_2O_3-MgO ternary diagram (Figure 1) which graphically distinguishes between the two smectites in which iron is an essential and major constituent: nontronite (dioctahedral; FeO = 0–1%) and iron-rich saponite (trioctahedral; FeO = 1–8%). Chemical analyses to delineate the smectite fields shown in Figure 1 were selected from various sources: saponites are from Ross and Hendricks (1945, analyses 77–79) and Deer et al. (1962, analysis 13); nontronites are from Ross and Hendricks (1945, analyses 55–67); iron-rich saponites are from Calliere and Henin (1951, analyses 4–5), Faust (1955), and Sudo (1959).

TABLE 3.—*Semiquantitative chemical analyses of iron-rich saponite,* Thomas Washington *1965–1, Station THV–4, Sample 2–17*, and Station THV–18, Sample 10–116†*

Constituent	*Chemical analyses (weight percent)*	
	2–17[1]	10–116[2]
SiO_2	43.0	41.6
Al_2O_3	7.2	5.0
Fe_2O_3	7.79	11.32
FeO	2.53	0.78
MgO	21.0	18.3
CaO	0.4	0.6
Na_2O	3.3	2.2
K_2O	0.4	0.5
TiO_2	<0.05	0.3
H_2O (total)	18.9	20.6

* Saponite from veins in mylonitized olivine basalt.

† Saponite derived by the hydrothermal alteration of basaltic glass.

[1] Performed by electron microprobe analysis of lithium tetraborate fusion using an enlarged electron microprobe spot and classically analyzed oceanic basalt lithium tetraborate fusions as standards. FeO and Fe_2O_3 contents were determined by classical methods.

[2] Performed by X-ray fluorescence, using the method of Rose et al. (1963). H_2O determined by Penfield method; Na_2O and K_2O by flame photometry; FeO and Fe_2O_3 by classical methods.

The combined X-ray and chemical results indicate that the clay is iron-rich saponite. The (001) reflection for the clay shifts from nearly 12.5Å to 16.6Å upon treatment with ethylene glycol, and the critical (060) reflection is greater than 1.52Å which is indicative of trioctahedral smectite (see Table 3). In addition, the semiquantitative chemical analyses of the clay plot very nicely in the iron-rich saponite region of the FeO-Fe_2O_3-MgO diagram (Figure 1). I suspect that the high Fe_2O_3 content of sample 10–116 (Table 3) is the direct result of the participation of heated sea water with a high Eh in the formation of the clay. The high Na_2O content and the low CaO content of both samples may very well be a primary feature, but Na saturation may also result from cation exchange during weathering of a normal, Ca-rich saponite in contact with sea water.

Textural relations of saponite in rocks from the 22°N area suggest several modes of origin for the saponite: (1) hydrothermal alteration, by heated sea water, of basaltic glass and silicates in the matrix of basaltic tuffs during cooling and movement of the tuffs; (2) low-grade metamorphism of basalts and basaltic tuffs at a maximum temperature of 300°C (Melson and van Andel, 1966) and a pH_2O of about 500 bars; and (3) deuteric alteration of basaltic glass, olivine, plagioclase and augite in the massive basalts.

I am indebted to Eugene Jarosewich, who provided the semiquantitative chemical data for sample 10–116 and the total and ferrous iron analyses for sample 2–17, and to Dr. Joel Arem who kindly assisted in the preparation of samples for X-ray analysis. Special thanks are due to Kenneth Towe and William G. Melson for their helpful discussions of many of the problems encountered during the course of this study.

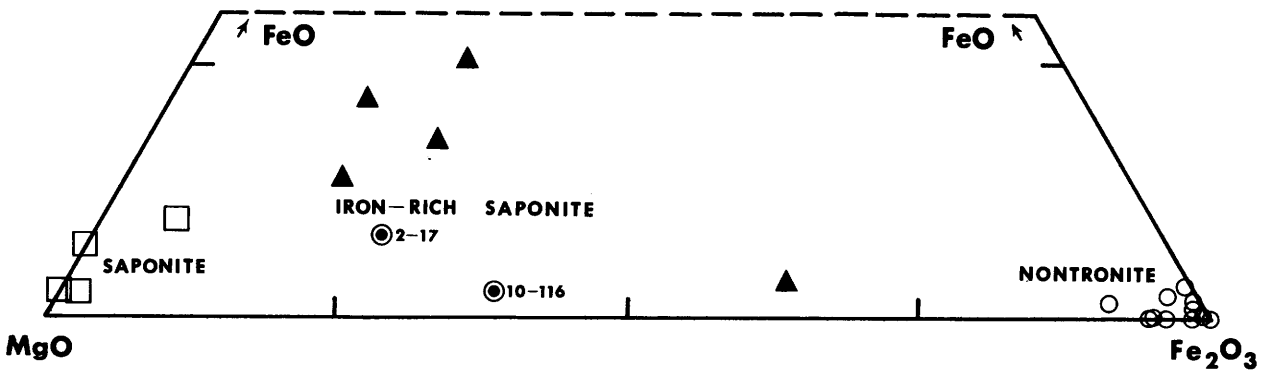

FIGURE 1.—Semiquantitative chemical analyses of saponite from the Mid-Atlantic Ridge (samples 2–17 and 10–116, open circles with solid centers) plotted on the ternary diagram FeO-Fe_2O_3-MgO. Open circles are nontronites selected from Ross and Hendricks (1945); open squares are saponites selected from Ross and Hendricks (1945) and Deer et al. (1962); solid triangles are iron-rich saponites selected from Calliere and Henin (1951), Faust (1955), and Sudo (1959).

Literature Cited

Banks, H. H., Jr., and W. G. Melson
1966. Saponite from the Mid-Atlantic Ridge, 22° N Latitude. *1966 Annual Meeting Geological Society of America,* Abstracts: 9–10.

Brown, G.
1955. Report of the Clay Minerals Group Subcommittee on Nomenclature of Clay Minerals. *Clay Minerals Bulletin,* 2:294–302.

Caillere, S., and S. Henin
1951. The Properties and Identification of Saponite (Bowlingite). *Clay Minerals Bulletin,* 1:138–144.

Deer, W. A., R. A. Howie, and J. Zussman
1962. *Rock-Forming Minerals,* 3:226–245. New York: John Wiley & Sons.

Faust, G. T.
1955. Thermal Analysis and X-Ray Studies of Griffithite. *Washington Academy of Science Journal,* 45:66–70.

Melson, W. G., and Tj. H. van Andel
1966. Metamorphism in the Mid-Atlantic Ridge, 22° N Latitude. *Marine Geology,* 4:165–186.

Melson W. G., G. Thompson, and Tj. H. van Andel
1968. Volcanism and Metamorphism in the Mid-Atlantic Ridge, 22° N Latitude. *Journal of Geophysical Research,* 73:5925–5941.

Rose, H. J., Jr., I. Adler, and F. Flanagan
1963. X-Ray Fluorescence Analysis of the Light Elements in Rocks and Minerals. *Applied Spectroscopy,* 17:81–85.

Ross, C. S., and S. B. Hendricks
1945. Minerals of the Montmorillonite Group. *U.S. Geological Survey Professional Paper,* 205B:23–77.

Siever, R., and M. Kastner
1967. Mineralogy and Petrology of some Mid-Atlantic Ridge Sediments. *Journal of Marine Research,* 25:263–278.

Sudo, Toshio.
1959. *Mineralogical Studies on Clays of Japan.* Tokyo: Maruzen. Pages 227–268.

van Andel, Tj. H., and C. O. Bowin
1968. The Mid-Atlantic Ridge Between 22° and 23° North Latitude and the Tectonics of Mid-Ocean Rises. *Journal of Geophysical Research,* 73: 1279–1298.

van Andel, Tj. H., V. T. Bowen, P. L. Sachs, and R. Siever
1965. Morphology and Sediments of a Portion of the Mid-Atlantic Ridge. *Science,* 148:1214–1216.

Warshaw, C. M., and R. Roy
1961. Classification and a Scheme for the Identification of Layer Silicates. *Geological Society of America Bulletin,* 72:1455–1492.

George Switzer, William G. Melson, and Geoffrey Thompson

Olivine Crystals from the Floor of the Mid-Atlantic Ridge near 22° N Latitude

Remarkably fresh, small, gemmy, single crystals of olivine were found in the heavy mineral fraction of foraminiferal sand dredged from the eastern flank of the mid-Atlantic Ridge near 22°N. This occurrence of euhedral, free olivine crystals in a marine sediment is highly unusual in our experience. These olivine crystals clearly grew in basaltic lava, and were then freed by growth of vesicles, with gas exsolution commonly initiating at crystal-liquid boundaries. Ultimate freeing of the crystals from the lava may entail more than this. Conditions in a vesiculating, turbulent, submarine lava fountain may be particularly favorable to the final freeing of these crystals.

Olivine phenocrysts, along with plagioclase phenocrysts, are the most common phenocrysts in deep-sea basalts from the mid-ocean ridges. Thus, the occurrence of olivine in the central, volcanically active zone of the mid-Atlantic Ridge is not surprising, but its occurrence free of a basaltic matrix is.

The dredge which recovered the olivine crystals is from the eastern slope of the median valley of the mid-Atlantic, a zone of active sea-floor spreading, characterized by frequent earthquakes and volcanic eruptions. The rocks of the 22°N area are dominantly fresh basalts and greenschist facies metabasalts (Melson and van Andel 1966, Melson et al. 1968). The median valley here is essentially a rifted submarine basalt field, where volcanism is manifested mainly by fissure eruptions, some on the flanks, and others along the floor of the median valley. The ridge from which the olivine was obtained is a major bathymetric feature, rising to within 1400 meters of the sea surface. This same ridge elsewhere produced pillow lavas, massive basalts, and massive to schistose greenschist facies metabasalts. The bathymetry and geology of this portion of the mid-Atlantic Ridge is also described by van Andel and Bowin (1968). Details of the recovery are as follows:

Cruise: R. V. *Chain,* cruise 44, of the Woods Hole Oceanographic Institution.

Location: Dredge tract from 22°50.0'N, 45°05.6'W at 3200 meters, to 22°50.6'N, to 45°04.2'W at 3400 meters.

Description: 450 grams of coarse foraminiferal sand from a 4-inch pipe dredge, taken in dredge 8.

At Woods Hole, a portion of the sample was leached with dilute hydrochloric acid and subjected to grain size analysis and to density separations. The grain size distribution was as follows: 27.35 gms greater than 590 microns; 0.54 gms greater than 297 microns, but less than 590 microns; and 43.32 gms less than 297 microns. Remarkably pure concentrates of euhedral olivine crystals were produced in the size fraction between 297 and 590 microns in the density range of 2.9 to 3.3 gm/cc. These crystals compose less than 1 percent of the total untreated sample.

George Switzer and William G. Melson, Department of Mineral Sciences, National Museum of Natural History, Smithsonian Institution, Washington, D.C. 20560. Geoffrey Thompson, Woods Hole Oceanographic Institution, Woods Hole, Massachusetts 02543.

The crystals occur with fresh fragments of basaltic glass (n=1.596). Olivine commonly occurs in this glass as phenocrysts, which have in some places been partially separated from their matrix by growth of gas pockets (vesicles) along the crystal-lava contact. It is thus quite clear that the free olivine crystals originally crystallized from basaltic lava, but were freed by growth of gas cavities around their surfaces, evidently a favored site for gas exsolution during vesiculation.

The olivine crystals are transparent, pale yellowish green and range from about one-half to one milli-

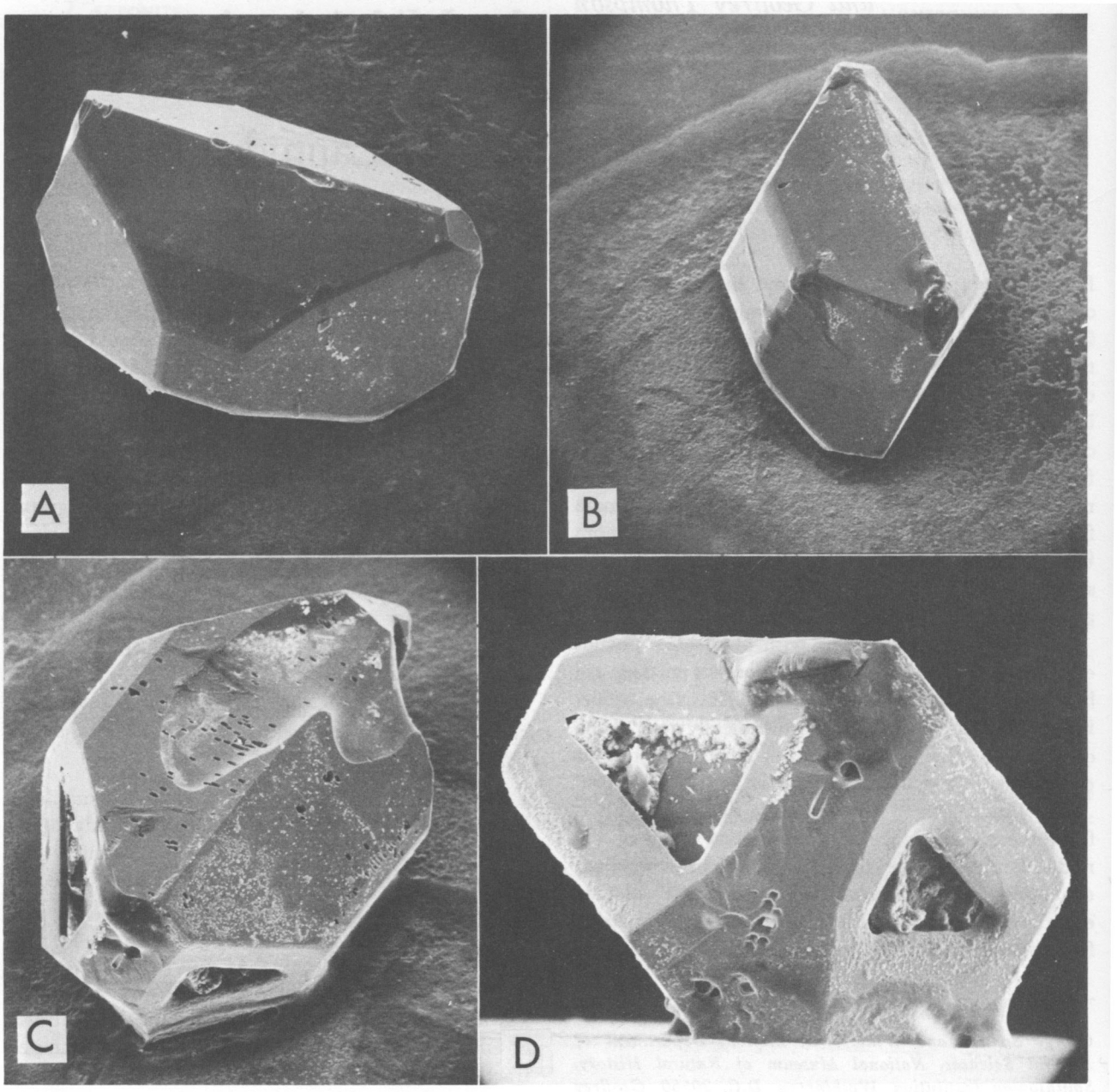

FIGURE 1.—A–B, Complete individuals showing typical olivine morphology. ×100. C–D, Two views of a crystal showing pitting and skeletal growth. (C ×95, D ×140). Scanning electron microscope photographs by Walter Brown, Smithsonian Institution.

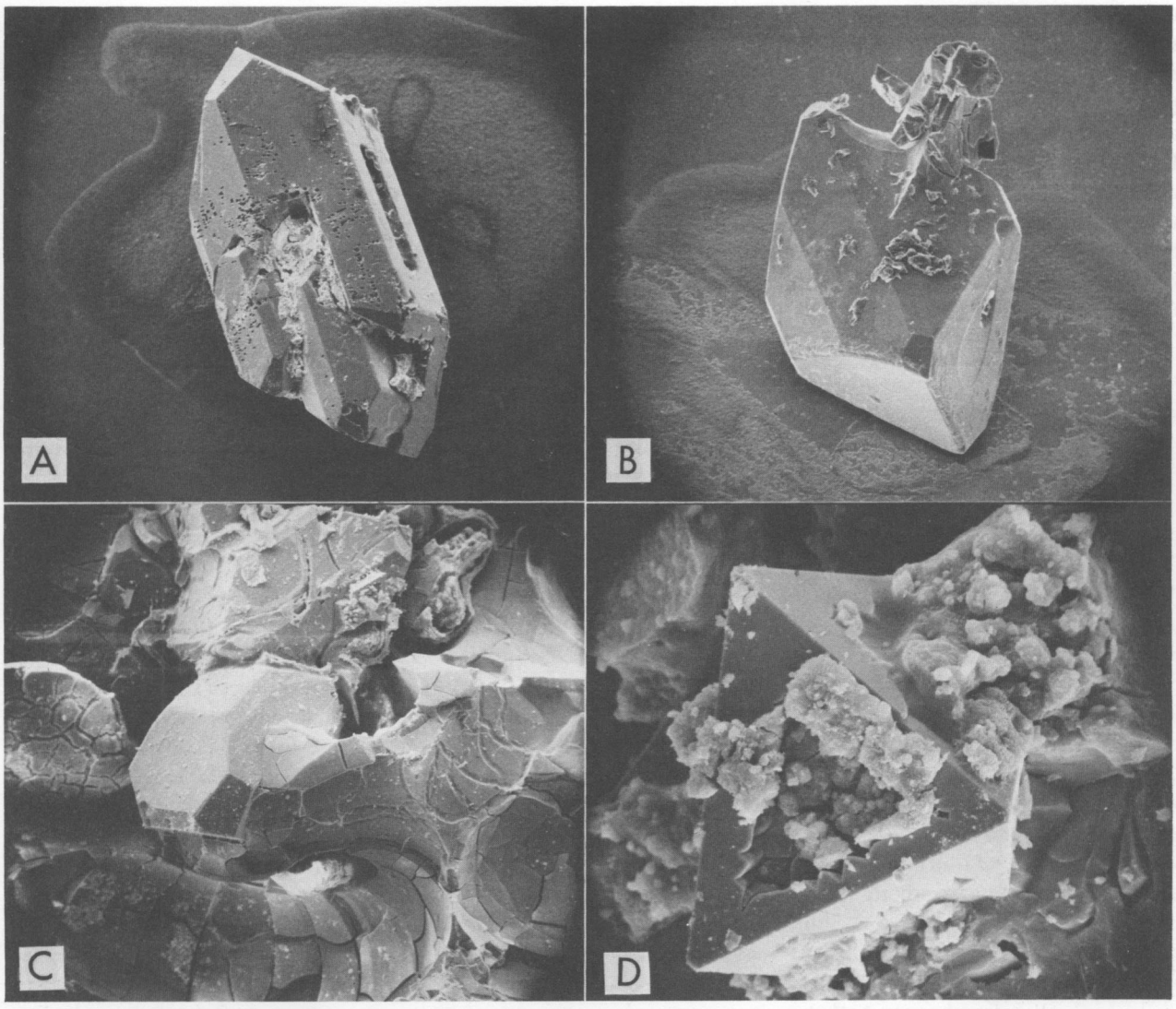

FIGURE 2.—A, Crystal showing pitting and skeletal growth. B, Crystal with attached glass fragments ×95. C, Crystal in cavity in vesiculated glass, ×40. D, Spinel crystal in glass matrix, ×140. Scanning electron microscope photographs by Walter Brown, Smithsonian Institution.

meter in maximum length. Their edges are remarkably sharp, and they have highly reflective faces. There is no evidence whatsoever of abrasion. These features, and the interesting skeletal forms shown by some crystals are illustrated in the accompanying scanning electron microscope photographs. The composition from microprobe analysis is Fo_{82}. We did not determine nickel and other minor and trace element contents. Small octahedra of a chromian spinel are associated with the olivine.

The olivine crystals are similar in composition to olivine phenocrysts (Fo_{85}) described from pillow lavas in this region (Melson et al. 1968, page 5929).

Acknowledgments

We wish to acknowledge the assistance of Dr. V. T. Bowen, Chief Scientist, and the officers and crew of

the R. V. *Chain,* for their assistance in obtaining these samples. Dr. Tj. H. van Andel has contributed substantially, both in published accounts and in discussions, to our information on the 22°N area. Support for various aspects of this study aboard ship and at Woods Hole came from the United States Atomic Energy Commission, the Office of Naval Research, and the National Science Foundation. The work at the Smithsonian was supported partially by the Smithsonian Research Foundation. This paper will be contribution No. 2665 from the Woods Hole Oceanographic Institution.

Literature Cited

Melson, W. G., and Tj. H. van Andel
1966. Metamorphism in the Mid-Atlantic Ridge, 22° N Latitude. *Marine Geology,* 4:165–186.

Melson, W. G., G. Thompson, and Tj. H. van Andel
1968. Volcanism and Metamorphism in the Mid-Atlantic Ridge, 22° N. Latitude. *Journal of Geophysical Research,* 73:5925–5941.

van Andel, Tj. H., and C. O. Bowin
1968. The Mid-Atlantic Ridge Between 22° and 23° North Latitude and the Tectonics of Mid-Ocean Rises. *Journal of Geophysical Research,* 73: 1279–1298.

George Switzer and William G. Melson

Origin and Composition of Rock Fulgurite Glass[1]

A great deal of attention has been given recently to natural glasses, especially tektites, impact glasses, and the glass phases of lunar rocks. However, fulgurites, natural glasses formed as a result of fusion of rock by lightning, have not been the subject of modern study.

Fulgurites may be conveniently divided into two types, those formed by fusion of loose sand, or *sand fulgurites,* and those formed by fusion of solid rock, usually referred to as *rock fulgurites.*

Sand fulgurites are normally of simple composition, from about 90 to 99 percent SiO_2 depending on the purity of the sand. They are quite common and have been described in detail by numerous investigators beginning in the year 1711.

Rock fulgurites on the other hand appear to be relatively uncommon, or at least have been observed less frequently than sand fulgurites. Also, they are petrologically more interesting since they may result from fusion of any rock type. They have been described as formed from rocks ranging as widely as andesite, granite, hornfels, glaucophane schist, and serpentinite.

Investigation of rock fulgurite glass composition by microprobe has revealed that these glasses are extremely hetergeneous. As examples, we have looked at the composition of glasses formed by fusion of andesite from Little Ararat, Turkey; quartz diorite porphyry from Crested Butte, Colorado; and hornfels from Castle Peak, Colorado.

George Switzer and William G. Melson, Department of Mineral Sciences, National Museum of Natural History, Smithsonian Institution, Washington, D.C. 20560.

[1] Presented orally at the International Mineralogical Association Seventh General Meeting, Tokyo and Kyoto, Japan, August 1970.

Little Ararat

Little Ararat, in eastern Turkey, elevation 12,877 feet, has the most extensive development of fulgurites reported anywhere in the world. The fulgurites are in hypersthene diopside andesite.

Detailed chemical analyses were made of areas in two thin sections of specimen USNM 52094. Figure 1A shows a partially melted plagioclase phenocryst. A microprobe step scan, at five micron intervals, was made along the line shown, and the results of the analysis as given in Figure 1B. The plagioclase-glass interface shows clearly in the photograph but is not so clearly discernible from the chemistry. For some distance beyond the interface the glass has plagioclase composition. It then changes abruptly to a composition representing melted groundmass.

Figure 2A shows a partially melted diopside phenocryst. Two interfaces are clearly discernible, one between diopside and diopside glass, and the other between diopside glass and glass derived by melting of groundmass. The same boundaries are reflected in the chemistry, as shown in Figure 2B.

Crested Butte, Colorado

Crested Butte, elevation 12,172 feet, is a Tertiary quartz diorite porphyry laccolith lying about 3 miles northeast of the town of Crested Butte in west central Colorado. The specimens used in this study

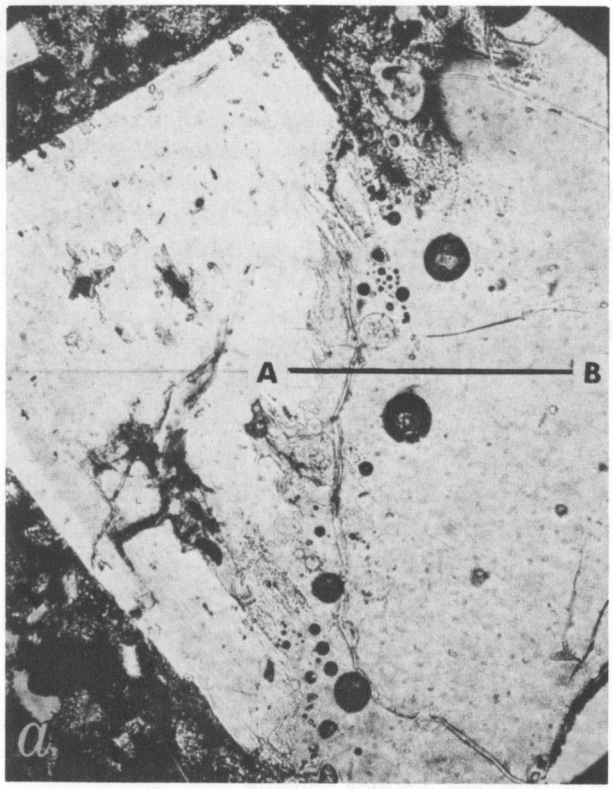

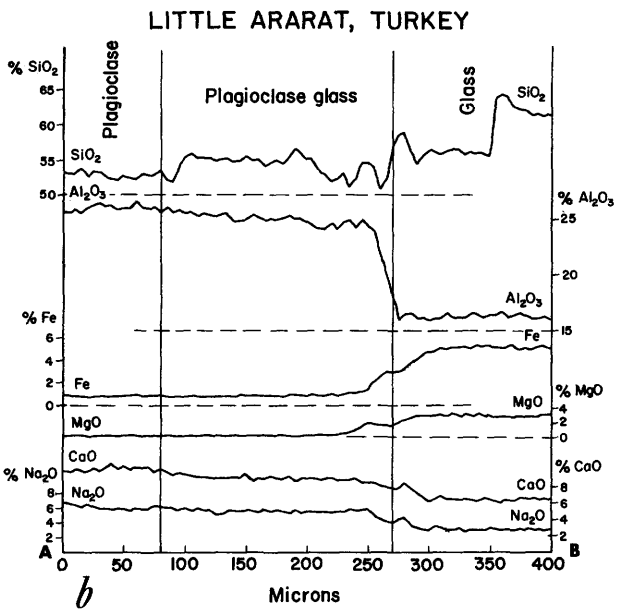

FIGURE 1.—*a*, (Photo) Partially melted plagioclase phenocryst. Andesite, Little Ararat, Turkey. *b*, (Graph) Composition of glass along AB, Figure 1*a*.

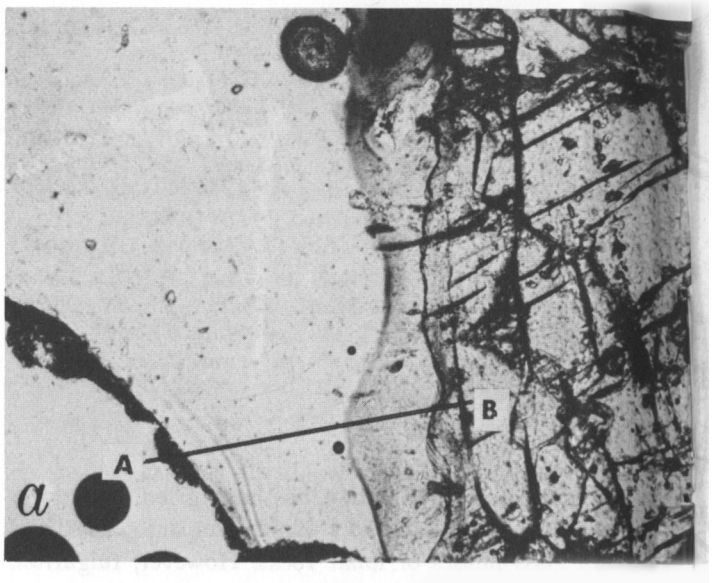

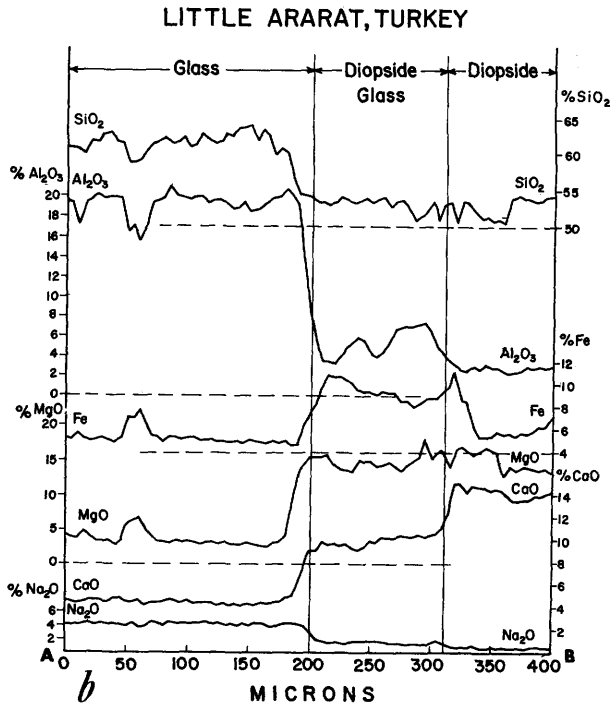

FIGURE 2.—*a*, (Photo) Partially melted diopside phenocryst. Andesite, Little Ararat, Turkey. *b*, (Graph) Composition of glass along AB, Figure 2*a*.

(USNM 52981) were collected by Whitman Cross in 1885.

The extreme hetergeneity of rock fulgurite glass, resulting from essentially no mixing while in the

molten state, is especially well exemplified by this material. In thin section, shown in Figure 3A, the plagioclase-glass interface is clearly seen, and heterogeneity of the glass is indicated by swirl marks, not visible in the photograph.

A step scan was made along the line shown and the results are shown in Figure 3B. There has been so little mixing that areas of glass representing the original phase can be recognized. Moving from left to right the composition is first that of plagioclase, then plagioclase glass. It then changes to quartz glass (as shown by SiO_2 nearly 100 percent, all other elements near zero), back to plagioclase glass, then quartz glass, plagioclase glass once again, and finally a glass high in Fe and Mg, probably representing fused biotite. The areas cannot be detected optically, but their dimensions correspond closely to the groundmass grain size of the rock.

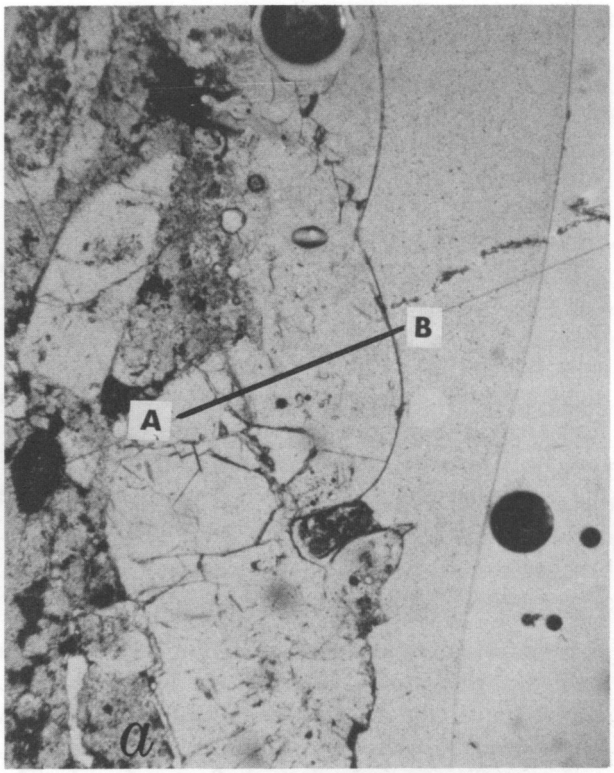

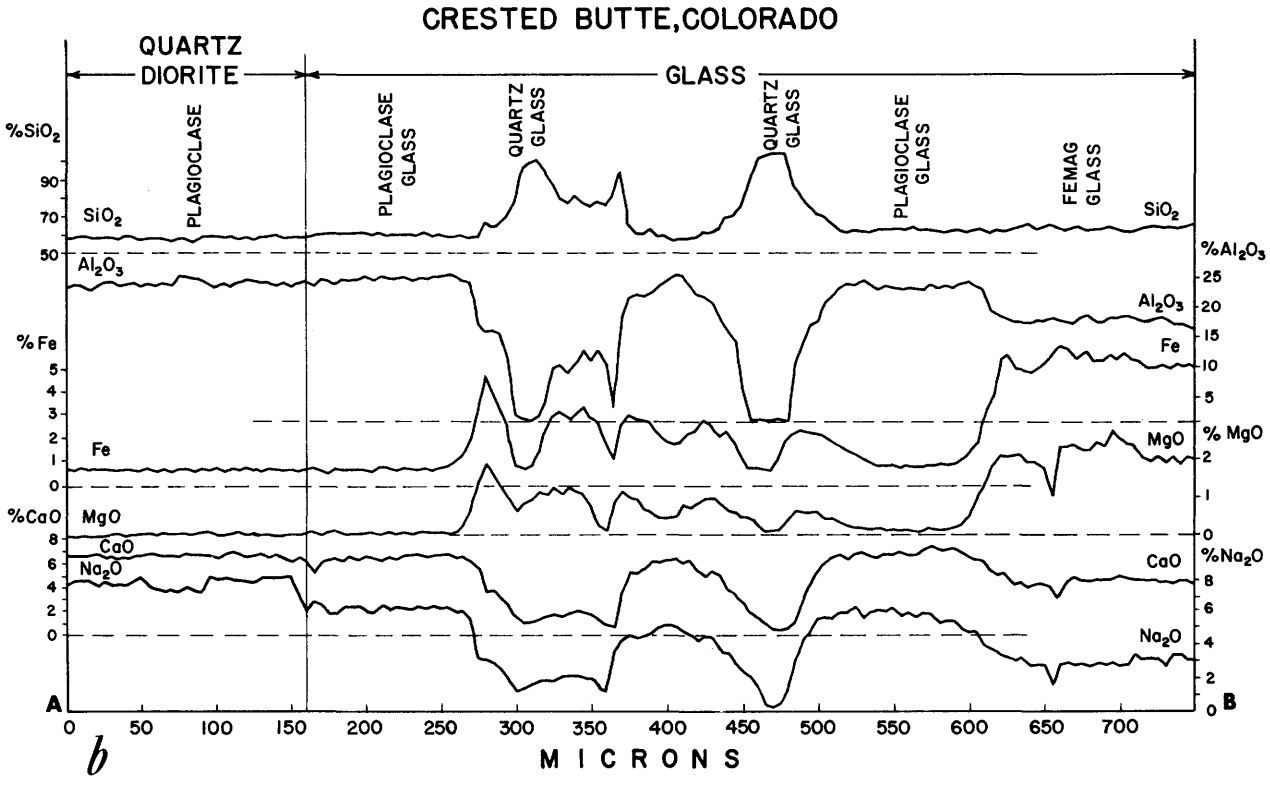

FIGURE 3.—*a*, (Photo) Fusion crust on quartz diorite, Crested Butte, Colorado. *b*, (Graph) Composition of glass along AB, Figure 3*a*.

Castle Peak, Colorado

Castle Peak, elevation 14,265 feet, is in west central Colorado and is the highest point in the Elk Mountains. The specimens studied (USNM 52980) were collected by Whitman Cross in 1887. The rock is an albite-quartz hornfels, with minor epidote, andradite, hornblende, calcite, and pyrite.

A photomicrograph of the glass analyzed, a bleb attached to the wall of a tube, is shown in Figure 4A. Because of the fine grain size, the glass appears optically homogeneous, and isochemical melting of individual grains cannot be seen. The results of a step scan analysis along the line shown are given in Figure 4B. This analysis reflects the fine grain size of the rock, but shows that even on this scale there has been relatively little homogenization.

Discussion

A remarkable feature of some of the rock fulgurites studied is the physical effect of the lightning strike. For example, the hornfels from Castle Peak has a nearly straight, glass-lined tube, 4 mm in diameter, and extending entirely through 9 cm of rock. The "entrance" of the tube is spalled and glass spattered, and the "exit" has a raised glass lip.

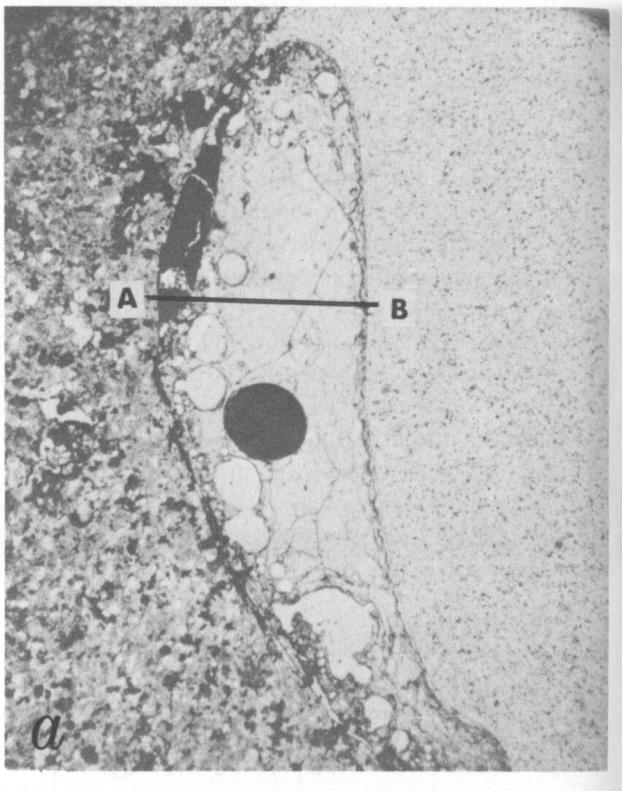

FIGURE 4.—*a*, (Photo) Fusion crust on hornfels, Castle Peak, Colorado. *b*, (Graph) Composition of glass along AB, Figure 4*a*.

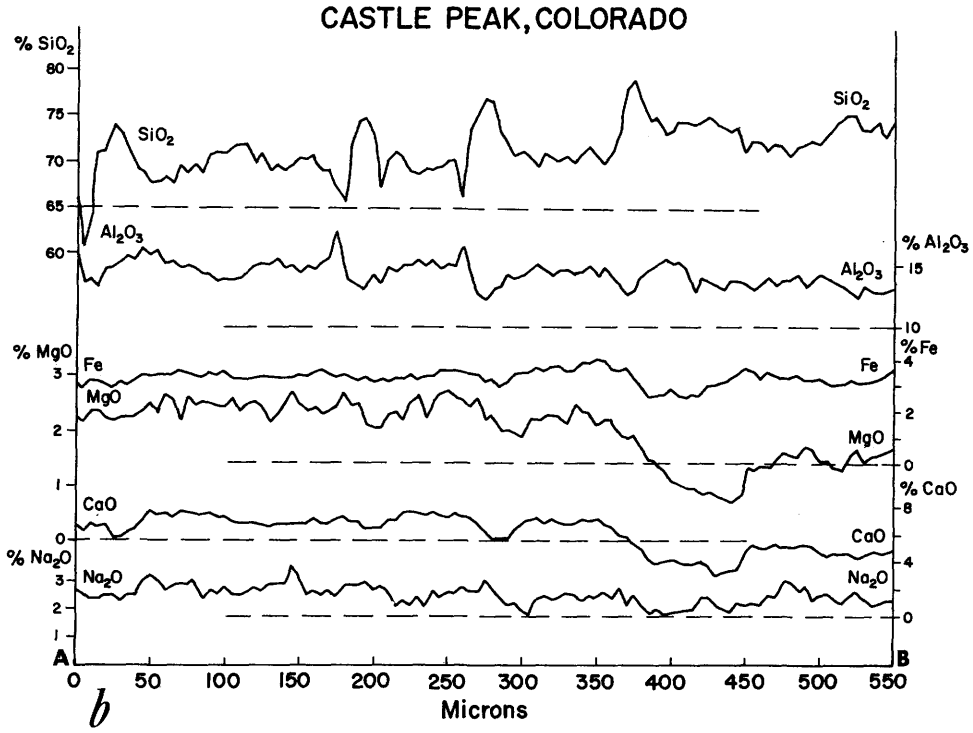

Specimens from other localities, such as Little Ararat, show both broad surfaces covered by a thin fusion crust, as well as irregular, sometimes branching, glass-lined tubes.

The rock fulgurite glasses examined contain no crystallites. This feature, combined with the observed isochemical melting of individual mineral grains and the extreme heterogeneity of the glasses, indicates rapid melting and cooling. These features are predictable since the duration of a lightning strike is of the order of one millisecond.

Measurements of lightning made by many investigators have shown that:

1. The potential difference between cloud base and ground is of the order of 100,000,000 volts.

2. Peak current may be as high as 10,000 amperes, and during most of the duration of the strike is of the order of 1,000 amperes.

3. Air particles within a radius of 2 cm of the channel are ionized at a temperature of about 30,000°K.

The tubes, such as the one described in hornfels, if formed by lightning, must also have been formed in a time interval of the order of millisecond. This is a phenomenon difficult for us to comprehend even knowing the vast amount of energy released by a lightning stroke. Other explanations for the formation of these remarkable tubes must be considered, particularly for the unusually straight tube in the sample from Castle Peak, although as yet none more plausible has occurred to us.

The extremely high temperatures conceivably reached by fulgurites might lead to volatilization of metallic oxides, particularly silica and those of the alkalies. All the sand and rock fulgurites we examined contain gas cavities, but these appear to have formed mainly by boiling off of surface and combined water; we have detected no loss of metallic oxides.

METEORITES

Joseph Nelen and Brian Mason

The Estherville Meteorite

The Estherville meteorite fell near the town of the same name in eastern Iowa on May 10, 1879. It belongs to the small class of mesosiderites, and is one of only six that were observed falls. The material is particularly suitable for research since it was collected immediately after the fall and has not suffered from the weathering that has seriously deteriorated most other mesosiderites. No complete chemical analysis has been published of the silicate material of this meteorite, hence the present investigation.

Material was taken from specimen number 1722 in the meteorite collection of the United States National Museum of Natural History. The material was crushed to pass through a 50-mesh sieve, and nickel-iron particles were removed with a hand magnet. This procedure evidently failed to remove all the included metal, since 0.14% Ni was determined in the analysed sample; using the figure of 8.57% Ni in the metal phase of Estherville (Powell 1970), this corresponds to 1.6% of nickel-iron. The analysed sample also showed 1.05% S, equivalent to 2.88% troilite. From the total iron determined by analysis the appropriate amounts were allotted to nickel-iron and troilite, and the remainder is reported as FeO. The analysis is set out in Table 1, together with partial analyses of Estherville silicates by Powell (1970) and Jérome (1970). Powell's data were obtained by X-ray fluorescence analysis; Jérome's data by semi-micro wet chemical analysis except for Cr_2O_3, obtained from instrumental neutron activation anlysis.

The normative mineralogical composition calculated from the analysis is (in weight percent): pyroxene ($En_{71}Fs_{25}Wo_4$), 72.6; plagioclase (An_{89}), 18.4; troilite, 2.9; nickel-iron, 1.6; tridymite, 1.6; chromite, 1.1; whitlockite, 0.7; ilmenite, 0.5. This is consistent with the observed mineralogical composition, except that a little olivine (estimated 2%) is present; the amount of modal pyroxene is therefore less than normative pyroxene by about 2%, and the amount of modal tridymite will be somewhat greater than the 1.6% in the norm. Modal chromite and ilmenite will be somewhat less than the normative amount, because some chromium and titanium are combined in the pyroxenes. Fuchs (1967) has shown that the whitlockite in Estherville is accompanied by stanfieldite, $Ca_4Mg_3Fe_2(PO_4)_6$.

Estherville is a polymict breccia, and different samples of the silicate material are likely to give somewhat different analyses. This certainly explains, at least

TABLE 1.—*Analyses of silicate material of the Estherville meteorite*

Constituent	*Chemical analyses (weight percent)*		
	*1**	*2**	*3**
SiO_2	50.03	55.42	
TiO_2	0.29	0.43	0.29
Al_2O_3	6.24	8.44	7.10
Cr_2O_3	0.76		0.95
FeO	12.27	11.80	18.68
MnO	0.51	0.47	0.43
MgO	18.88	14.16	17.40
CaO	5.18	5.62	5.50
Na_2O	0.22		0.26
K_2O	0.02		0.02
P_2O_5	0.31	0.74	
FeS	2.88		
Fe	1.46		
Ni	0.14		
Total	99.19		
FeO/FeO+MgO (mole percent)	26.8	31.9	37.6

* Column *1:* Analyst, Joseph Nelen.
Column *2:* Powell (1970).
Column *3:* Jérome (1970).

Joseph Nelen and Brian Mason, Department of Mineral Sciences, National Museum of Natural History, Smithsonian Institution, Washington, D.C. 20560.

in part, the discrepancies between the different analyses in Table 1. The FeO/FeO + MgO molecular percent given by Jérome's analysis is too high to be consistent with the average composition of the pyroxenes; probably his sample contained some troilite and nickel-iron whose iron was determined and reported as FeO. The SiO_2 figure in Powell's analysis appears to be somewhat too high; he gives a figure of 10.1% for normative tridymite, which is considerably higher than the amounts we have observed.

Literature Cited

Fuchs, L. H.
1967. Stanfieldite, a New Phosphate Mineral from Stony-Iron Meteorites. *Science,* 158:910–911.

Jérome, D. Y.
1970. *Composition and Origin of Some Achondritic Meteorites.* Thesis, University of Oregon.

Powell, B. N.
1970. Petrology and Chemistry of Mesosiderites. I. Textures and Composition of Nickel-Iron. *Geochimica et Cosmochimica Acta,* 33:789–810.

A. F. Noonan,
Kurt A. Fredriksson,
and Joseph Nelen

Forest Vale Meteorite

ABSTRACT

The Forest Vale meteorite is a typical olivine-bronzite chondrite. Chemical, mineralogical, and textural evidence indicates that all phases are genetically related, crystallized at high temperature, and the later formed agglomerate was lithified with no subsequent thermal metamorphism.

Introduction

At about 3 p.m. on August 7, 1942, a shower of meteorites fell near Forest Vale, New South Wales, Australia. Forest Vale is about 12 miles (19.2 km) northeast of Tullibigeal (Latitude 33°30′S; Longitude 146°48′E), which is on the Wyalong-Cargellico railway line. The countryside has low relief with hills of Devonian sedimentary rocks, granite, and Tertiary lava flows.

Details are reported by Hodge-Smith (1942, 1943). Five fragments were recovered which fitted together to form an almost complete stone. Of these, three have been preserved. The two smaller fragments have been destroyed or lost since their discovery. It is estimated that the two lost specimens weighed nearly 4.5 kg, and the total weight of the stone was about 26 kg. In addition, another stone was discovered in the immediate vicinity and its probable weight was about 2 kg. Hodge-Smith (1943) wrote:

> Both stones are chondritic. On the fractured surface the color is bluish-grey and the texture is fine granular somewhat resembling a grey sandstone in appearance. The chondrules vary in size from 1 mm. to 0.1 mm. in diameter. They are very numerous, and many consist of olivine or enstatite, or both. The groundmass consists mainly of the same two minerals. Nickel-iron is present in a very finely divided state, fairly evenly distributed throughout the mass. It constitutes roughly 20% by weight of the stone. Chemical analysis and further optical studies have yet to be undertaken.

Mason (1963) determined the composition of the olivine in the Forest Vale meteorite. The purpose of this study is to expand the mineralogic and petrologic data and, if possible, obtain some indications about the conditions of formation of this meteorite and of chondrites in general.

Chemical Composition

In addition to the wet chemical analysis by Jarosewich (1967), detailed phase analyses were made with an ARL (Applied Research Laboratories) electron probe microanalyzer. The instrument was operated at 20 KV with a specimen current of about 0.03 microamps. All measurements were corrected for deadtime, drift, background, and mass absorption. In addition, secondary fluorescence corrections were made for the metal phases. For details on the technique see Keil (1967). For the quantitative analyses, pure metallic iron and nickel, Marjalahti olivine (Fe = 8.7, Mg = 29.0 weight percent), and Johnstown hypersthene (Ca = 0.99, Mg = 16.40 weight percent) were used as standards.

Wet Chemical Analysis

The chemical analysis in Table 1 was published by Jarosewich (1967). However, the reported FeO value (5.84%) is too low to be consistent with the composition of the olivine and pyroxene as determined from microprobe analyses. This is probably due

A. F. Noonan, Kurt A. Fredriksson and Joseph Nelen, Department of Mineral Sciences, National Museum of Natural History, Smithsonian Institution, Washington, D.C. 20560.

to analytical error, since FeO was determined as the difference between total iron and iron in metal and sulfide. The analysis has been corrected by calculating the amount of FeO (8.75%) required to make Fa_{17} from the acid-soluble MgO (23.95 weight percent). Combined with the acid insoluble FeO, the total FeO would then be 8.61%. This will in turn necessitate lowering the metallic iron to 17.24%, which is much closer to the average of two recent analsyes for metallic iron—17.57%—obtained by Jarosewich on two other small pieces from this meteorite.

In Table 2 the data are also presented in the conventional form expressed as metal, troilite, and oxides; in terms of the elements in weight percentages; and in atom percentages after the elimination of O, C, H, and S. The presentation in conventional form (column A) assumes that all S exists as FeS, that Fe in excess of free metal and FeS is present in the ferrous state, and that all Ni and Co are present in the metal phase. The second method of presentation (column B) more closely reflects the results actually obtained in analysis. The amounts of the different elements are determined with the exception of O, which is later added to make 100 percent. The expression of the analysis in atom percentages after the elimination of O, C, H, and S, was introduced by Wiik (1956). This provides a method for comparing all stony meteorites regardless of the abundance or lack of volatiles. The normative mineral composition, calculated from the chemical composition as recommended by Wahl (1950), and expressed in weight percentages, is given in Table 3 (A).

TABLE 1.—*Analysis of the Forest Vale meteorite (Jarosewich 1967, with revised figures for Fe and FeO)*

Constituent	*Chemical analyses (weight percent)*		
	1 *Acid Soluble* 56.59	*2* *Acid Insoluble* 43.41	*3*
Fe			17.24
Ni			1.76
Co			0.09
FeS			5.54
SiO_2	24.00	55.01	37.46
TiO_2	0.03	0.27	0.13
Al_2O_3	0.14	4.38	1.98
Cr_2O_3			0.46
FeO	8.75	8.44	8.61
MnO			0.31
MgO	23.95	22.31	23.23
CaO	0.58	3.15	1.69
Na_2O			0.85
K_2O			0.11
P_2O_5			0.31
H_2O (+)			0.72
H_2O (−)			0.06
C			0.18
Total			100.73
Total Fe	43.48	6.56	27.45

CARBON DISTRIBUTION

The carbon content as reported by Moore and Lewis (1967) (0.18%—Table 1) appears somewhat higher than normal. In an attempt to determine the distribution of carbon within this meteorite, a sample was selectively drilled under a low-power microscope with a dental drill (Fredriksson and Nelen 1969). The collected material consisted of some finely powdered matrix material and a few small chunks with adhering chondrules. After separating powder and chunks, both fractions were analyzed for carbon content with a Leco low-carbon analyzer. The powdered matrix fraction contained 1.04% carbon, the chunks 0.19% carbon.

In a second experiment, two small samples were gently crushed in a mortar. The coarser pieces were then manually picked out and the remaining material separated in several size fractions by sieving. With this technique the softer, fine-grained matrix material tends to concentrate in the finer fractions, while the harder chondrules and metal tend to remain with the coarser material. Carbon content of the separates is given in Table 4. Similar results have been obtained for other normal (i.e., with constant olivine-pyroxene composition) H and L group chondrites. Apparently these chondrites have a carbonaceous matrix similar to that in unequilibrated or carbonaceous chondrites, although in smaller amounts. The presence of a carbonaceous low-temperature fraction (Fredriksson and Keil 1964; Anders 1964) would argue against a high-temperature metamorphic event such as suggested by Dodd (1969) after the agglomeration of the chondrites.

TABLE 2.—*Chemical composition of the Forest Vale meteorite*

A[a]		*B*[b]		*C*[c]	
Constituent	*Weight percent*	*Constituent*	*Weight percent*	*Constituent*	*Atom percent*
Fe	17.24	Fe	27.45	Si	33.84
Ni	1.76	Si	17.44	Mg	31.39
Co	0.09	Mg	14.01	Fe	26.78
FeS	5.54	S	2.02	Al	2.11
SiO_2	37.46	Ni	1.76	Ca	1.65
TiO_2	0.13	Ca	1.21	Ni	1.63
Al_2O_3	1.98	Al	1.05	Na	1.49
Cr_2O_3	0.46	Na	0.63	Cr	0.32
FeO	8.61	Cr	0.31	P	0.25
MnO	0.31	Mn	0.24	Mn	0.24
MgO	23.23	C	0.18	K	0.13
CaO	1.69	P	0.14	Ti	0.09
Na_2O	0.85	Co	0.09	Co	0.08
K_2O	0.11	K	0.09		
P_2O_5	0.31	H	0.09	Total	100.00
H_2O (+)	0.72	Ti	0.08		
H_2O (−)	0.06	O	33.21		
C	0.18				
		Total	100.00		
Total	100.73				

[a] Chemical analysis expressed as nickel-iron, troilite, and oxides (Jarosewich 1967, with revised figures for Fe and FeO).

[b] Chemical analysis expressed as elements, with oxygen added to make 100 percent.

[c] Chemical analysis expressed as atom percentages, with the elimination of O, C, H, and S.

TABLE 3.—*Normative composition of the Forest Vale meteorite*

Constituent	*A Bulk*	*B Matrix*
Nickel-iron	19.1	11.1
Troilite	5.5	2.9
Bronzite	31.6	36.2
Olivine	28.5	17.2
Diopside	4.0	9.0
Albite	7.2	16.2
Anorthite	1.3	2.9
Orthoclase	0.7	1.5
Chromite	0.7	0.4
Apatite	0.7	1.5
Ilmenite	0.2	0.4

A. Normative composition calculated from chemical analysis according to Wahl (1950).

B. Matrix (44.6%) = Bulk normative minerals (column A) minus modal amounts in weight percent of recognizable mineral grains.

TABLE 4.—*Carbon content of separates of the Forest Vale meteorite*

Size fraction	*Sample 1 (% Carbon)*	*Sample 2 (% Carbon)*
Coarse pieces	0.13	0.19
>80 Mesh	0.51	0.40
80–100 Mesh	0.86	0.78
<100 Mesh	1.27	1.23

Mineralogy and Petrology

OLIVINE

In a crushed sample, olivine grains are abundant, colorless, and frequently inclusion-filled. The fractures are characteristically conchoidal.

The refractive indices are $\alpha = 1.665 \pm 0.002$, $\gamma = 1.702 \pm 0.002$, indicating a content of 16 mole percent

of the Fe_2SiO_4 (Fa) component, according to the determinative curve of Poldervaart (1950). The (130) peak at 2.771Å appears sharp and symmetrical on the diffractograms indicating uniform composition. According to the data of Yoder and Sahama (1957), this peak shows the composition of olivine to be 16.5 mole percent Fe_2SiO_4.

Five or six points on each of about ten randomly selected olivine grains, or a total of 55 points, were analyzed with the microprobe. The olivine proved Ni-poor (less than 0.02%) and with an essentially homogeneous composition of $Fa_{17.6}$.

In thin section, the crystal habit of olivine is variable. Subhedral grains are most common, although euhedral crystals do exist. The well-developed crystals are commonly elongated parallel to the C-axis, six-sided, and show (010) cleavage. Poikilitic inclusions of small olivine grains in pyroxene are common. Grain orientation is random, and crystals attain a maximum length of 0.7 mm. Euhedral grains are length-slow with parallel extinction.

Pyroxene

Pyroxene is also abundant and occurs as large prismatic crystals or fibrous aggregates. The grains are colorless to opaque depending on the abundance of inclusions, often part along cleavage planes, and frequently display both simple and polysynthetic twins.

The refractive indices are $\alpha = 1.670 \pm 0.002$, and $\gamma = 1.684 \pm 0.002$, indicating a composition of 15 mole percent of the $FeSiO_3$ component, according to Kuno's data (1954). This falls in the compositional range of bronzite. The diffractograms indicate both abundant bronzite and one or more clinopyroxenes. These are probably clinobronzite with accessory diopside.

Both orthorhombic and monoclinic pyroxene revealed a near constant composition of $Fs_{15.8}$ in both twinned and untwinned crystals. A few anomalously high Ca areas prompted the use of electron beam scanning pictures taken of pyroxene grains and measured for Ca and Fe distribution, only one revealed distinct Ca-rich rims (Figure 1). The enrichment oc-

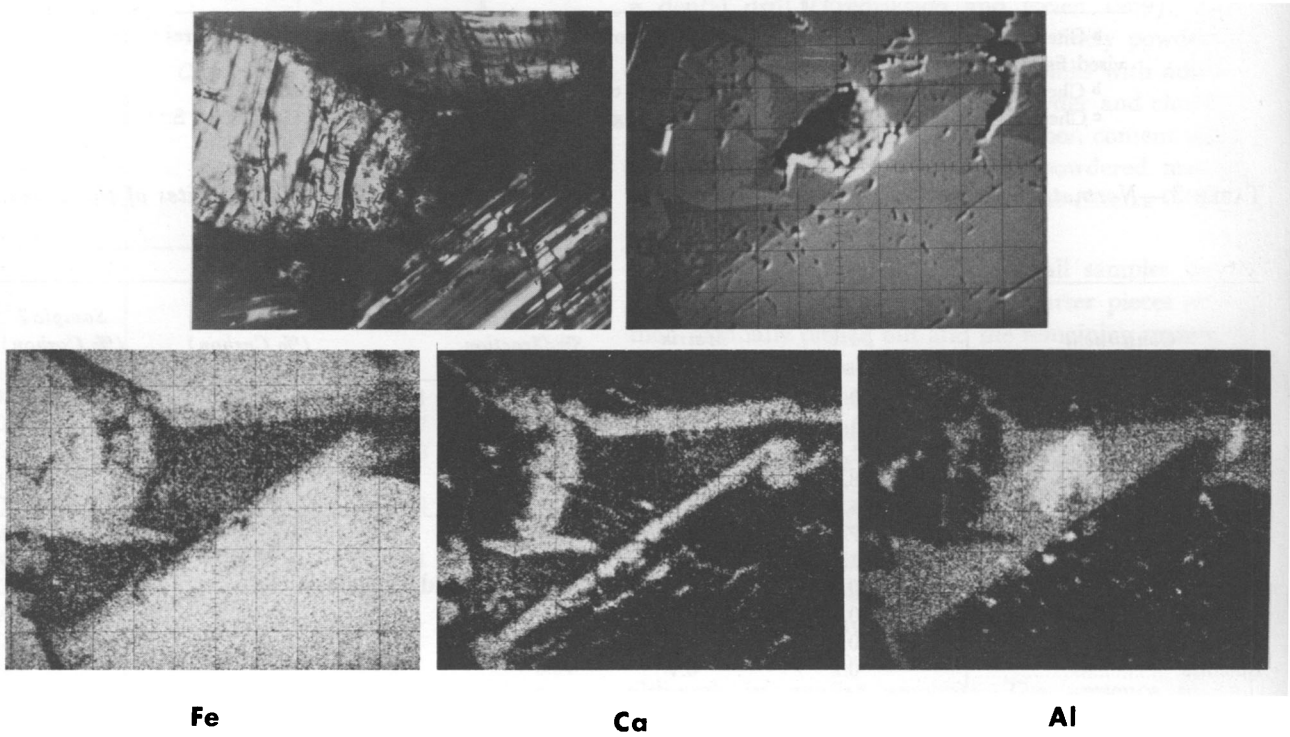

FIGURE 1.—Photomicrograph of twinned and untwinned pyroxene viewed by polarized transmitted light at 450×, upper left, the nearly correlative secondary electron emission photograph, upper right, and electron probe elemental scans, lower three photographs, of iron, calcium, and aluminum, moving from left to right.

curred on both twinned and untwinned crystals, and the rims had a uniform composition of $Wo_{34.9}Fs_{10.6}En_{54.5}$. This Ca-armoring noted on only some rhombic and monoclinic pyroxene grains seems to eliminate any significant equilibrating influence which might be attributed to thermal metamorphism.

The pyroxene crystals range in external shape from finely fibrous to the characteristic prismatic habit. The (110) cleavage and (010) partings are present on the numerous large distinct crystals. Orthopyroxene is most abundant, but half of the well-developed grains, although of similar composition, are clinopyroxene and these display what appears to be polysynthetic twinning. The grains are randomly oriented with the exception of the eccentrically radiating chondrules made of fibrous crystals. The large crystals, which attain a maximum length of 0.8 mm, are riddled with inclusions, and are length-slow with parallel extinction.

Oligoclase

Although oligoclase was not identified optically, the X-ray diffractograms suggest it to be a minor constituent. The recalculated normative composition also suggests that the dark matrix and devitrified glass in barred chondrules is in part Na-rich plagioclase.

Nickel-Iron

In reflected light, nickel-iron appears white, structureless, and in some grains bi-reflectant (possibly as a result of deformation). The alloy appears grey and nearly always isotropic under crossed nicols.

The maximum dimension of these irregularly shaped masses, which occur most frequently between the chondrules, is approximately 0.5 mm. The silicate chondrules appear to control the shape and distribution of the large metal grains, but smaller, rounded, nickel-iron particles are found in the matrix and are included in chondrules. It is generally inclusion-free and a limonitic alteration product usually exists around the perimeters of the grains.

A very limited microprobe study of the Fe-Ni phases was undertaken. Three tracks across two distinct grains were run at a speed of eight micron/minute (Figure 2). The intensities for both Fe Kα and Ni Kα were recorded while the pulses were simultaneously counted on the scalers at 10-second intervals. The taenite appeared Ni-deficient when compared to normal chondritic taenite, whereas the kamacite was rather high in Ni. Also, there were no low-Ni zones in the kamacite at the taenite-kamacite interfaces. This suggests that equilibration of the Ni-Fe was retained only through relatively high temperatures and that the metal was probably subject to rapid cooling across the taenite-kamacite phase boundary, thus restricting Ni diffusion.

Troilite

Plane polarized light reveals this iron sulfide to be distinctly yellow in color and slightly bi-reflectant. Its anisotropism is distinct, with colors ranging from silver-grey to brown revealing polycrystalline troilite as the typical texture. This accessory mineral, which usually occurs in close association with nickel-iron, attains maximum dimensions of approximately 0.5 mm. Like nickel-iron, the borders are highly irregular, and its distribution seems to be controlled by the surrounding silicate chondrules. Besides occurring as large, distinct masses within the matrix, minute grains are included in the chondrules and the larger of the nickel-iron fragments.

Chromite

The accessory chromite grains, which are grey, isotropic, and structureless, occur most commonly as extremely fine-grained aggregates within the matrix. They do, however, attain a maximum dimension of 0.2 mm when included in chondrules.

Matrix

The fine-grained, nearly isotropic matrix has very low bi-refringence and occurs as interstitial aggregates between chondrules. It does, however, merge with the boundaries of some fine-grained chondrules. Although the material could not be identified optically, the recalculated norm suggests it is principally pyroxene, plagioclase, and metallic iron.

Chondritic Texture

The Forest Vale meteorite is composed of olivine and pyroxene chondrules uniformly distributed throughout the stone and quite variable in their degree of crystallinity. They often range up to 1 mm in diameter,

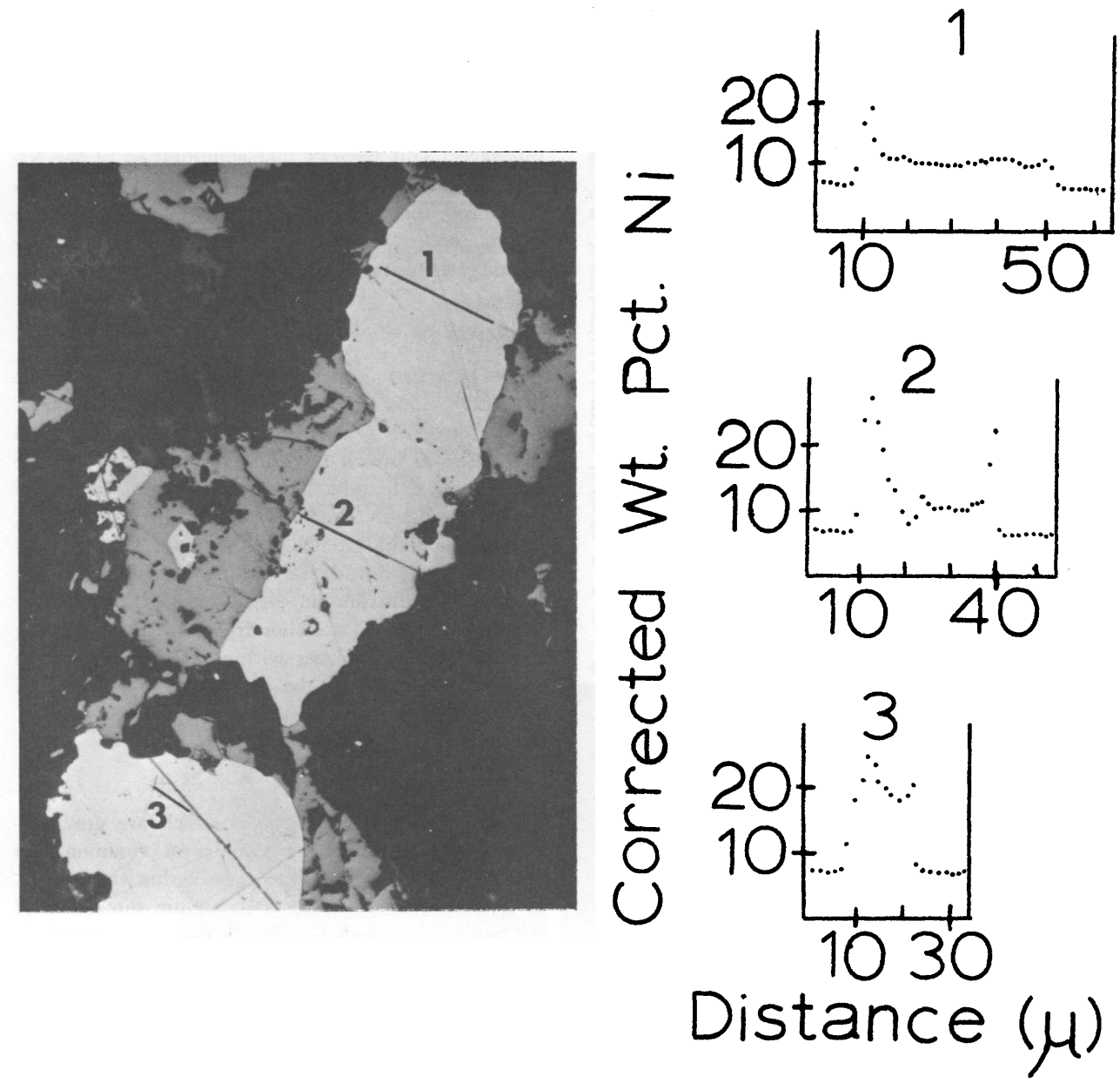

FIGURE 2.—Photomicrograph of nickel-iron observed at 190× and corresponding electron probe compositional tracks. The low nickel content of the taenite and the lack of Ni depletion in the kamacite at the taenite-kamacite interface is noteworthy.

retain their sphericity, and are set in a matrix of fine-grained crystallites and opaque minerals (Figure 3).

MODAL ANALYSIS

A total of 5000 points were counted on two polished thin sections. The mineralogical composition as calculated from the mode (in weight-percent) is: nickel-iron 14.2; chromite 0.5; troilite 4.2; olivine 20.9; pyroxene 15.6; and 44.6 percent fine-grained matrix material which could not be identified. The abundance of pyroxene is higher in the norm than in this mode, which suggests a large amount of the pyroxene exists as fine-grained groundmass material, or as fine-grained or glassy material within the chondrules, or

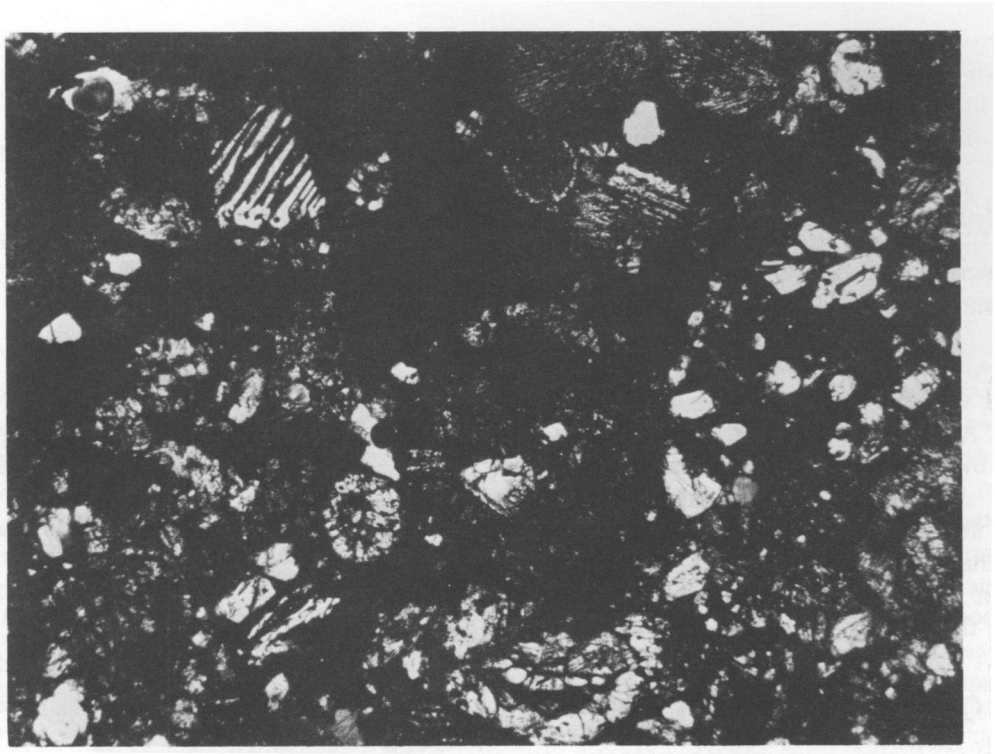

FIGURE 3.—Chondritic texture of the Forest Vale meteorite at 30× using polarized transmitted light.

both. Assuming that the insignificant amount of material was lost during polishing, and recalculating the norm with the elimination of nickel-iron, troilite, and silicates noted in the modal analysis, the fine-grained matrix material is probably rich in pyroxene, plagioclase, and metallic iron and poor in olivine (Table 3, column B). The gross similarity of the norms, however, seems to suggest that matrix and chrondules are cogenetic.

Classification

If the amount of nickel-iron and the ratio of MgO to FeO in the silicates are considered, as suggested by Prior (1920), the Forest Vale meteorite is an olivine-bronzite chondrite. With regard to both the total iron content and the oxidation state of the iron, it would be placed in the high-iron (H) group of Urey and Craig (1953), while the amount of reduced iron would place it in Wiik's group (1956) of chondrites with 15 percent to 19 percent metallic iron. The ratio Fe/Fe+Mg) in both olivine and pyroxene, as suggested by Keil and Fredriksson (1964), would again classify it as an H group chondrite. The Forest Vale meteorite corresponds to that of the petrologic type 4 in the chemical-petrologic classification of Van Schmus and Wood (1967). This group is characterized by well-developed chondrules, olivine and pyroxene of uniform or nearly uniform composition, and an abundance of clinopyroxene.

Conclusions

1. If not attributable to shock, the high-temperature nickel-iron and devitrified glass in barred chondrules indicate a brief cooling history for the chondrite.

2. Ca-rich coronas occurring on only some pyroxene grains indicate that the crystallization conditions were not identical for all fragments.

3. The presence of metal particles in, and adjacent to, chondrules, and the gross similarity in normative mineralogy of both matrix and included fragments suggest that although crystallization conditions were not identical they may have been nearly the same.

4. The degree of chondrule integration, the hetero-

geneous pyroxene, the high C content in the matrix and the high-temperature nickel-iron suggest accumulation and lithification of the genetically related fragments but with no subsequent metamorphism.

Acknowledgments

This manuscript is an extension of preliminary data gathered and submitted in thesis form by A. F. Noonan in partial fulfillment of the M.S. degree at the University of Tennessee. This initial research was carried out under a Smithsonian Research Foundation Grant. Additional costs for extended studies were supported by NASA and United States Air Force grants. We are indebted to the Department of Geology faculty at the University of Tennessee for an early review of the paper, and to Dr. Brian Mason of the Smithsonian Institution for many helpful suggestions throughout the study.

Literature Cited

Anders, E.
1964. Origin, Age and Composition of Meteorites. *Space Science Reviews,* 3:583–714.

Dodd, R. T.
1969. Metamorphism of the Ordinary Chondrites: A Review. *Geochimica et Cosmochimica Acta,* 33: 161–203.

Fredriksson, K., and K. Keil
1964. The Iron, Magnesium, Calcium, and Nickel Distribution in the Murray Carbonaceous Chondrite. *Meteoritics,* 2:201–217.

Fredriksson, K., and J. Nelen
1969. Carbon Distribution in Chondrites. *Meteoritics,* 4:271–272.

Hodge-Smith, T.
1942. A Fall of Meteorites at Forest Vale, New South Wales. *Australian Museum Magazine,* 8:45–48.
1943. A Shower of Meteoritic Stones at Forest Vale, New South Wales. *Australian Journal of Science,* 5:154–156.

Jarosewich, E.
1967. Analysis of Seven Stony Meteorites and One Iron with Silicate Inclusions. *Geochimica et Cosmochimica Acta,* 31:1103–1105.

Keil, K.
1967. The Electron Microprobe X-Ray Analyzer and its Application in Mineralogy. *Fortschritte der Mineralogie,* 44:4–66.

Keil, K., and K. Fredriksson
1964. The Fe, Mg, and Ca Distribution in Coexisting Olivines and Rhombic Pyroxenes in Chondrites. *Journal of Geophysical Research,* 69:3487–3515.

Kuno, H.
1954. Study of Orthopyroxene from Volcanic Rocks. *American Mineralogist,* 39:30–46.

Mason, B.
1963. Olivine Composition in Chondrites. *Geochimica et Cosmochimica Acta,* 27:1011–1023.

Moore, C. B., and C. F. Lewis
1967. Total Carbon Content of Ordinary Chondrites. *Journal of Geophysical Research,* 72:6289–6292.

Poldervaart, A.
1950. Correlation of Physical Properties and Chemical Composition in the Plagioclase, Olivine, and Orthopyroxene Series. *American Mineralogist,* 35: 1067–1079.

Prior, G. T.
1920. The Classification of Meteorites. *Mineralogical Magazine,* 19:51–63.

Urey, H. C., and H. Craig
1953. The Classification of the Stone Meteorites and the Origin of the Meteorites. *Geochimica et Cosmochimica Acta,* 4:36–82.

Van Schmus, W. R., and J. A. Wood
1967. A Chemical and Petrologic Classification for the Chondritic Meteorites. *Geochimica et Cosmochimica Acta,* 31:747–765.

Wahl, W.
1950. The Statement of Chemical Analysis of Stony Meteorites and the Interpretation of the Analysis in Terms of Minerals. *Mineralogical Magazine,* 29: 416–426.

Wiik, H. B.
1956. The Chemical Composition of Some Stony Meteorites. *Geochimica et Cosmochimica Acta,* 9:279–289.

Yoder, H. S., and T. G. Sahama
1957. Olivine X-Ray Determinative Curve. *American Mineralogist,* 42:475–491.

Roy S. Clarke, Jr.
and Eugene Jarosewich

Iron Meteorite Compositions

During the past several years chemical analyses for the elements nickel, cobalt, and phosphorus have been performed on twelve meteorite specimens from the Smithsonian collection. Classification or curatorial considerations have normally prompted individual investigations. The data are summarized in the accompanying table in order to make them available to others.

Recent analyses of four of these same meteorites have been given by Moore et al. (1969), and their paper includes a general discussion of the problems of iron meteorite analysis. Our results on these four meteorites are in excellent agreement with their results. Nickel analyses have also been performed on all twelve of these meteorites by Wasson as part of his comprehensive study of chemical groupings among iron meteorites (John T. Wasson, personal communication, 1970). Agreement is again good, but it was noted that our nickel values are normally 0.1 to 0.2 percent higher than Wasson's. Older analyses of these meteorites and references to descriptive papers are cited by Hey (1966).

Roy S. Clarke, Jr. and Eugene Jarosewich, Department of Mineral Sciences, Division of Meteorites, National Museum of Natural History, Smithsonian Institution, Washington, D.C. 20560.

TABLE 1.—*Chemical analyses for nickel, cobalt, and phosphorous on twelve meteorite specimens from the Smithsonian collections*

Name	*NMNH cat. no.*	*Structure class**	*Weight percent*			*Notes*
			Ni	*Co*	*P*	
Angelica, Wisconsin	2177	Om	7.50	0.50	0.11	
Arlington, Minnesota	627	Om	8.55	0.41	0.02	(1)
Bodaibo, Siberia	2149	Of	8.05	0.36	0.04	(1)(4)
Cacaria, Mexico	1480	Om	7.74	0.46	0.11	
Cruz del Aire, Mexico	1441	Of	9.19	0.50	0.30	(1)
Cumpas, Mexico	1591	Om	8.14	0.47	0.18	
Elbogen, Bohemia	309	Om	10.25	0.64	0.22	
El Capitan, New Mexico	2754	Om	8.80	0.48	0.43	
Monahans, Texas	1303	D	10.79	0.52	0.09	(1)(2)(3)
New Westville, Ohio	1412	Of	9.38	0.34	0.18	
Obernkirchen, Germany	1611	Of	7.67	0.36	0.02	
St. Genevieve County, Missouri	454	Of	7.96	0.36	0.24	(2)(5)

* Buchwald and Munck (1965).
(1) Recent analysis reported by Moore et al. (1969).
(2) Recent analyses reported by Wasson (1967).
(3) A doubtful analysis for Ni in Monahans was reported by Cobb (1967).
(4) Analysis reported by Dyakonova and Kharytonova (1963).
(5) Recent analyses reported by Lewis and Moore (1971).

All of the meteorites in this group are finds and have, therefore, been subjected to varying degrees of terrestrial weathering. In each case material was carefully selected to be free of oxidation and obvious inclusions. Samples were in the size range of 1.2 to 3.0 g, large enough to be representative of the metallic phases. They were dissolved in an HCl-HNO_3 mixture, and then evaporated to dryness several times with HCl. Residues were taken up with 5 ml of concentrated HCl, diluted with H_2O and filtered into a 100 ml volumetric flask. Appropriate aliquots were taken for the determination of nickel, cobalt, and phosphorus. Nickel was precipitated with dimethylglyoxene and determined gravimetrically, cobalt spectrophotometrically with nirosto-R salt, and phosphorus spectrophotometrically using the molybedenum blue method (Moss et al., 1961).

Literature Cited

Buchwald, V. F., and Sole Munck
1965. Catalogue of Meteorites. *Analecta Geologica,* 1: 1–81.

Cobb, James C.
1967. A Trace-Element Study of Iron Meteorites. *Journal of Geophysical Research,* 72:1329–1341.

Dyakonova, M. Y., and V. Y. Kharytonova
1963. Composition of Nickel-Iron in Some Iron and Stony-Iron Meteorites of Various Types. *Meteoritika,* 23:42–44.

Hey, Max H.
1966. *Catalogue of Meteorites.* lxviii+637 pages. The British Museum (Natural History).

Lewis, Charles F., and Carleton B. Moore
1971. Chemical Analyses of Twenty-eight Iron Meteorites. *Meteoritics,* 6:195–205.

Moore, Carleton B., Charles F. Lewis, and David Nava
1969. Superior Analyses of Iron Meteorites, in *Meteorite Research.* P. M. Millman, editor. Pages 738–748. Dordrecht, Netherlands: D. Reidel Publishing Company.

Moss,, A. A., M. H. Hey, and D. I. Bothwell
1961. Methods for the Chemical Analysis of Meteorites: I. Siderites. *Mineralogical Magazine,* 32:802–816.

Wasson, John T.
1967. The Chemical Classification of Iron Meteorites: I. A Study of Iron Meteorites with Low Concentrations of Gallium and Germanium. *Geochimica et Cosmochimica Acta,* 31:161–180.

Roy S. Clarke, Jr., Eugene Jarosewich, and Joseph Nelen

The Nejo, Ethiopia, Meteorite

A stony meteorite fell 16 km due west of Nejo, near the village of Jarso, Wollega Province, Ethiopia, at 11:30 a.m. local time on May 11, 1970. The coordinates of the fall site are 9°30′N, 35°20′E. The fall was observed by local residents and reported to Professor Pierre Gouin, Director, Geophysical Observatory, Haile Selassie I University, Addis Ababa, Ethiopia. Professor Gouin visited the site and reported obtaining three pieces weighing a total of 2.4 kg that had been recovered, apparently from an individual stone. The stone had made a small hole in hard ground, and he estimated that its impact weight was 4–4.5 kg.

Professor Gouin's reports on the meteorite fall and visit to the site were circulated by the Smithsonian Institution Center for Short-Lived Phenomena on July 23, 1970, and August 4, 1970. On July 21, 1970, Professor Gouin sent the Smithsonian Institution a 287 g specimen (NMNH 5420) of the Nejo meteorite to be made available for time-dependent research. Material was distributed for this purpose to Edward Fireman, Smithsonian Astrophysical Observatory, Cambridge, Massachusetts 02138, Louis A. Rancitelli, Battelle Memorial Institute, Richland, Washington 99352, and G. D. O'Kelley, Oak Ridge National Laboratory, Oak Ridge, Tennessee 37830. Reports on these investigations will appear elsewhere. We have undertaken a brief mineralogical and chemical characterization that will be summarized here. A detailed petrographic investigation is being undertaken by Dr. Bill Moreton, Geology Department, Haile Selassie I University, Addis Ababa.

Roy S. Clarke, Jr., Eugene Jarosewich, and Joseph Nelen, Department of Mineral Sciences, National Museum of Natural History, Smithsonian Institution, Washington, D.C. 20560.

Mineralogy and Chemistry

The Nejo meteorite is a hypersthene chondrite, an L6 meteorite in the classification of Van Schmus and Wood (1967). It is coarsely crystalline with a recrystallized matrix, and no distinct chondrules were observed. The olivine and pyroxene were examined by the electron microprobe and found to be equilibrated. The olivine compositions clustered closely around 25 mole percent fayalite (Fa_{25}) and the pyroxene around 20 mole percent ferrosilite (Fs_{20}). Plagioclase, chlorapatite, and chromite were identified by the microprobe and the troilite was observed to be essentially free of nickel. The presence of both kamacite and taenite was observed microscopically on etched polished sections and confirmed by the microprobe. Kamacite and taenite occur as individual grains, in association with one another, and in association with troilite. Troilite grains are comparatively large and monocrystalline or coarsely crystalline. The larger kamacite grains frequently contain slightly distorted Neumann bands. Evidence of strong shock appears to be lacking.

Our specimen contained a small area of well-developed fusion crust. The vesicular glass crust ranged up to 0.3 mm thick and was seen in polished section to contain precipitated magnetite. It is underlain by a zone injected with sulfide veins penetrating as far as 1 mm below the surface (Ramdohr 1967). Within this zone, particularly near the surface, are

TABLE 1.—*Chemical composition of the Nejo, Ethiopia, meteorite, NMNH 5420* (Eugene Jarosewich, analyst)

Constituent	*Percent*
Fe	7.10
Ni	1.27
Co	0.06
FeS	6.47
SiO_2	39.98
TiO_2	0.12
Al_2O_3	2.27
Cr_2O_3	0.56
FeO	14.22
MnO	0.32
MgO	24.83
CaO	1.82
Na_2O	0.92
K_2O	0.10
P_2O_5	0.24
$H_2O(+)$	<0.1
$H_2O(-)$	0.03
C	0.01
Total	100.32
Total Fe	22.26
D(g/cm^3)	3.59

eutectic structures resulting from the melting of metallic phases and troilite. Kamacite grains throughout this zone have been transformed to alpha-2 structure, indicative of heating to temperatures around 500°C.

The bulk chemical analysis of the Nejo meteorite, typical of hypersthene chondrites, is given in the accompanying Table 1. The analytical procedures employed are outlined in an earlier paper (Jarosewich 1966).

Literature Cited

Jarosewich, Eugene
1966. Chemical Analyses of Ten Stony Meteorites. *Geochimica et Cosmochimica Acta,* 30:1261–1265.

Ramdohr, Paul
1967. Die Schmelzkruste der Meteoriten. *Earth and Planetary Science Letters,* 2:197–209.

Van Schmus, W. R., and J. A. Wood
1967. A Chemical-Petrologic Classification for the Chondritic Meteorites. *Geochimica et Cosmochimica Acta,* 31:747–765.

Joseph A. Nelen
and Kurt Fredriksson

The Nakhon Pathom Meteorite

ABSTRACT

The Nakhon Pathom meteorite from Thailand has been chemically analyzed and found to be an olivine-hypersthene chondrite, belonging to the L-group, with 24 mole percent Fe_2SiO_4 in olivine and 21 mole percent $FeSiO_3$ in orthopyroxene. It shows dark-light structure of light gray areas surrounded by dark gray bands, probably caused by hypervelocity shock. The chemical composition of both parts is similar.

Introduction

The meteorite fell on December 21, 1923, at about 2100 hours. It was found in the province of Nakhon Pathom, Thailand, probably shortly after the fall, since it is fresh and unaltered. The place (13°44′N, 100°05′E) is a swampy area in the Don Yai Nom subdistrict about 10 kilometers south-south-east of the town of Nakhon Pathom. Two stones were placed in a case of curios in the National Museum in Bangkok, because of their unusual properities. When Dr. and Mrs. Edward P. Henderson were visiting Thailand in 1960, Mrs. Henderson saw the stones and suspected them to be of meteoritic origin. The picture showing both stones (Figure 1) was taken at that time by Dr. Henderson. Eventually, the smaller stone was loaned to the United States National Museum for study. Mason (1967) has described the meteorite briefly, giving full data and olivine composition. It is not otherwise reported in the literature. The main mass is in the National Museum in Bangkok, Thailand. The United States National Museum has 413 grams of the smaller piece in its collection (NMNH 3192).

The total weight of the two pieces was 32.2 kilograms. The meteorite shows light-dark structure, the density of the lighter part being 3.56 gm/cc of the darker part, 3.51 gm/cc. The average density of a piece containing 41% dark material and 59% light is 3.53. Stones with a light-dark structure were first described by Reichenback (1865). Similar meteorites include Walters (Roy et al. 1962), Ställdalen (Fredriksson et al. 1963), and Lanzenkirchen (Kurat and Kurzweil 1965).

Description

The meteorite Nakhon Pathom broke in two pieces. The smaller piece, weighing 9.6 kilograms, is covered on two sides with a dark brown fusion crust 2 millimeters thick. The side oriented toward the front during the fall shows well-formed "thumbprints," covered by a smooth dull crust (Figure 2). The back side is flat and is covered with a rougher crust, traversed by cracks.

A cross-section (Figure 3) shows a brecciated structure of light gray material surrounded by areas of darker gray. In the darker parts many smaller round to angular light gray bodies can be observed. The lighter parts are broken pieces of a well-crystallized chondrite. They contain only a few recognizable chondrules or parts of chondrules, strongly intergrown with the coarsely crystalline matrix (Figure 4). The chondrules and crystals show strong mechanical deformation. The cracks are frequently filled with droplets or angular particles of troilite and nickel-

Joseph A. Nelen and Kurt Fredriksson, Department of Mineral Sciences, National Museum of Natural History, Smithsonian Institution, Washington, D.C. 20560.

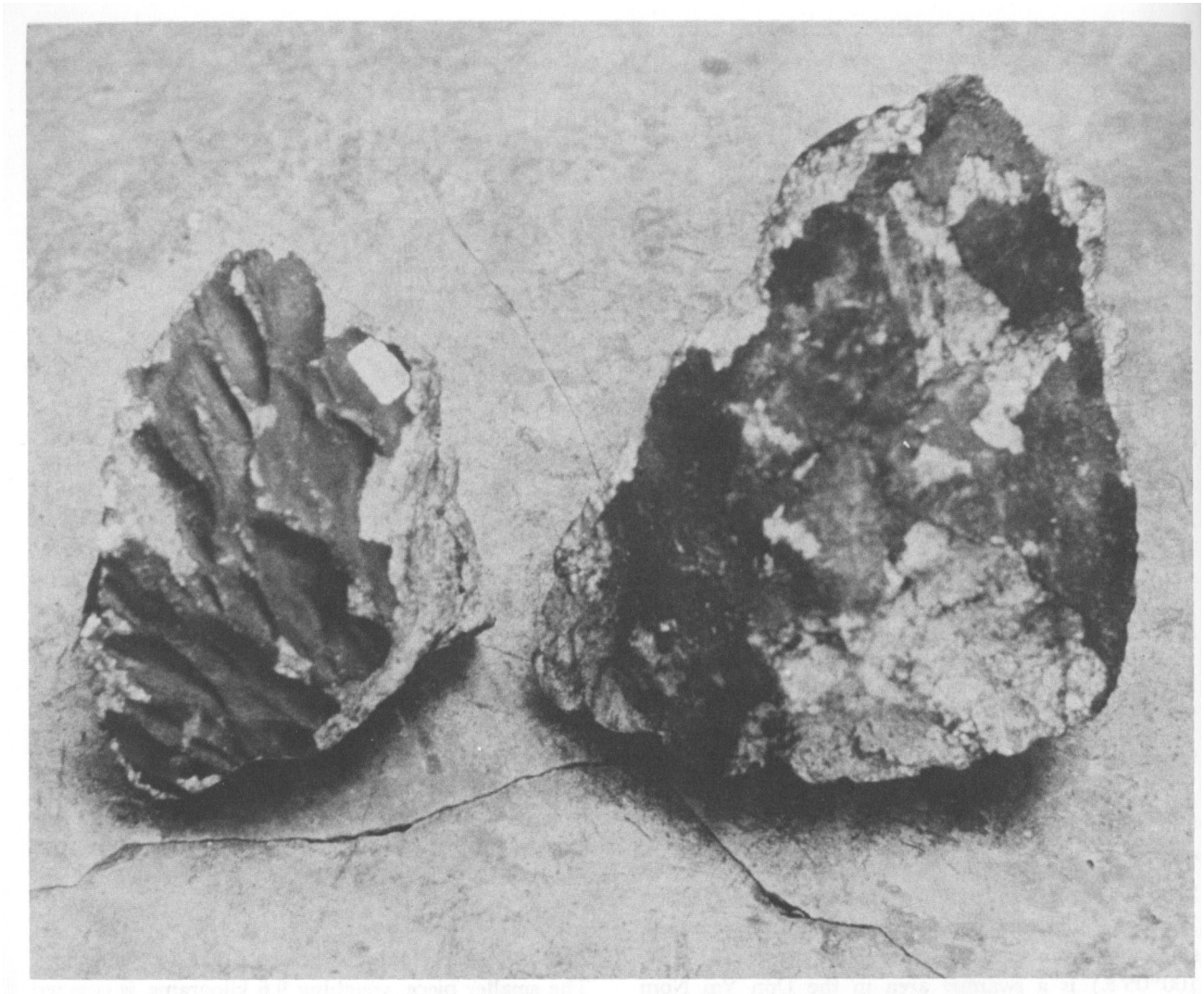

FIGURE 1.—The two pieces of the Nakhon Pathom meteorite in the National Museum, Bangkok, Thailand (smaller stone 210 × 160 mm).

iron. The black veins penetrating the lighter mass consist mostly of comminuted silicates and opaque minerals.

Mineralogy

The minerals identified in a polished thin section of the meteorite are olivine, orthopyroxene, clinopyroxene, plagioclase, whitlockite, chromite, kamacite, and taenite.

Olivine is mostly xenomorphic, has a wavy extinction, and is often, especially in the dark part, mixed with nickel-iron and troilite. The composition in both dark and light parts as determined by electron microprobe analysis is given in Table 1.

The average fayalite content, Fa_{24}, is the same as that given by Mason (1967) who obtained his figure by X-ray diffraction. Orthopyroxene is also mostly xenomorphic, shows strong wavy extinction, and is mixed with nickel-iron and troilite in the same manner as olivine. The composition is given in Table 2; it averages 21 mole percent $FeSiO_3$.

Most of the clinopyroxene exhibits similar properties. A little calcium-rich clinopyroxene was also observed. Plagioclase with wavy extinction occurs occasionally as interstitial grains, both in chondrules

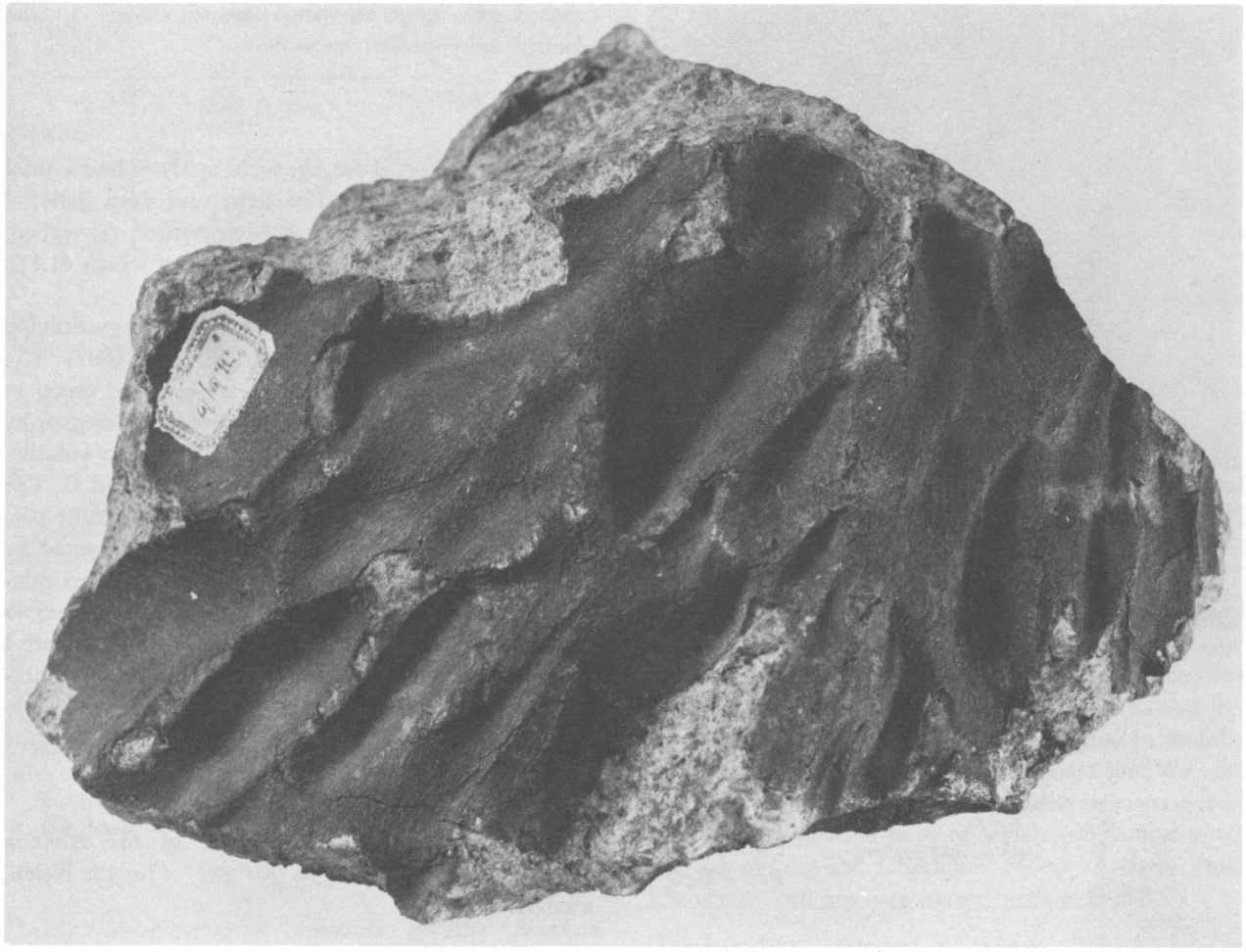

FIGURE 2.—The smaller piece of the Nakhon Pathom meteorite, showing comparatively thick fusion crust and prominent regmaglypts (210 × 160 mm).

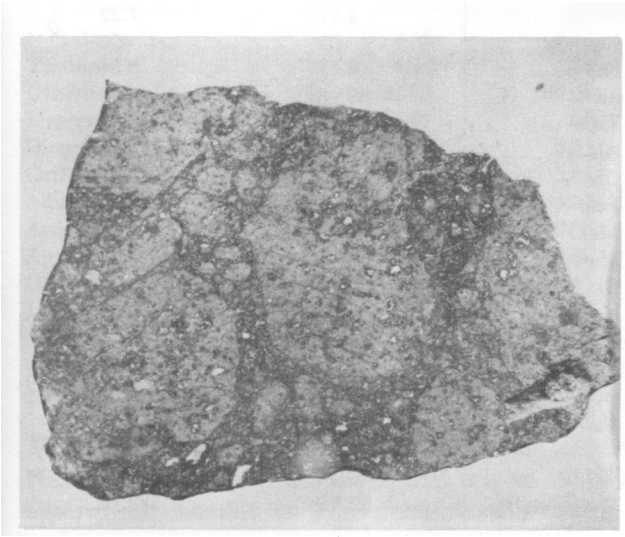

and in the groundmass. Whitlockite is common as interstitial crystals or aggregates of fairly large size, especially in the light gray areas. Chromite occurs together with nickel-iron and troilite, as well as intergrown with silicates; it is fairly large and almost xenomorphic. Troilite is mixed with nickel-iron in the larger aggregates. Separately it occurs as small droplets and irregular-shaped aggregates in the interstices of the silicates. Kamacite and taenite occur separately from each other and could not be distin-

FIGURE 3.—Polished surface on the main mass of the Nakhom Pathom meteorite, showing prominent light-dark structure, together with veining and brecciation (130 × 90 mm).

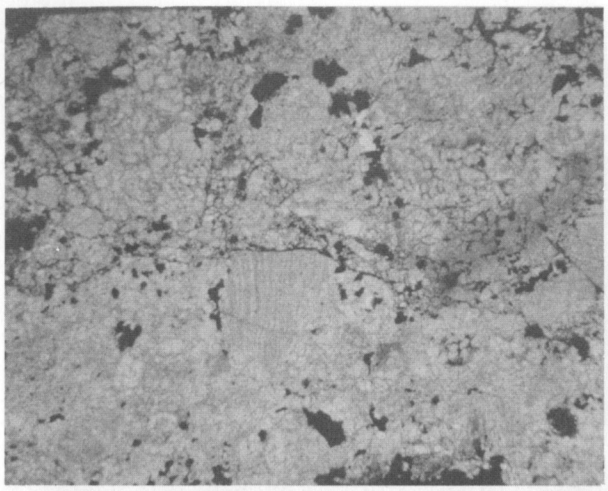

FIGURE 4.—Photomicrograph of thin section of the Nakhon Pathom meteorite in ordinary light. The dark part, upper half, has barely recognizable chondrules and a brecciated texture. In the light, lower part chondrules and matrix are almost entirely intergrown. The black areas consist of nickel-iron and troilite. The length of the section is 9 mm.

TABLE 1.—*Olivine composition of the Nakhon Pathom meteorite in light and dark portions*

Area	*FeO weight percent*		$\frac{FeO}{FeO+MgO}$
	Range	*Average**	*Mole percent Fa*
Light	21.9–22.5	22.2	24.0
Dark	21.9–23.4	22.5	24.3

* The averages represent ten to fifteen grains with about three to four measurements in each grain.

TABLE 2.—*Orthopyroxene composition of the Nakhon Pathom meteorite in light and dark portions*

Area	*FeO weight percent*		$\frac{FeO}{FeO+MgO+CaO}$
	Range	*Average**	*Mole percent Fs*
Light	13.8–14.7	14.2	21.1
Dark	13.9–14.8	14.2	21.2

* The averages represent ten to fifteen grains with one to three analyses in each grain.

guished microscopically, but were identified with the electron microprobe.

Chemistry

The sample selected for chemical analyses had a total weight of 18.8 grams. The light and dark material was carefully separated and each portion reweighed. Total recovery was about 18.6 grams of which 41.1% was dark and 58.9% light.

Each portion was analyzed separately by techniques previously described by Jarosewich (1966, 1967). The results are expressed as oxides, troilite, and metal in Table 3. The elemental composition with oxygen by difference and the elements calculated on a volatile-free basis are given in Table 4 under A and B. The normative mineral content, expressed as weight percentages in Table 5, was calculated as suggested by Wahl (1950). It agrees well with the observed mineral abundances. The phosphorus was calculated as apatite. Microscopic observation and semiquantitative microprobe measurements indicate that the phosphorus mineral is whitlockite. The titanium is probably associated with the silicate phases, since ilmenite was not found.

TABLE 3.—*Chemical composition of the Nakhon Pathom meteorite (weight percent)* (Joseph Nelen, analyst)

Constituent	*Dark portion 41.06%*	*Light portion 58.94%*
Fe	7.08	8.15
Ni	1.17	1.22
Co	.05	.06
FeS	6.46	5.84
SiO_2	39.98	40.00
TiO_2	0.17	0.17
Al_2O_3	1.81	1.79
Cr_2O_3	0.60	0.51
FeO	13.52	13.26
MnO	0.31	0.31
MgO	24.71	24.45
CaO	1.84	1.83
Na_2O	0.98	0.97
K_2O	0.10	0.10
P_2O_5	0.26	0.24
H_2O+	0.58	0.66
H_2O-	0.07	0.04
C	0.08	0.14
Total	99.77	99.74
Fe (Total)	21.69	22.17

TABLE 4.—*Elemental composition of the Nakhon Pathom meteorite*

Constituent	*Dark portion*		*Light portion*	
	A	*B*	*A*	*B*
H	0.07		0.08	
C	0.08		0.14	
O	37.04		36.90	
Na	0.73	1.21	0.72	1.19
Mg	14.90	24.70	14.75	24.32
Al	0.96	1.59	0.95	1.57
Si	18.69	30.98	18.70	30.83
P	0.11		0.10	
S	2.36		2.13	
K	0.08	0.13	0.08	0.13
Ca	1.32	2.19	1.31	2.16
Ti	0.10	0.16	0.10	0.16
Cr	0.41	0.67	0.35	0.58
Mn	0.24	0.40	0.24	0.40
Fe	21.69	35.95	22.17	36.55
Co	0.05	0.08	0.06	0.10
Ni	1.17	1.94	1.22	2.01
Total	100.00	100.00	100.00	100.00

A. Chemical analysis in weight percent of the elements, with oxygen to bring the sum to 100.

B. Atomic percent of the elements on a volatile (C,H,O, S)-free basis.

TABLE 5.—*Normative minerals of the Nakhon Pathom meteorite (weight percent)*

Constituent	*Dark portion*	*Light portion*
Nickel-iron	8.30	9.43
Troilite	6.46	5.84
Olivine (Fa 24)	41.14	39.40
Hypersthene (Fs 21)	26.07	27.38
Diopside	5.81	5.83
Orthoclase	0.61	0.61
Albite	8.20	8.17
Anorthite	0.22	0.22
Apatite	0.60	0.57
Chromite	0.95	0.83
Ilmenite	0.32	0.32

Summary

The chemical and mineralogical composition of the Nakhon Pathom meteorite shows that it is an olivine-hypersthene chondrite in Prior's classification (1920). The total iron content, about 22 percent, places it in the low-iron (L) group of Urey and Craig (1953). The olivine composition, Fa_{24}, determined by microprobe analysis, also confirms that this meteorite is an L-group chondrite (Keil and Fredriksson 1964). The minerals present are the same in the light and dark parts both according to microscopic observations and chemical composition. The microprobe analyses appear to show a slightly higher iron content and more variability for olivines in the dark portion. The difference, however, is practically within the limits of analytical error and is not considered significant. The bulk chemical composition, Table 3, is also similar in both parts and the meteorite may therefore be classified as a monomict breccia (Wahl 1952).

The meteorite was severely shocked. The dark and light structure and the black veins, containing small troilite bodies, are similar to the black veins and the darkening produced in the gray chondrite Ställdalen by artificial shock as described by Fredriksson et al. (1963).

It should also be noted that the carbon content is lower in the dark part than in the light (Table 3), and consequently the dark color is not caused by carbon as suggested by Wlotzka (1963) for the Pantar meteorite. The carbon values are averages of five analyses of each part, of which two of each were carried out by Dr. Charleton Moore, Arizona State University. All analyses agreed with ±0.03%C.

Acknowledgments

We wish to thank Dr. Louis Walter and Dr. Brian Mason for their critical review of the paper.

Part of the expenses of this paper have been met by grants from the National Aeronautics and Space Administration (Grant NsG–688) and the United States Air Force (Contract AF19(628)–5552).

Literature Cited

Fredriksson, K., P. S. De Carli, and A. Aaramae
1963. Shock-Induced Veins in Chondrites. *Space Research* III:974–983. North Holland Publishing Company, Amsterdam.

Jarosewich, E.
1966. Chemical Analyses of Ten Stony Meteorites. *Geochimica et Cosmochimica Acta,* 30:1261–1265.
1967. Chemical Analyses of Seven Stony Meteorites and One Iron with Silicate Inclusions. *Geochimica et Cosmochimica Acta,* 31:1103–1106.

Keil, K., and K. Fredriksson
1964. The Iron, Magnesium and Calcium Distribution in Coexisting Olivines and Rhombic Pyroxenes of Chondrites. *Journal of Geophysical Research,* 69:3487–3515.

Kurat, G., and H. Kurzweil
1965. Der Meteorit von Lanzenkirchen. *Annalen des Naturhistorischen Museums in Wien,* 68:9–24.

Mason, B.
1965. The Chemical Composition of Olivine-Bronzite and Olivine-Hypersthene Chondrites. *American Museum Novitates,* 2223:38.
1967. Olivine Composition in Chondrites—A Supplement. *Geochimica et Cosmochimica Acta,* 31: 1100–1103.

Prior, G. T.
1920. The Classification of Meteorites. *Mineralogical Magazine,* 19:51–63.

Reichenbach, C. V.
1865. Die schwarzen Linien und Ablosungen in den Meteoriten. *Poggendorff's Annales der Physik und Chemie,* 125:308–325, 420–441, 600–618.

Roy, S. K., J. J. Glass, and E. P. Henderson
1962. The Walters Meteorite. Chicago National History Museum Fieldiana. *Geology,* 10:539–550.

Urey, H. C., and H. Craig
1953. The Composition of the Stone Meteorites and the Origin of the Meteorites. *Geochimica et Cosmochimica Acta,* 4:36–82.

Wahl, W.
1950. The Statement of Chemical Analyses of Stony Meteorites and the Interpretation of the Analyses in Terms of Minerals. *Mineralogical Magazine,* 29:416–426.
1952. The Brecciated Stony Meteorites and Meteorites Containing Foreign Fragments. *Geochimica et Cosmochimica Acta,* 2:91–117.

Wlotzka, F.
1963. Uber die Hell-Dunkel-Structur der urgashaltigen Chondrite Breitscheid and Pantar. *Geochimica et Cosmochimica Acta,* 27:419–429.

MINERALOGY

J. J. Gurney

Gorceixite in the Buffels River, Namaqualand, South Africa

Gorceixite is a hydrated basic phosphate of barium and aluminium of uncertain formula but approximating to $[BaAl_3(PO_4)_2(OH)_5H_2O]$ (Hussak 1906). The mineral has been reported to be present in carbonatites such as Mrima Hill, Kenya, (Binge and Joubert 1966), but is better documented as a "Fava" or pebble in the diamantiferous gravels of Brazil, British Guiana, West Africa, Rhodesia, and now South Africa. Gorceixite is of no economic value in itself but is generally thought to be a good indicator of the presence of diamonds (Beard 1941).

In Brazil the mineral has been reported to occur as pebbles in the diamantiferous gravels of the rivers Abiete Bagagem and Douradinhos in the Minas Geraes, the Paranhijba and Verissimo in Goyaz, and the Patrocinio de Sapucahy and the Canoas in São Paulo. Gorceixite has also been reported to be associated with diamonds at Issineru, British Guiana; Bonsa River, Gold Coast; Oiyi District, Sierra Leone; and at Somabula, Rhodesia (Palache, Berman, and Frondel 1951). More recently it has been discovered in the Bongou River in French Equatorial Africa (Miller 1959).

Pebbles of gorceixite contain some impurities, usually of silica, iron, and titanium. Calcium and the rare earth elements may substitute for barium and a strontium analogue of the mineral (goyazite) has been reported from the same gravel deposits.

The pebbles found in the Buffels River were obtained from the heavy mineral concentrate of the diamond mining operations of the Buffelsbank Diamante Edms. Bpk. This company is recovering diamonds from a quaternary drainage channel of the Buffels River in the Spektakel Valley, west of Springbok, Namaqualand.

The pebbles range from greyish white to light brown to dark brown and are up to 2 cm across. An analysis of a light brown pebble is given in Table 1. This pebble had a porcelaneous fracture, hardness of about 6, specific gravity of 3.14, and vitreous lustre. An X-ray diffractogram confirmed that the mineral was gorceixite.

In the analysis reported, some calcium, strontium, and rare earth substitution of barium is apparent. Neither the ideal formula, nor that suggested as an alternative by Palache, Berman, and Frondel (1951) are identical to the analytical result seen after the obvious impurities are ignored (see Table 1).

The source of the gorceixite in the Buffels River is unknown and there is no reported association between gorceixite and diamond except in river gravels. It seems probable that similarity in specific gravity was the chief agent in bringing the two minerals into close association in this environment. Possibly gorceixite is more common than might be supposed from its sparsely reported occurrences. It is unimpressive in appearance and can easily be overlooked.

Acknowledgments

The author would like to thank Mssrs F. Hoffman and F. Mostert, Managing Director and Mine Manager of the Buffelsbank Diamante Edms. Bpk, for

J. J. Gurney, Department of Mineral Sciences, National Museum of Natural History, Smithsonian Institution, Washington, D.C. 20560.

TABLE 1.—*Analysis of gorceixite from the Buffels River, Cape Province, South Africa*

Constituent	*Chemical anlaysis (weight percent)*			
	*1** $BaAl_3(PO_4)_2(OH)_5H_2O$	*2** *Gorceixite Buffels River*	*3** *Recalculated less impurities*	*4** $BaAl_4(PO_4)_2(OH)_5H_2O$
BaO	29.98	23.38	25.12	26.02
CaO		0.92	1.00	
Total R. E.		1.71	1.86	
SrO		1.50	1.62	
Al_2O_3	29.96	27.64	29.70	34.59
P_2O_5	27.75	19.76	21.23	24.10
H_2O+	12.31	16.11	17.11	15.29
SiO_2		2.63	Impurities	
TiO_2		0.95		
Fe_2O_3		2.49		
Na_2O		0.29		
K_2O		0.15		
H_2O-		0.32		
Total	100.00	97.85	97.64	100.00

* Column *1:* Theoritical composition.

Column *2:* New analysis, J. J. Gurney.

Column *3:* Recalculation after subtraction of probable impurities (SiO_2, TiO_2, Fe_2O_3, Na_2O, K_2O, H_2O-).

Column *4:* Ideal composition.

submitting the samples investigated for examination. Permission to publish the results was kindly granted by the Board of Directors of the operating company and the X-ray diffraction work was carried out by P. Hofmeyr.

Literature Cited

Beard, E. H.
1941. Recent Discoveries of Gorceixite. *Bulletin of Imperial Institute,* 39(2):160–164.

Binge, J, and P. Joubert
1966. The Mrima Hill Niobium Deposit, Coast Province Kenya. *Information Circular No. 2 Republic of Kenya Geological Survey.*

Hussak, E.
1906. Uber die Sogenannten 'Phosphat—Favas' der Diamantfuhrenden Sande Brasiliens. *Mineralogische und Petrographische Mittheilungen,* 25:336.

Miller, M.
1959. Sample Submitted to Smithsonian Institution 3/2/59. Locality Bongou River, French Equatorial Africa.

Palache, C., H. Berman, and C. Frondel
1951. *Dana's System of Mineralogy,* 7th edition, 2:833. New York: John Wiley and Sons.

Brian Mason

Tocornalite

In 1968 I received from Sir Maurice Mawby (Melbourne, Australia) a mineral specimen from Broken Hill, New South Wales, for identification. The mineral for identification filled a small cavity in a coralloid mass of embolite; it was soft, mealy, bright yellow in color but extremely photosensitive, rapidly turning gray-green and then black on exposure to bright light. Sir Maurice had obtained it in 1922 from the underground manager of the Block 14 mine at Broken Hill (the Block 14 mine is now part of the North Broken Hill property).

The association with embolite and the photosensitivity immediately suggested a silver halide. However, an X-ray powder photograph gave a distinctive pattern (Table 1) which could not be matched with any of the silver halides in the ASTM index. On checking against the silver halide minerals in the literature, my attention focused on the obscure mineral tocornalite, as described in Palache et al. (1951):

> A name given to a supposed iodide of silver and mercury found with other ill-defined chloride-iodides of silver and mercury at Chanarcillo, Chile. Granular massive. Color pale yellow, becoming darker on exposure. Streak yellow. An analysis of impure material gave Ag 33.80, Hg 3.90, I 41.77, siliceous residue 16.65, total 96.12; the loss is due to some water belonging in the residue, and probably some iodine. A mineral referred to tocornalite was found at the Proprietary Mine, Broken Hill, New South Wales, as a deep yellow powder, blackening in sunlight, associated with iodyrite and cinnabar.

In the mineral collection of this department was one small specimen (No. C906) labeled "Tocornalite, Chanarcillo, Chile"; material from this specimen gave an X-ray powder photograph identical with that from the Broken Hill specimen.

The published identification of tocornalite at Broken Hill was the work of Mr., George Smith (1926), who was associated with the mines for many years from 1888 onward, first as an ore buyer and assayer, then as a mine manager, and subsequently as Inspector of Mines for twenty-one years. It is eloquent testimony to his discerning eye and his mineralogical knowledge that he was able to recognize tocornalite in the Broken Hill material from the description of the Chilean mineral published many years earlier. The Proprietary Mine, from which his material came, was contiguous with the Block 14 Mine.

Tocornalite was described by Ignacio Domeyko in 1867. I have attempted to find type material of this mineral, both in Chilean and in European collections, without success. However, the Chanarcillo specimen in our collection does correspond well with the origi-

TABLE 1.—*X-ray powder photograph of tocornalite, Broken Hill, Australia (Cu Kα radiation, intensities visually estimated)*

Line	*Intensity*	*d-spacings*
1	7	6.37
2	2	4.67
3	2	4.51
4	9	3.76
5	9	3.61
6	1	3.39
7	4	3.29
8	4	3.19
9	3	2.998
10	4	2.894
11	10	2.644
12	1	2.468
13	2	2.309
14	7	2.254
15	3	2.127
16	5	2.036
17	4	1.877
18	2	1.834
19	2	1.743
20	3	1.695
21	4	1.634
22	3	1.583

Brian Mason, Department of Mineral Sciences, National Museum of Natural History, Smithsonian Institution, Washington, D.C. 20560.

nal description. Unfortunately, neither in this specimen nor in the Broken Hill material is there sufficient tocornalite for a quantitative chemical analysis to check the composition arrived at by Domeyko. Experiments at synthesizing this mineral have so far been unsuccessful; a variety of products has been obtained by precipitating mixed silver and mercury solutions with potassium iodide, but none of the precipitates has given an X-ray powder photograph agreeing with that of tocornalite. Attempts at indexing the powder photograph of tocornalite and thereby determining its crystal system, cell dimensions, and ultimately its structure have also been unsuccessful.

Tocornalite is evidently a valid species, occurring at both Chanarcillo and Broken Hill, but additional work on better material is needed to characterize it completely.

I am indebted to John S. White, Jr., for the preparation of numerous X-ray powder photographs.

Literature Cited

Domeyko, Ignacio
1867. *Mineralojia de Chile, Appendix* II:41.
Palache, C., H. Berman, and C. Frondel
1951. *Dana's System of Mineralogy,* 7th edition, 2:1124. New York: John Wiley and Sons.
Smith, George
1926. A Contribution to the Mineralogy of New South Wales. *New South Wales Mines Department, Mineral Resources,* 34: 145.

STANDARDS FOR CHEMICAL ANALYSIS

Eugene Jarosewich

Chemical Analysis of Five Minerals for Microprobe Standards

There is a growing need for the availability of reliable microprobe standards for chemical analysis of various materials, in our particular case for the analysis of minerals.

Unfortunately, there are a very limited number of acceptable standards. Perhaps one of the main reasons for this is lack of homogeneous materials, an essential property of microprobe standards. Homogeneity should be the micron level, and the material should be stable under the electron beam. Also, there should be sufficient material for a chemical analysis.

We have analyzed five minerals which have been successfully used as microprobe standards. These standards served very well in plotting the calibration curves with standards from other sources, and excellent results were obtained. Nevertheless, we still are contemplating a more thorough study of homogeneity. These standards were obtained by crushing hand specimens of a rock or mineral and then selecting a fraction between 80 and 60 mesh for heavy liquid and Franz magnetic separations. Each sample was visually inspected for impurities. In this manner between 0.8 g to 1.5 g of sample was obtained. Approximately 20 grains of each sample were mounted on a one-inch

Eugene Jarosewich, Department of Mineral Sciences, National Museum of Natural History, Smithsonian Institution, Washington, D.C. 20560.

TABLE 1.—*Chemical analyses of minerals for use as microprobe standards (weight percent)*

Constituent	*Kakanui Hornblende*	*Kakanui Pyrope*	*Omphacite (USNM 110607)*	*Garnet (USNM 87375)*	*Garnet (USNM 110752)*
SiO_2	40.37	41.46	55.42	39.47	40.16
Al_2O_3	14.90	23.73	8.89	22.27	22.70
Fe_2O_3	3.30	N.D.	1.35	2.77	2.17
FeO	7.95	10.68	3.41	13.76	9.36
MgO	12.80	18.51	11.57	6.55	7.17
CaO	10.30	5.17	13.75	14.39	18.12
Na_2O	2.60	N.D.	5.00	N.D.	N.D.
K_2O	2.05	N.D.	0.15	N.D.	N.D.
H_2O+	0.90	N.D.	N.D.	N.D.	N.D.
H_2O-	0.04	<0.01	0.02	<0.01	<0.01
TiO_2	4.38	0.47	0.37	0.39	0.35
P_2O_5	0.00	N.D.	N.D.		
MnO	0.09	0.28	0.10	0.59	0.19
Total	99.66	100.30	100.03	100.19	100.22

glass and checked for major elements homogeneity on the microprobe. The chemical analyses were performed employing classical methods (Hillebrand 1953 and Peck 1964). Sodium and potassium were determined by flame photometry.

Omphacite USNM 110607 was separated from eclogite, garnet USNM 87375 and garnet USNM 110752 were separated from kyanite eclogite, all from Robert Victor Mine, South Africa. Kakanui hornblende and pyrope were prepared from nodules described by Brian Mason (1966).

Literature Cited

Hillebrand, W. F., G. E. F. Lundell, H. A. Bright, and J. I. Hoffman
1953. *Applied Inorganic Analysis.* 2nd edition, 1034 pages. New York: Wylie and Sons.

Mason, B.
1966. Pyrope, Augite and Hornblende from Kakanui, New Zealand. *New Zealand Journal of Geology and Geophysics,* 9.

Peck, L.
1964. Systematic Analysis of Silicates. *Geological Survey Bulletin,* 1170.

THE COLLECTIONS

Paul E. Desautels

Acquisition of the Carl Bosch Collection of Minerals and Meteorites

A five-year effort by the Division of Mineralogy to acquire ownership of the Carl Bosch Collection of minerals and meteorites was brought to a successful conclusion in 1970. This collection, once belonging to the late Nobel Prize winner, Professor Dr. Carl Bosch (Figure 1), is a very large and important collection of about 25,000 specimens including almost 600 meteorites. It is especially strong in specimens from old, exhausted, Central European localities. The representative suites of older species in a wide range of variation from many now-extinct mines are unmatched in any other private collection. These and many other specimens in it are of materials that are most difficult or impossible to acquire today. The meteorite segment of the collection is a major collection in its own right, consisting largely of falls which are unavailable now. Considering the difficulty and expense of acquiring any new meteoritic material this is an incredible accumulation. As is true with most large collections, the Bosch Collection contains several pre-existing collections. Among the best of these is the well-known Seligmann Collection which contains a large number of specimens that have been described in the mineralogical literature of the past.

Assembled and enjoyed by Dr. Carl Bosch, the collection was transported, for safekeeping, to the United States from Germany in 1951. Arrangements were made for its deposition at Yale University on a fifteen-year loan. By 1966, with the loan period expiring and Yale University having made no move to acquire the collection, the heirs of Dr. Bosch decided to dispose of the collection through sale. Although little used by Yale in the fifteen-year period, the collection had been kept intact and in relatively good condition. Its original catalog was in rather good agreement with the contents of the collection.

For several reasons it was considered imperative to acquire and place the collection in the Smithsonian Institution for conversion to maximum use as part of the National Collection of minerals and meteorites. Firstly, the collection was of major size with its 25,000 specimens including the nearly 600 meteorites. Collections of such size rarely become available for wholesale reinforcement of constantly changing specimen needs of the National Collection. In numbers, though not in quality or species representation, it would be the largest single collection of minerals ever acquired by the National Museum of Natural History. Also, the collection contained extensive suites of rare reference specimens unobtainable through normal channels. Even those specimens duplicating others already in the Museum were considered usable for supplying additional material to meet ever-increasing research and exchange demands. Several hundred pieces were thought to be of public exhibit quality. The strong representation of old Central European mineral occurrences was specially significant because of the new support which would be available for the weakest part of our Museum collection. Being an older collection, much of the specimen material was of a type totally unavailable today through normal sources. Of course, the presence of the included Seligmann Collection with its many described specimens increased the number of scientifically significant pieces generally unavailable at any price. The meteorite materials had

Paul E. Desautels, Department of Mineral Sciences, National Museum of Natural History, Smithsonian Institution, Washington, D.C. 20560.

FIGURE 1.—Dr. Carl Bosch—late Nobel Prize winner—who assembled the Bosch Collection of minerals and other natural history collections in the early 1900s. Photograph supplied by Dr. Henning Borchers.

unusually high, current, scientific importance and needed to be carefully conserved. Our meteorite collections were already under such careful control that conservation-research procedures were already set up. Finally, the excellent state of preservation and organization of the collection would make it possible to convert it to maximum use in minimum time (Figure 2).

The Bosch Collection had already been openly offered for sale by the time the decision had been made to attempt acquisition. When it appeared that there was a distinct possibility the collection would be sold outside the United States, negotiations were accelerated. There was no established price but our own appraisal and independent appraisals were arranged and a reasonable price of $250,000 was agreed upon. In retrospect, faced with a continuing rapid rise in

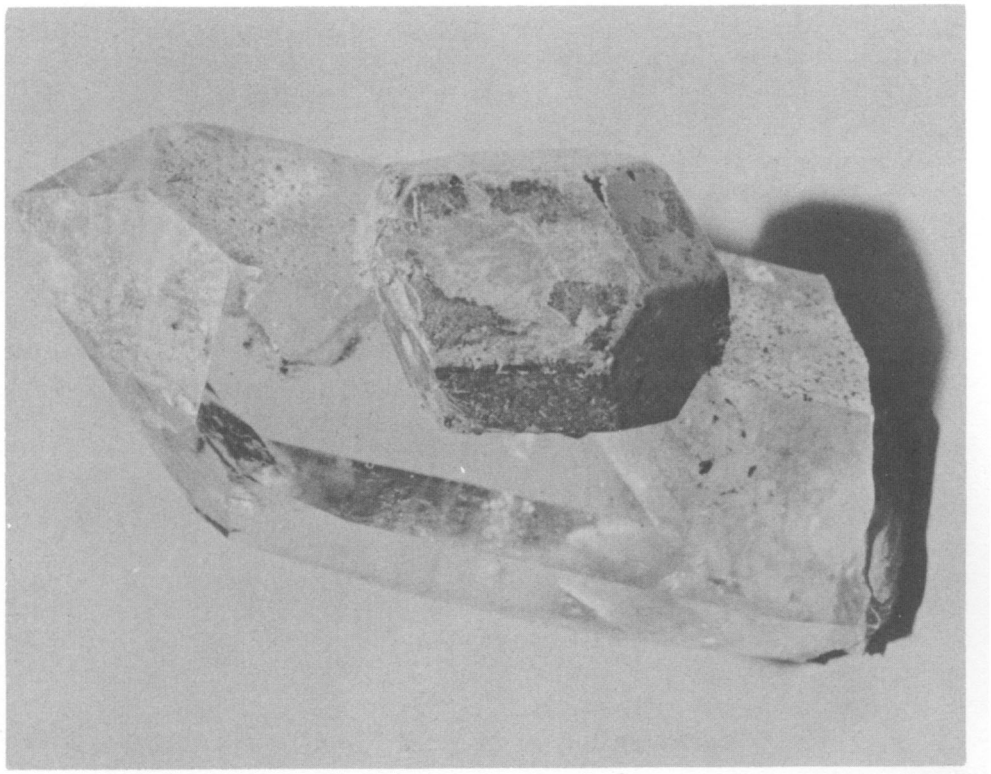

FIGURE 2.—Cafarsite—a newly (1966) described mineral species. This very fine specimen was found in the Bosch Collection where it had been labeled as an "unknown." Thus, Dr. Bosch had discovered the species long before its "official" discovery.

the market price of mineral specimens, this was a very fair agreement. By this time, Dr. Carl Bosch, Jr., had concluded that the Smithsonian was the logical repository for his father's collection. When it became obvious that there was little hope of our raising the total payment, he was willing to help as much as possible. Accordingly, Dr. Bosch agreed to donate $70,000 of the value with the remaining $180,000 to be paid over a period of five years. With the aid of a $47,000 grant from the National Science Foundation and $13,000 in available private funds, an initial payment was made in the spring of 1966. Necessary packing and moving arrangements were made and the collection was transferred promptly to Washington in two large vans. The problems of packing and moving such a large collection containing much fragile material were anticipated in advance and the moving company was so cooperative that there were no mishaps of any account during the transfer. Most of the actual handling of specimens was, of necessity, done by our own staff.

Without waiting for complete ownership, the sorting, relabeling, cataloging and integration of the collection into our existing operation were begun. To date, about 14,500 specimens have been processed. Since the original collection's cataloging and labeling are not up to our present standards, the task is difficult. German script of names and localities—often abbreviated—must be translated and related to modern speciation and geography. These difficulties, together with the necessary physical handling and the shortage of trained personnel, have made cataloging the collection slow work but completion of the project is expected in 1971. The size and nature of this collection as a unit suggested the possibility of using it for a pilot program in computerization of the mineral collection. Accordingly, cataloging has been arranged in such a way as to make the necessary information available eventually for the computer.

Meanwhile, this important collection has already been pressed into service for our normal research, educational, and exhibits programs.

THIN-SECTION PREPARATION

Grover Moreland,
Frank Ingram,
and Harold H. Banks, Jr.

Preparation of Doubly Polished Thin Sections

A technique for preparing polished thin sections which show greater textural and mineralogical detail has been developed for stony meteorites, rocks, and minerals.

The preparation of polished thin sections—sections which can be examined in both reflected and transmitted light and used for electron microprobe studies—has been discussed at length by Moreland (1968). This procedure, in summary, is to cement an optically flat surface of a specimen, which has been sized for a petrographic section or for a circular microprobe section, to a glass slide and then to hand-grind the specimen to a thickness of 30 microns. Next, the opaques are given a rough polish, then the non-opaques are polished, and lastly the section is subjected to a final polish.

In the course of preparing polished thin sections of deep-sea basalts, volcanic ejecta, and Apollo 11 and 12 samples, it was observed that the polishing of both sides of a sample enhanced the optics by yielding sharper images, particularly of groundmass minerals in fine-grained rocks and of inclusions in minerals.

The first step in the preparation of a doubly polished thin section is to cut a wafer of the specimen, approximately 7/8 inch square and 3/16 inch thick with smooth parallel surfaces, using a 5-inch by 0.015-inch diamond saw blade. The wafer is then ground on one face to an optically flat surface, using a water slurry of 600 aluminum oxide on an 850 rpm, 12-inch cast-iron lap.

Grover Moreland and Harold H. Banks, Jr., Department of Mineral Sciences, National Museum of Natural History, Smithsonian Institution, Washington, D.C. 20560. Frank Ingram, Ingram Laboratories, Griffin, Georgia 30223.

After washing the wafer with water and drying it for approximately 30 minutes at 200°F, it is immersed, under vacuum, in a mixture composed of equal portions of Araldite AY105 and Hardner 935F (Moreland 1968:2071) dissolved in three parts of toluene. The vacuum occasionally is broken and restored to help force the impregnating solution into the pores and cavities of the sample. The wafer is removed from the vacuum and the impregnating solution, after two to three hours, and placed on a hot plate or in a drying oven to allow the impregnating medium to cure, which takes about one hour at 200°F and 15 minutes at 300°F. The wafer is reground to expose the sample and the impregnation procedure is repeated.

The next step is polishing the ground face of the wafer. For this, a double thickness of kraft, heavy-duty, wrapping paper is used instead of a lap cloth. The paper is cut to the size of the lap and evenly smeared with a one-half-inch length of 3-micron diamond abrasive and a small amount of polishing oil, until it appears moist. Unlike a lap cloth, the kraft paper minimizes plucking and subsequent scratching of the sample and ultimately gives a much better polish; in addition, it is inexpensive. The polishing technique is described by Moreland (1968:2073). However, it must be noted that the lap should turn at 200 rpm. After the final polish, the wafer is mounted with the polished face down on a glass slide, using Araldite AY105 and Hardner 935 (Moreland 1968:2071).

An Ingram Model 103 thin section cut-off saw is used to reduce the wafer to a thickness of 0.020 inches, and an Ingram Model 303 thin section grinder with a diamond wheel is utilized to still further reduce the thickness. Additional grinding is done by hand, using

a slurry of 600 aluminum oxide and water on a 850 rpm horizontal lap, until the desired thickness is reached. A standard thickness of 30 microns is obtained using a glass plate with a slurry of 1500 aluminum oxide and water.

Final step in the preparation of the doubly polished thin section is polishing of the wafer, which is described by Moreland (1968).

Doubly polished thin sections of grain mounts are prepared in essentially the same manner. Grains between 177 and 105 microns (80 to 150 mesh) are sprinkled one layer thick onto a glass slide, which has been smeared with a mounting medium of equal portions of Araldite AY105 and Hardner 935F and heated to 200°F on a hot plate.

After curing, an Ingram thin section grinder is used to expose the individual grains which are then ground to an optically flat surface and polished in the same manner as a doubly polished thin section. A 0.015-inch diamond saw blade is used to remove all outer regions of the glass slide devoid of grains; the slide is then mounted, polished face down, on another glass slide. Once the mounting medium has cured, the sample is placed in an Ingram thin section cut-off saw and the thickness of the slide containing the unpolished surface of the grains is reduced so that the grains are just barely exposed. The section is then ground and polished to a standard thickness of 30 microns.

Literature Cited

Moreland, G.
1968. Preparation of Polished Thin Sections. *American Mineralogist,* 53:2070–2074.

☆ U.S. GOVERNMENT PRINTING OFFICE: 1972 O—484–316/18